"Aggregation-Induced Emission'' of Transition Metal Compounds: Design, Mechanistic Insights, and Applications

Parvej Alam[a], Clàudia Climent[b], Pere Alemany[c] and Inamur Rahaman Laskar[a]*

[a]*Department of Chemistry, Birla Institute of Technology and Science, Pilani Campus, Pilani, Rajasthan, India.* **ir_laskar@bits-pilani.ac.in**

[b]*Departamento de Física Teórica de la Materia Condensada, Universidad Autónoma de Madrid, E-28049 Madrid, Spain.*

[c]*Departament de Ciència de Materials i Química Física and Institut de Química Teòrica i Computacional (IQTCUB), Universitat de Barcelona, Barcelona, Spain.*

Abstract: In the last decades**,** compounds with 'Aggregation-Induced Emission' (AIE), which are weakly or non-emissive at all in solution but exhibit a strong luminescence in aggregated states, have emerged as an extraordinary breakthrough in the field of luminescent materials, allowing to circumvent 'Aggregation Caused Quenching' (ACQ), which in many cases prevents the development of efficient solid-state materials for optoelectronic applications.

Since the discovery of AIE, many AIE-active materials have been developed, most of them composed of organic molecules, and thus fluorescent in nature. Although a wide range of applications such as bioimaging, sensing, multi-stimuli responsive materials, and optoelectronic devices have been proposed for this new class of materials, triplet harvesting phosphorescent materials have much longer lifetimes as compared to their singlet harvesting analogues, and for this particular reason, the development of AIE-active phosphorescent materials seems to be a promising strategy from the applications point of view. In this respect, the synthesis of new AIE-active systems including heavy metals that would facilitate the population of low-lying excited triplet states via spin-orbit coupling (SOC), for which the strength increases as the fourth power of atomic number, i.e. Z^4, is highly desirable. This review covers the design and synthetic strategies used to obtain the AIEgens reported in the literature that contain either d-block metals such as Cu(I), Zn(II), Re(I), Ru(II), Pd(II), Ir(III), Pt(II), Au(I), and Os(IV) describing the mechanisms proposed to explain their AIE. New emerging high-tech applications such as

OLEDs, chemical sensors or bioimaging probes proposed for these materials are also discussed in a separate section.

Keywords: Aggregation-induced emission, transition-metal complexes, Stimuli-responsive materials, Bioimaging probes, chemo-sensing materials, OLEDs

Index

4. Conclusions

Acknowledgements

References

Introduction

Currently there is a great interest, both from academia and industry, in the study and development of new, strongly emitting luminescent solid state materials as promising candidates for applications such as organic light-emitting diodes (OLEDs) [1-10], bioimaging agents [11-19], chemosensors, detectors of microenvironmental changes [14, 20-28], or dynamic functional materials [7, 8, 18, 29-32]. Most of the known molecular luminescent materials contain planar π-conjugated aromatic rings, and after the pioneering works of Scheibe [33] and Jelly [34], it is well known that formation of aggregates might have a large influence on the intensity of the luminescent emission of a given compound, either enhancing it or, in most of the cases, leading to a quenching of the luminescence sometimes designated in the literature as aggregation caused quenching (ACQ) [35-39]. An excellent review on the research developed in the last 80 years on the effects of aggregation, and in particular on the formation of the so-called J-aggregates, can be found in reference [40].

To overcome ACQ, which severely limits the solid-state application of many known luminescent materials, several strategies have been developed, basically aimed towards preventing close intermolecular interactions in order to limit the possibility of excimer formation [41-44] that is thought to be at the origin of ACQ in many cases [45-47]. These approaches have found a limited success since while they solve in part the issue of unwanted excimer formation, it is at the cost of creating other issues. The discovery in 2001 by Tang and co-workers that the 1-Methyl 1,2,3,4,5-pentaphenylsilole molecule, which was hardly emissive in common organic solvents, but highly emissive in aggregated or solid state [48] led to a new boost to the search for new suitable ways to circumvent the problems of ACQ. Tang and co-workers introduced the term "aggregation induced-emission" (AIE) for this phenomenon [49-52] (Fig. 1), a denomination that is now widespread in the field of luminescent materials, although other related terms (see below) have also been indiscriminately employed to describe this phenomenon or other closely related observations.
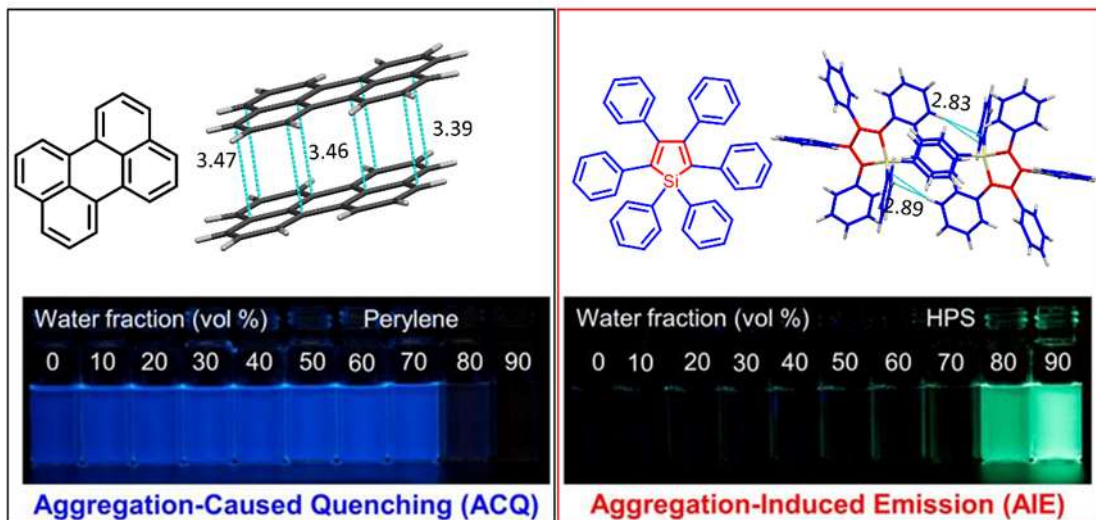
Fig. 1. Top; Chemical structure and molecular conformation (or configuration) in the respective crystals of perylene and hexaphenylsilole, **Bottom**; ACQ effect and fluorescence photographs of perylene (20 μM) in THF/water mixtures with increasing water fraction (right), AIE effect of hexaphenylsilole (HPS; 20 μM) in THF/water mixtures with increasing water fraction (left). Adapted from Ref. [52] with permission from The American Chemical Society.

Many purely organic and heteroatom-containing AIE-active molecules such as tetraphenylthiophene derivatives, dithiole nitrofluorene derivatives, indolo [3,2-b] carbazole derivatives [53], or organoboron compounds were synthesized in the following years, a work that has been extensively reviewed in several recent articles [49, 51, 52, 54-59].

Despite the obvious advantages of organic luminogens, the chemical nature of these compounds often poses some serious drawbacks to the development of new optoelectronic devices since efficient organic phosphorescent molecules are very scarce due to the inefficient spin-orbit coupling in compounds incorporating only light elements [60-63]. The presence of a heavy atom which facilitates intensity borrowing of the lowest triplet state from bright singlet states, combined with the photophysical properties of π-conjugated ligands is thus seen as a promising strategy for obtaining new luminescent functional materials. There have been some attempts to introduce heavy main group atoms such as Hg, Pb, Bi, Sb, or Te [64] but, most of the attention has been paid to coordination compounds containing transition metals such as Ir(III), Pt(II), Au(I), Re(I), or Cu(I) with an excellent phosphorescent emission capability [16, 65, 66]. The d-block metal luminescent complexes are renowned for their long luminescence lifetimes (up to

5

ms), large stokes shifts (hundreds of nm), high quantum yields in the visible region, and straightforward synthetic routes. The rich photophysics of these complexes, due to the variety of different charge transfer electronic states (^{3}MLCT, ^{3}LLCT, ^{3}LMCT, ^{3}ILCT, ^{3}MMLCT) and intense local π-π^* transitions on the ligands (Fig. 2), makes them potential candidates for optoelectronic applications [67-71], allowing the design of optical materials by a fine tuning of their photophysical properties through chemical modification. Although luminescence in the solid state for this type of compounds has been described as early as 1853 [72], these transition metal complexes suffer also often from ACQ effects: In thin films with 4,4'-bis(*N*-carbazolyl)-2,2'-biphenyl as a host material doped with Ir(ppy)$_3$, a remarkable quantum yield of $\Phi_P = 97\%$ was measured when the dopant concentration is low (about 1.5 mol%). As the concentration of Ir(ppy)$_3$ was increased, significant decreases in Φ_P were observed, resulting in a value Φ_P below 3% in the neat film. This observation points clearly towards the existence of Ir(ppy)$_3$ self-quenching interactions at large dopant concentrations that limit the applicability of such materials in solid-state devices [73]. For this reason, the search for new AIE-active phosphorescent components is actually a very active field of research in luminescent materials.
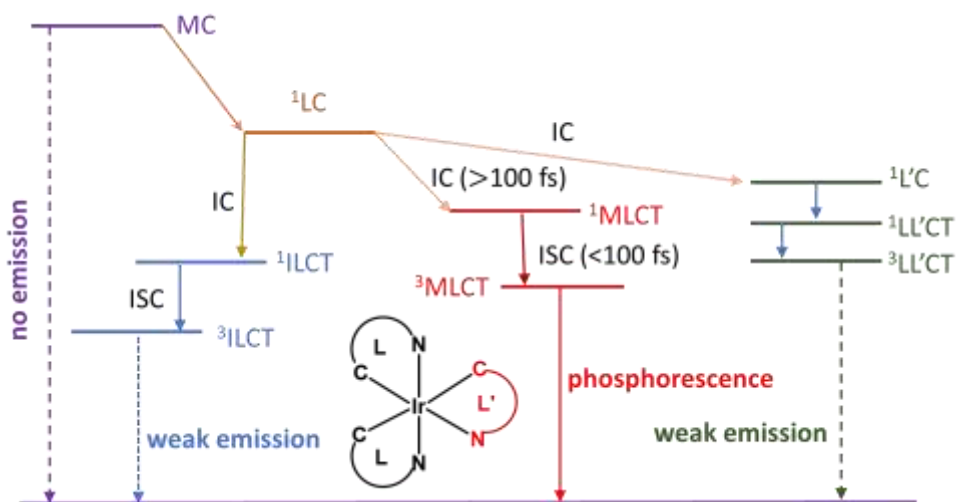
Fig. 2. Schematic diagram indicating the relevant low-lying excited states and transitions between them for a generic octahedral Ir(III) complex. Acronyms: MC-Metal Centered, ILCT – Intra-ligand Charge Transfer, LC - Ligand Centered, MLCT - Metal to Ligand Charge Transfer, LL'CT - Ligand to Ligand Charge Transfer, IC - Internal Conversion, ISC - Inter System Crossing. Adapted from Ref. [71] with permission from The Royal Society of Chemistry.

With the quest for efficient transition metal based phosphorescent materials in the solid state, especially in the field of OLEDs, the term AIPE (aggregation-induced phosphorescence enhancement) has been introduced also in the literature to stress the phosphorescent nature of the emission, although AIE and AIEE (aggregation induced-emission enhancement) are commonly used, both in the case of fluorescence and phosphorescence, without further distinction. In some cases, when a special emphasis on the solid nature of the studied systems is made, the denomination EPESS (enhanced phosphorescence emission in the solid state) is used instead of the more generic AIPE [17]. In the special case that the emission or emission enhancement is observed only in crystalline samples, the terms CIE (crystallization induced emission), CIEE (crystallization-induced emission enhancement) or CIPE (crystallization-induced phosphorescence enhancement) have also been used to describe these phenomena [65, 74-77]. Since all these experimental observations have a common origin, that is, the change in the luminescent behaviour upon aggregation, in the following, to avoid confusion we will use the most commonly accepted term, AIE, in a general sense to refer to all these phenomena and reserve the use of terms such as AIPE or CIPE for those cases where it is important to further indicate the specific features of a given AIE system.

While after the initial bloom of organic AIE systems, a thorough task of reviewing the available literature on these compounds has been undertaken, only scarce references to transition metal containing AIE systems can be found in these reviews and most of the studies on these compounds are still scattered in the literature [50, 55, 65, 66]. Additionally, some confusion in the nomenclature used to describe the photophysical behaviour of these compounds upon aggregation and the lack of a unified description of related phenomena such as vapochromism or mechanochromism, appearing often in conjunction with the AIE behaviour, has led us to the recompilation of this information in a single review paper. To limit its scope, we will focus our attention mainly to transition metal based phosphorescent materials. Our main aim is to give a unified vision on their AIE properties, the underlying mechanisms, as well as of some of the most interesting applications that have been proposed for these new materials.

1. Origin of AIE in transition metal complexes

Although from the experimental point of view it is quite simple to detect the presence of either ACQ or AIE (Fig. 1), a clear explanation at the atomic level of the mechanisms underlying these observations is quite elusive since different causes may lead to similar phenomenological

observations for different classes of luminescent molecules [37, 78-83]. ACQ has been extensively studied since Förster's report of the concentration quenching effect in 1954 [84]. The absorption and emission properties of π-conjugated luminophores are basically determined by the nature of their conjugated backbone, but they may change dramatically upon aggregation. The main factors responsible for such changes are explained adducing the establishment of specific inter-molecular interactions that may modify the nature of the emitting state (excimer formation), although the detailed mechanisms behind ACQ may be more involved, as for instance in non-radiative deactivation processes in polycrystalline samples arising from the presence of (structural) trap states located especially at grain boundaries [85].

Although there is not a single general mechanism capable to explain the origin of ACQ or AIE in all cases, some general trends may be anticipated. Since the observed behaviour emerges because of competing radiative and non-radiative de-excitation paths, selective enhancement or blocking of these channels will lead to one or the other result. Experiments with different molecules and theoretical work, mainly by the group of Shuai, has shown that the restriction of internal motion (RIM) [86-88], in which no differentiation is made on the detailed nature of the low frequency large amplitude motions (internal rotations or vibrations) that quench the luminescence in solution via internal conversion, lead in many cases to AIE when the non-radiative de-excitation channel gets blocked by the rigidification of the molecular environment due to the establishment of intermolecular interactions. Although the RIM mechanism seems to provide a widely accepted explanation for the emergence of AIE, let us note that the question is not totally settled as shown by some recent computational work where photochemical decay is suggested to play an important role, at least for systems with accessible conical intersections (CIs) [89, 90].

Besides blocking an effective non-radiative deactivation pathway by RIM, an alternative, but not mutually excluding, possibility is to achieve efficient AIE inducing a change in the nature of the emitting state when bringing the isolated molecules into contact. If emission from this new state is more efficient than from the state from which molecules were originally emitting in solution, an enhancement of the luminescence could be expected. In the case of transition metal complexes, metal-metal intramolecular interactions may lead simultaneously to changes in the nature of the emitting state that give an additional complication to the establishment of the mechanisms behind AIE for a particular family of compounds.

In the next section we will review the most relevant papers discussing the synthesis of AIE-active transition metal complexes, describing briefly the experimental and computational

evidences that have been given in each case to support or discard a given mechanism for the observed AIE. We have divided the section in two main parts, considering separately the cases where there are no significant metal-metal interactions and those where their presence leads to a change in the nature of the emitting state. A third shorter section gives account of some particular cases where the emergence of AIE has been attributed to specific mechanisms other than RIM or a change in the nature of the emitting state.

2.1 Restriction of Intramolecular motion (RIM)

2.1.1 Ir (III) complexes

In 2008, the group of Huang synthesized three Ir(III) complexes [91], with two of them, Ir(ppy)$_2$(DBM) (**1**) and Ir(ppy)$_2$(SB) (**2**) (where ppy = 2-phenylpyridine, DBM = 1,3-diphenyl-1,3-propanedione and SB = 2-(naphthalen-1-yliminomethyl)-phenol), showing AIE in H$_2$O/CH$_3$CN mixtures and in the solid state (Fig.3a). The origin of the AIE behaviour was analysed by searching for relevant intermolecular contacts in crystal data and periodic DFT calculations. The crystal structure revealed π-stacking interactions between adjacent pyridyl rings of ppy ligands that were suggested to give rise to different energy level orderings in the aggregated state compared to solution (Fig. 3b). In solution, the DBM ligand would dominate the excited state properties of **1** instead of ppy due to the lower energy of the ^{3}LX$_{DBM}$ state, leading to very weak emission. In the solid state, however, strong π-π interactions between the adjacent ppy ligands of neighbouring molecules reduce the energy of the π^*_{ppy} orbital, lowering the metal-to-ligand–ligand charge-transfer (^{3}MLLCT) charge transfer state from Ir(III) to ppy that would become the lowest emitting state.
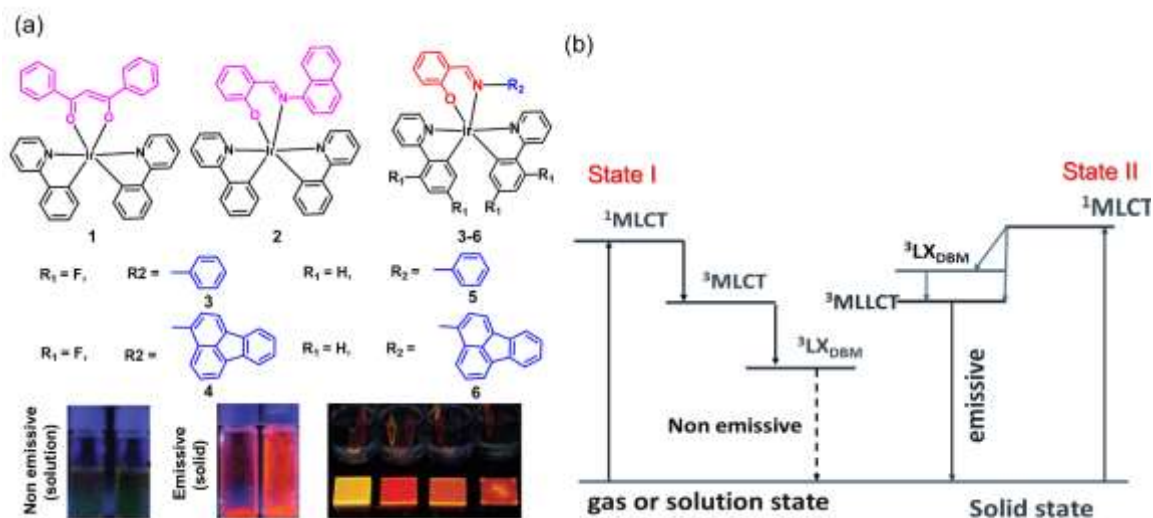
9

Fig. 3. (a) Molecular structures and luminescence photographs of AIE Ir(III) complexes (**1-6**), (b) Possible mechanism of phosphorescence emission in State I (gas or solution) and State II (solid state). Adapted from Ref. [91, 92] with permission from The Royal Society of Chemistry.

In the same year, Park and co-workers questioned the origin of AIE for these complexes as reported in reference [92]. According to these authors, AIE should be due to RIM in the aggregated state rather than to the supposed intermolecular excimer formation. To support this claim they synthetized a new series of complexes using 2-(2,4-difluoro-phenyl)pyridine (dfppy) and 2-phenylpyridine (ppy,) as cyclometalating ligands and imine-based ancillary ligands, 2-(phenyliminomethyl) phenol (pip) and 2-((fluoranthen-3-ylimino)methyl) phenol (fip) (**3-6**) (Fig. 3) that were non-luminescent in solution, while strong emission could be observed for thin films. According to the mechanism suggested in reference [91], the cyclometalating ligand's excimeric states of **3** and **4** (or **5** and **6**) should be responsible for the AIE effect and, hence, λ_{max} for **3** and **4** (or **5** and **6**) should be identical. However, **4** and **6** exhibit a solid-state phosphorescence that is bathochromically shifted with respect to that of **3** and **5**, respectively, from which it can be deduced that the observed colour change should be directly related to the chemical structure of the ancillary ligand. A more convincing evidence for the origin of the AIE was obtained from experiments in solution at different temperatures. When an initially non-phosphorescent fluid CHCl₃ solution (10 mM) containing **3**, was frozen, bright yellow phosphorescence was observed. The variation of the phosphorescence intensity of the frozen solution with temperatures in the range 80–240 K reveals a very abrupt decrease in phosphorescence intensity near the melting point of CHCl₃. This behaviour is reversible and

10

could also be reproduced in other solvents, leading to the conclusion that fast-non-radiative decay due to rotation around the N–aryl ring bond of the ancillary ligands was possible at high temperatures, while the restriction of this intramolecular motion would lead to the AIE observed at low temperatures or in the solid state.

The general principle of RIM as a key ingredient in the design of new organic AIEgens has been fruitfully exploited principally by Tang and co-workers [52] and the extension of these ideas to transition metal based AIE-active complexes has lead also to interesting results. In this line, the introduction of flexible triphenylphosphine groups as ancillary ligands in luminescent Ir(III) complexes (7-10) has been successfully exploited in our group (Fig. 4a) [93-101]. Analysis of molecular packing of crystal structures for this type of compounds reveals the presence of intermolecular C−H⋯π interactions between the mobile phenyl rings of the triphenylphosphine groups and the rigid bipyridine ligands of neighbouring molecules restricting severely the internal rotation of these rings as the principal source for RIM in these AIE-active complexes.
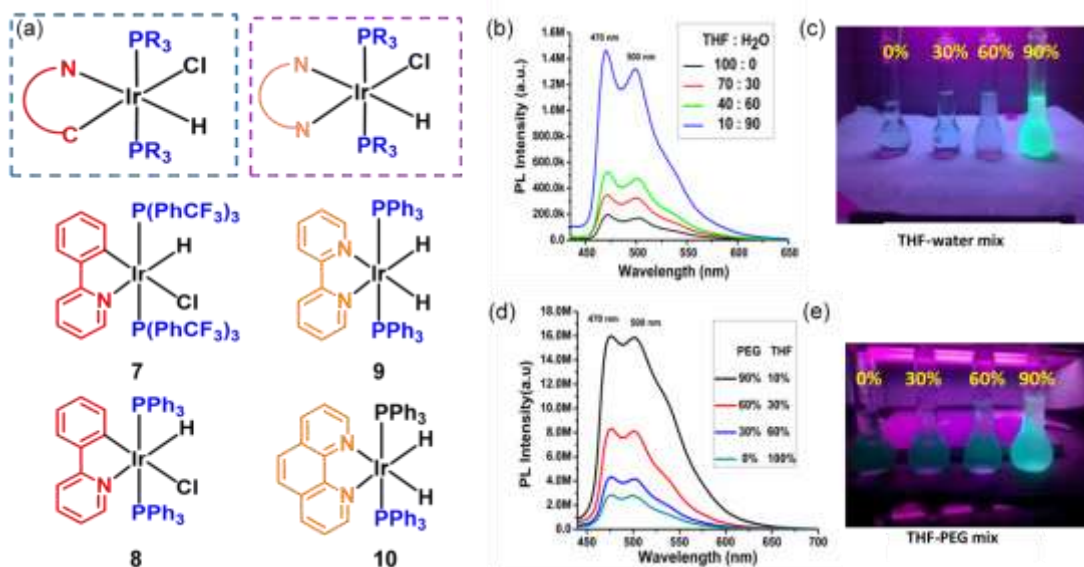

Fig. 4. (a) Molecular structures of two different kinds of AIE-active Ir(III) complexes with C^N and N^N as the chromophoric ligand, (7-10), PL spectra of complex **8,** (b) In THF/water mixtures, and (c) fluorescence photographs of **8** with different fractions of water (f_w), (d) In THF/PEG mixtures, and (e) fluorescence photographs of **8** with different fractions of PEG (f_{PEG}), Adapted from Ref. [98] with permission from The Royal Society of Chemistry.

The involvement of RIM can be inferred from fluorescent measurements in different solvent mixtures such as THF-water where aggregates form (Fig. 4b-c), or by changing the viscosity in

PEG-THF mixtures (Fig. 4d-e). The observed phenomena are also consistent with geometry optimizations using quantum chemical calculations that show that in solution the minimum energy disposition of those phenyl rings is markedly different from that adopted in the crystal structure (**11-13**) (Fig. 5). The hindered motion of the phenyl rotors in the crystal state is suggested to block the non-radiative decay channels enhancing the emission intensity significantly in aggregated state, as observed experimentally [99].
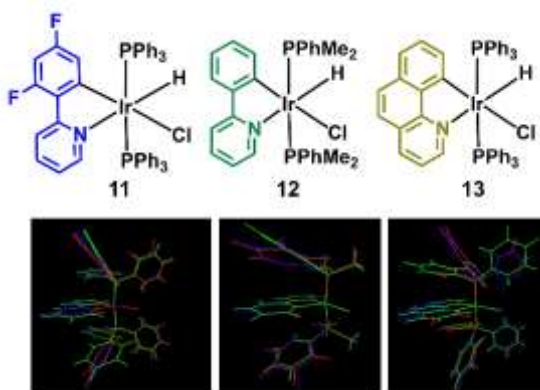

Fig. 5. Geometry comparison between the X-ray crystal structure (green), and the ground state (blue) and lowest triplet (red) optimized geometries in DMC solution of complexes **11**, **12** and **13.** Reprinted from Ref. [99] with permission from The Royal Society of Chemistry.

Su and co-workers have synthesized an AIE-active Ir(III) core with C^N cyclometalated ligand along with triazol-pyridine derivatives as ancillary ligands (**14-16**) [102, 103]. The substitution at positions 1 and 3 of the triazole ring leads to distinct photophysical behaviour while TD-DFT calculations show that for the AIE-active complexes, the emissive state has a predominantly intra-ligand charge transfer (^{3}ILCT) character, non-emissive in solution. However, in the solid or aggregate state, strong intermolecular packing drastically reduces the non-radiative decay rate via RIM, and the system becomes emissive (Fig. 6).
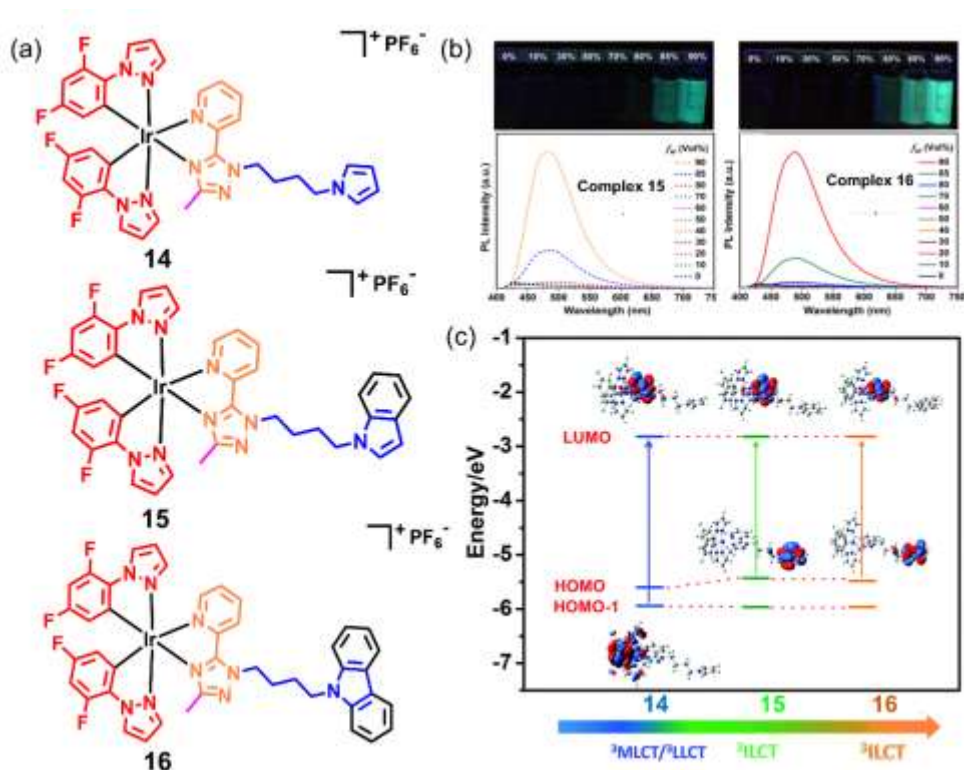
Fig. 6. (a) Molecular structures of AIE-active Ir(III) complexes **14-16**, (b) Luminescent photographs and emission spectra of complexes **15** and **16** in CH_3CN/H_2O mixtures with different water ratios, (c) Selected molecular orbitals involved in the T_1 states of complexes **14–16**. HOMO − 1 → LUMO for **14** and HOMO → LUMO for **15** and **16** are shown. Adapted from Ref. [103] with permission from The Royal Society of Chemistry.

Another class of dinuclear Ir(III) Schiff base complexes (**17-20**) were reported by Bryce and co-workers [61, 104-107]. TD-DFT calculations show that the lowest emitting state of these complexes has a mixture of metal-to-ligand charge transfer (^{3}MLCT), ligand-to-ligand charge transfer (^{3}LLCT) and ligand-centred (^{3}LC) character, resulting in a much more distorted geometry for the excited T_1 state than for the ground state. This finding is interpreted to result in a reduction of the radiative rate, making the complex non-emissive in solution. Further, close inspection of the crystal structure indicated that the presence of several short contacts (π–π and C–H⋯π interactions) between the phenyl rings stabilize a more planar geometry, resulting in a RIM and activating the AIE phenomenon (Fig.7). Additional recent work on AIE-active Ir(III) compounds may be found in references [108-112].
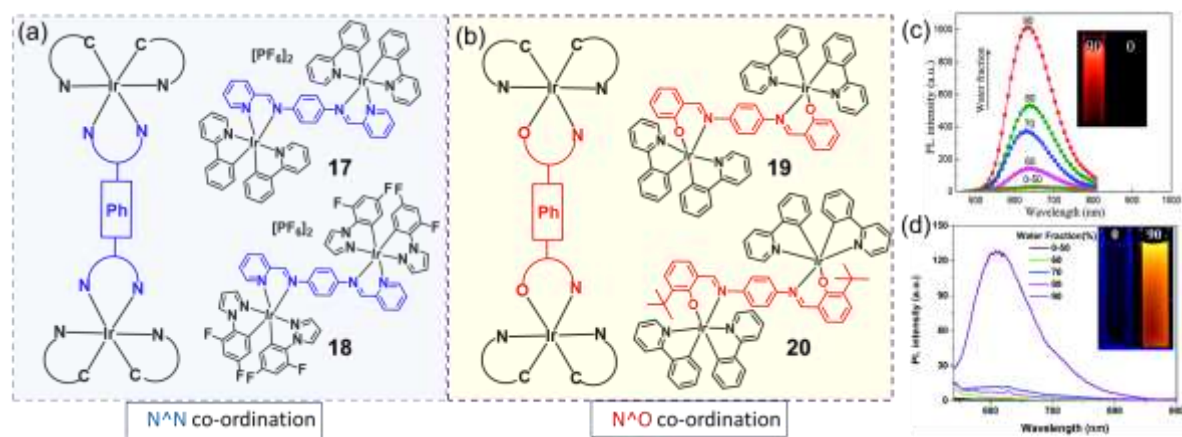
Fig. 7. (a) Molecular structures of AIE-active Ir(III) complexes having N^N coordination mode (**17-18**), (b) Molecular structures of AIE-active Ir(III) complexes having N^O coordination mode (**19-20**), (c) Emission spectra of complex **17** in CH_3CN–water mixtures with different water fractions (0–90% v/v) at room temperature. Inset: Emission image of **17** in pure ACN solution and ACN–water mixture (90% water fraction) under 365 nm UV illumination, (d) Emission spectra of **20** in THF–water mixtures with different water fractions (0–90% v/v) at room temperature. Inset: Emission image of **20** in pure THF solution and THF–water mixture (90% water fraction) under 365 nm UV illumination. Adapted from Refs. [61, 105] with permission from The Royal Society of Chemistry.

2.1.2 Pt (II) complexes

Recently, our group has synthesized a series novel Pt(II) complexes exhibiting AIE. Among them, complex **21**, a well-known precursor for the synthesis of Pt(II) complexes, was also investigated for AIE activity [113]. The design of the two other complexes (**22-23**) included propeller-type ligands, prone to AIE through a RIM mechanism (Fig. 8a). The AIE activity of complex **21** was studied adding different amounts of water to a pure THF solution, with the maximum emission intensity observed for $f_w = 90\%$ being about 12 times higher than in pure THF. DCM-Hexane mixtures were used to prove the AIE activity of complexes **22** and **23** for which ~ 20-fold enhancements of the PL intensity were found (Fig. 8b). To understand why aggregate formation was causing the AIE, the crystal structures of these complexes were examined, detecting short intermolecular contacts, mainly of the C-H.---π type, that restrict the motion of phenyl rings.

14

In 2014, Kanbara and co-workers reported the synthesis of two new Pt(II) complexes (**24-25**) with secondary thioamide units (Fig. 8a) exhibiting AIE behaviour [114, 115]. Analysing the crystal structures strong hydrogen bonds between the N–H moiety in the secondary thioamide group and chloride anions lead them to suggest a suppression of molecular motion in the solid state as the source for AIE. The gradual addition of hexane into chloroform solutions resulted in the emission enhancement (Fig. 8b-c), while dynamic light scattering (DLS) data support the formation of aggregates with particle sizes in the range 500-600 nm. Lifetimes for complex **24** in chloroform-hexane mixtures were found to be two times larger than in pure chloroform solution. The crystal structure reveals the absence of relevant Pt---Pt interactions that could lead to a ^{3}MMLCT state. On the basis of all these observations, the N–H$\cdots$Cl$^-$ hydrogen-bonding interactions with the counter anion were postulated to suppress the molecular motion in the aggregated state leading to the observed AIE.
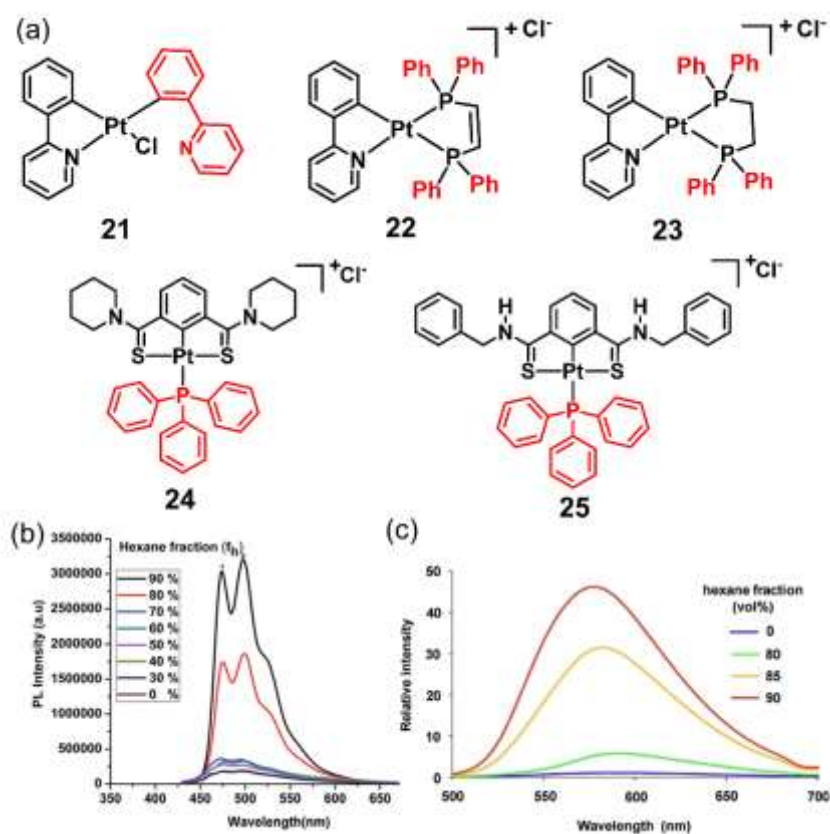

Fig. 8. (a) Molecular structures of AIE-active Pt(II) complexes (**21-25**), PL spectra in different hexane fractions for (b) complex **23** and (c) complex **25**. Adapted from Ref. [113] with

15

permission from The Royal Society of Chemistry and Ref. [114] with permission from WILEY-VCH.

2.1.3 Zn (II) complexes

In 2013, Su and co-workers reported the synthesis of a series of Zn(II) complexes with Schiff bases, Zn(L1)$_2$ (**26**), Zn(L2)$_2$ (**27**), Zn(L3)$_2$ (**28**), Zn(L4)$_2$ (**29**) and Zn(L5)$_2$ (**30**), where L1 to L5 stand for 2(((4-(diphenylamino)phenyl)imino)methyl)phenol, 1-(((4-(diphenylamino) phenyl)imino)methyl)naphthalen-2-ol, 2-(((4-(9H-carbazol-9yl)phenyl)imino) phenol, naphthalen-2-ol, and 2-((ethylimino)methyl)phenol, respectively (Fig. 9a) [116]. Inspired by the idea of the restriction of internal rotations as the source of AIEE, these authors synthesised diphenyl amine and carbazole based Zn(II) complexes. As predicted, complexes **26-29** were shown to exhibit AIEE in THF-water mixtures (Fig. 9b). To prove that RIM involving the rotation of phenyl (**26** and **27**) and carbazole rings (**28** and **29**) was a plausible mechanism for AIEE, complex **30** was synthesised, using in this case ligand L5, a ligand without mobile groups prone to experience internal rotations. In contrast to what was found for complexes **26-29**, the gradual addition of water to a solution of **30** in CH$_2$Cl$_2$ resulted in a gradual decrease of the PL intensity, attributed to an ACQ effect (Fig. 9c).
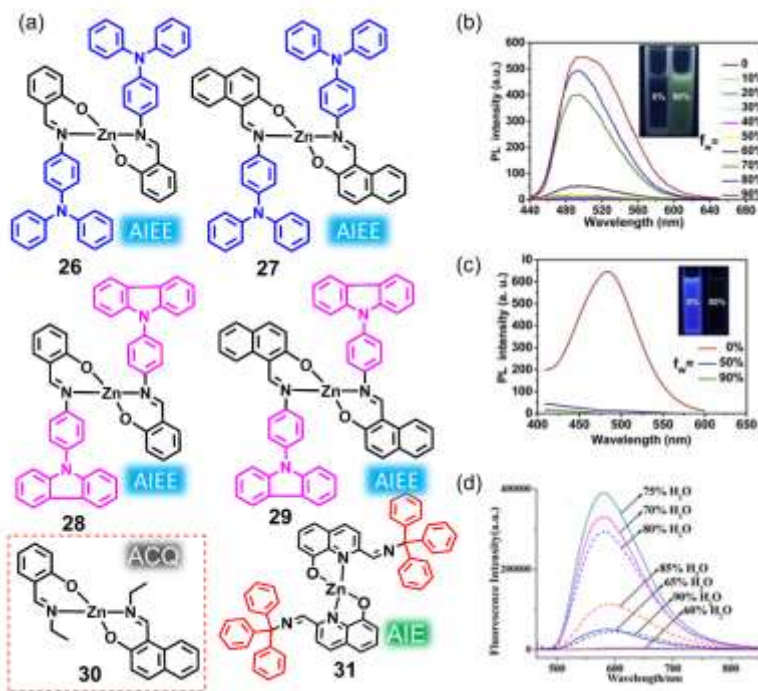

Fig. 9. (a) Molecular structures of AIEE, ACQ, and AIE-active Zn(II) complexes **(26-29, 30 &31)**, emission spectra of (b) **28** and (c) **30**, in water/THF mixtures with different water

16

fractions, (d) Emission spectra of **31** in THF/H$_2$O (HEPES buffer solution, 20 mM, pH = 7.4) with different H$_2$O fractions. Adapted from Ref. [116] with permission from Elsevier (b and c) and Ref. [117] with permission from American Chemical Society (d).

Recently, Jin and co-workers synthesized a Zn (II) complex including a Schiff base ligand **(31)** [117], which was weakly emissive in THF, but showed enhanced emission at f_w above 60% (Fig. 9a-d). AIE was attributed to RIM on the basis of the intermolecular $\pi-\pi$ interactions found in the crystal structure

2.1.4 **Cu (I) complexes**

Li and co-workers synthesized a series of binuclear mixed-ligand Cu(I) complexes **(32-35)**, [Cu$_2$(BrphenBr)$_2$(Ph$_2$P(CH$_2$)nPPh$_2$)$_2$](ClO$_4$)$_2$ (BrphenBr = 3,8-dibromo-1,10-phenanthroline; Ph$_2$P-(CH$_2$)$_n$ PPh$_2$ = bridging diphosphine ligands, n = 1, 4, 5, or 6) for which a distorted tetrahedral coordinated geometry for copper was found [118]. All complexes exhibited a remarkable AIE effect. The emission lifetimes were found to be in the range 2 - 9 μs, supporting their phosphorescent nature. In these complexes, the presence of propeller shaped phenyl rings was deemed to be responsible through a RIM mechanism of the observed AIE.

Similar results were reported by Li and co-workers for five mononuclear [Cu(BIPP)(PP)]ClO$_4$ (PP = dppe, **36**; dppp, **37**; bdpp, **38**; POP, **39**; xantphos, **40**) complexes (where BIPP = 4-bromo-2-(1H-imidazo[4,5-f][1,10]phenanthrolin-2-yl)phenol) (Fig. 10) [119]. The gradual addition of hexane to the solutions of **39** or **40** in DCM resulted in an emission enhancement attributed to the formation of aggregates at higher hexane content. Recent reports on further Cu(I) complexes with AIE activity can be found in references [120-122]
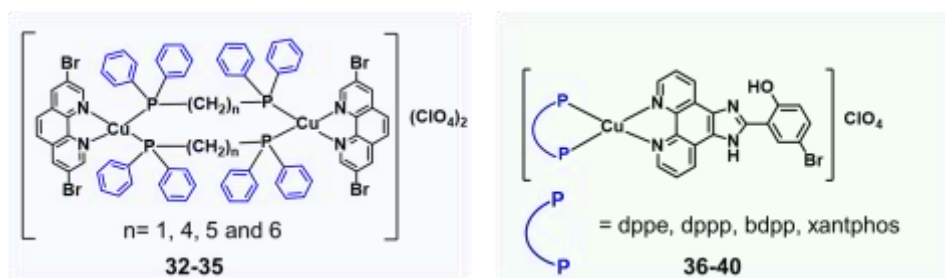

Fig. 10. Molecular structures of AIE-active Cu(I) complexes **(32-40).**

2.1.5 Re(I), Ru(II), Os(IV) and Pd(II) complexes

Tricarbonylrhenium(I) complexes containing chelating diimine ligands have been extensively studied because of their distinctive luminescent properties. In the first report on AIE for these types of compounds, Lu and co-workers observed an abnormal photophysical behaviour for complexes **41-43** (Fig. 11) [123]. The crystal structure showed a rectangular architecture with a rhenium atom at each corner and the coordinated bipyridine ligands perpendicular to the plane that contains the four metal atoms. The gradual addition of water to acetonitrile solutions of these complexes leads to an enormous enhancement in the emission intensity for **43** while the effect is moderate for the other two complexes with shorter alkyl chains. Although the shift observed for the absorption band is not especially large, the corresponding emission maximum is substantially blue-shifted with higher quantum yield, indicative of less solvent exposure and less distorted excited-state environments. RIM associated with molecular aggregation has been suggested as the most appropriate explanation for these experimental observations.
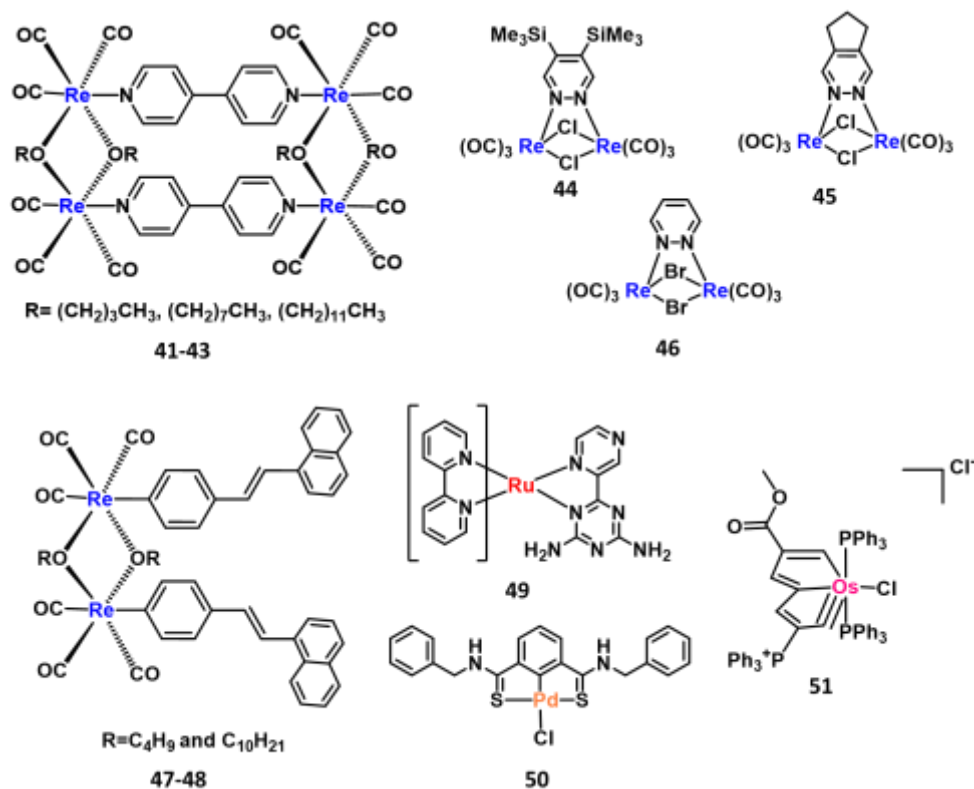

Fig. 11. Molecular structures of Re(I), Ru(II), Pd(II) and Os(IV) based AIE-active complexes (**41-51**).

In 2010, de Cola and co-workers synthesized a dinuclear complex $[Re_2(\mu\text{-Cl})_2(CO)_6(\mu\text{-4,5-}(Me_3Si)_2\text{-pyridazine})]$,(**44**) (Fig.11) [124] exhibiting a unique combination of unusual properties: a higher emission quantum yield in the solid state vs. solution (Fig. 12), formation of two highly luminescent polymorphs (yellow, **44Y** and orange **44O**), and clean single-crystal-to-single-crystal conversion of one form into the other. The observed enhancement of the emission in the solid state was attributed to the restricted rotation of the Me_3Si groups in the crystals, since all the alternative mechanisms proposed to explain the AIE appear not to be at work in this case, as the structural data rule out any π-π stacking intermolecular interactions.
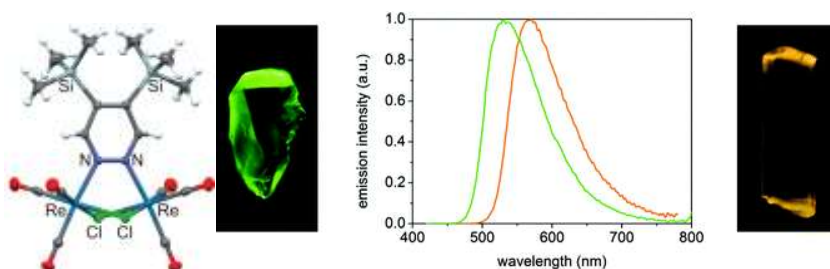

Fig. 12. ORTEP view of complex **44** referred to the molecule as found in the **44Y** phase. Emission spectra and colour for crystals of the two polymorphs of complex **44**. Adapted from ref. [124] with permission from American Chemical Society.

Interestingly, in a different study, similar photophysical properties were reported for $[Re_2(\mu\text{-Br})_2(CO)_6(\mu\text{-1,2-pyridazine})]$ **(45)** (Fig. 11) [125]. This complex displays a stronger and much brighter luminescence in solid state than in solution. A similar enhancement of the phosphorescence was also observed in poly(methyl methacrylate) (PMMA) thin-films. Since in this case there are no mobile groups that could justify a RIM mechanism for the observed enhancement of the emission, the lability of the $Re_2(\mu\text{-Br})_2(\mu\text{-diazine})$ core, as compared to the $Re_2(\mu\text{-Cl})_2(\mu\text{-diazine})$ **(46)** (Fig. 11) one, was considered to explain the poor quantum yields in solution. The enhancement of the emission in films or in solid state is supposed to be due to the lower mobility imposed by the more rigid environment in these cases.

The same $Re_2(\mu\text{-Cl})_2(\mu\text{-diazine})$core was also used to design complexes with amphiphilic character [126] in which the luminescent neutral dinuclear rhenium core represents the hydrophobic head, while the hydrophilic part is provided by a polar tail, either as a tri- or a tetra-ethylene glycol chain. It has been found that all the derivatives self-aggregate in dioxane/water mixtures at water content above 80%. The assembly process results in a strong increase of the

photoluminescence quantum yield in air-equilibrated conditions. Importantly, aggregation leads to a prolongation of the lifetime for the excited state, suggesting a strong shielding of the emitters from the environment once the supramolecular assemblies are formed. A similar approach was used by the same group merging the peculiar physico-chemical properties of transition metal complexes with the self-assembling ability of surfactant molecules using Ir(III) based emitters [127].

Recently, Rajagopal and co-workers reported two new AIE-active alkoxy-bridged binuclear Re(I) complexes (Fig. 11) bearing a long alkyl chain with the 4-(1-naphthylvinyl)pyridine (1,4-NVP) ligand (**47-48**) [128]. The complexes are insoluble in water and acetonitrile, but readily soluble in solvents such as dichloromethane and DMSO. The absorption spectrum showed two bands, assigned to a ligand-centered (LC) transition at ~235 nm and to metal-to-ligand charge transfer (MLCT) character at ~355 nm. The gradual addition of ACN in a DCM solution of **48** resulted in a blue shift of the MLCT band to 340 nm at $f_{ACN} = 90\%$.

The increase in emission intensity observed when a polar solvent such as acetonitrile is added to a solution of the complexes in DCM is explained by aggregate formation due to π-stacking interactions induced by the long alkyl chains that expel the solvent molecules. This aggregation is suggested to suppress vibrational motion, resulting in the lowering of the non-radiative decay rate. AIE effects have also been observed in other Re(I) complexes such as the dendrimers reported by Burn, Samuel, and co-workers [129] or the mononuclear complexes reported in reference [130].Recent reports on other AIE-active Re(I) complexes are given in references [131, 132].

Ji and co-workers report AIE activity for a Ru(II) complex, [Ru(bpy$_2$(pzta)]$^{2+}$(ClO$_4^-$)$_2$ [bpy = 2,2-bipyridine; pzta = 6-(pyrzin2-yl)-1,3,5-triazine-2,4-diamine] (**49**), [133]. This complex (Fig. 11) has red emission under irradiation with a 365 nm UV lamp, very faint in solution but strong in the aggregated state. Gradual addition of toluene to the acetonitrilic solution of the complex did show an abrupt change in the PL intensity at $f_{toluene} = 90\%$. By comparison with the crystal structure, the strong π–π stacking and hydrogen bonding interactions were suggested to promote the formation of aggregates with 3D ordered supramolecular structures, but no hints on a possible mechanism for the observed AIE is given in the paper. Two further reports on Ru(II) compounds with AIE-activity are given in references [134, 135].

Only one Pd(II) complex has been reported to exhibit AIE. Kanbara and co-workers synthesized a thioamide-based pincer Pd(II) complex, [2,6-bis(benzylami-nothiocarbonyl-kS)phenyl-kC1]

chloropalladium(II) (**50**) where two thioamide units work as H-bonding donors while the chlorine ligand acts as an H-bonding acceptor (Fig.11). [136]. Surprisingly, the complex showed a bright emission only at low temperature (77 K) with a 65% of absolute quantum yield, while it did not show any emission in solid state, as well as in solution. Complex **50** was crystallized from solutions of four different polar solvents (DMF, NMP, DMAc, and DMSO) acting as hydrogen-bonding acceptors. The co-crystals of **50**·DMF, **50**·NMP, and **50**·2DMSO exhibited greenish-yellow emission upon excitation, while the solutions of complex **50** do not exhibit any emission at room temperature. A zigzag arrangement of the complexes in the crystal structure was suggested to be unfavourable for emission because of the loose packing of the organopalladium molecules, whereas a dense packing arrangement and the H-bonding interactions was supposed to favour AIE at room temperature by suppressing the non-radiative de-excitation channel.

The synthesis of small cyclic alkynes is extremely difficulted by the angular strain arising from the triple bonds. The introduction of a metal fragment to reduce the ring strain is an efficient strategy to stabilize such compounds used by Xia and co-workers to obtain a series of remarkable stable osmapentalyne complexes (**51**) [137] that were found to be aromatic in nature (Fig. 11). These novel metal-aromatic complexes were found to exhibit near-IR emission in aggregate and crystal state (with their large Stokes shifts (up to 320 nm) and long lifetimes (up to 1 µs) hinting towards their potential use as novel near-infrared dyes. Unlike the behaviour found for many organic aromatic compounds, osmapentalynes did not suffer from ACQ, showing instead an interesting AIE effect. The addition of a large amount of water ($f_w = 95\%$) to an ethanol solution of the complex resulted in an enhancement of the emission intensity as well as the quantum yield. Although the emission enhancement was tentatively attributed in the original work to the restriction of intramolecular rotations, vibrations and intermolecular collisions in the aggregated state, in a recent computational study [138] it is claimed that the intensity enhancement should be attributed to the formation of H- and J-type dimers.

2.2 Metal-metal interactions

Changes in the nature of the emitting state are especially frequent for the d^8 and d^{10} metal complexes, where the establishment of metallophilic interactions (such as Pt···Pt or Au···Au) [139] can significantly influence the nature of the emitting excited state in aggregated phases [140]. Of course, formation of aggregates leads in these complexes in many cases also to RIM and the final observed AIE effect is often due to a combination both causes, a metal-metal

induced RIM and the change in the nature of the emitting state. Besides an enhancement of the luminescent emission upon formation of these M···M interactions in the aggregates [141], the change in the nature of the emitting state is usually accompanied with a change in the emission colour that may be exploited in the design of chemosensors [26] or other stimuli responsive materials. These changes in the emitting state are also often related to mechanochromism [142], the change of colour induced by mechanical forces. In the following we will briefly review some illustrative examples of this type of AIE-active complexes, while the applications that have been suggested for them will be described in the next section.

2.2.1 Au (I) complexes

In 2012, Au(I)–thiolate complexes exhibiting AIE were synthesized by Xie and co-workers [143]. Non-luminescent oligomeric Au(I)–thiolate complexes in aqueous solution where found to be strongly luminescent upon aggregation, with a tunable emission both in colour and intensity (Fig. 13). This discovery was used to design highly luminescent core-shell structured Au(0)-Au(I)-thiolate nanoclusters formed by the aggregation of Au(I)-thiolate complexes and in situ generated atomic Au. The addition of a weakly polar solvent (ethanol) to the aqueous solution of the complex disrupted the hydration shell resulting in a neutralization of the charge along with aggregate formation. The formation of aggregates was described as a mixture of solvent-induced and cation-induced aggregation. Rigid and denser aggregates were obtained after addition of excess ethanol (f_e>70%) due to multiple intra- and inter complex van der Waals interactions as well as aurophilic interactions, that were suggested to block non-radiative deexcitation via RIM.
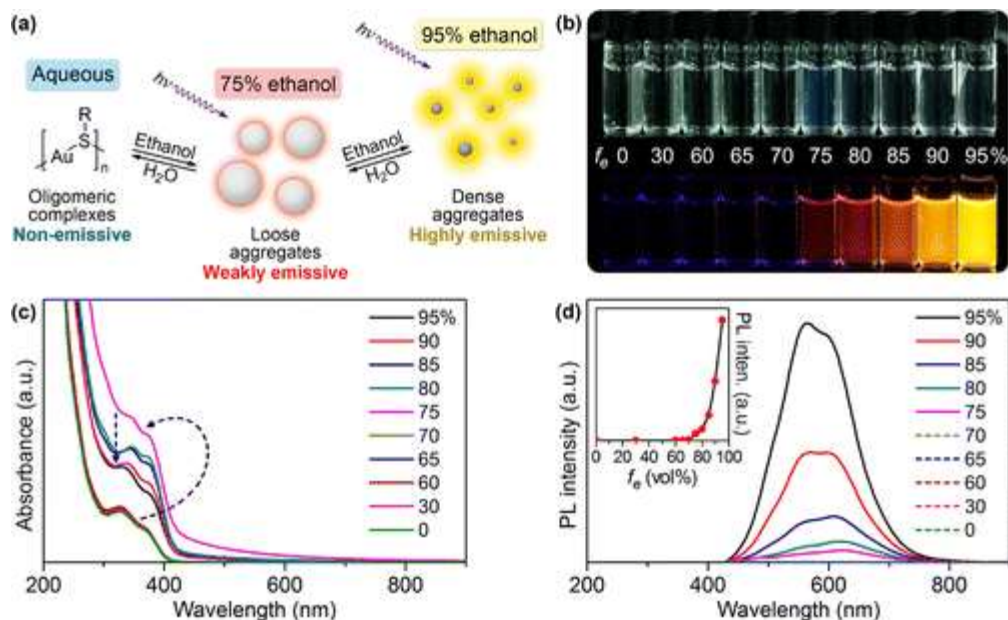
Fig. 13. (a) A Schematic illustration of solvent-induced AIE properties of the oligomeric Au(I)-thiolate complex, (b) The image of Au(I)–thiolate complex in different fractions of ethanol and water (0-95%) under visible (top row) and 365 nm UV irradiation (bottom row), (c) Absorption spectra of the of oligomeric Au(I)-thiolate complex in different ethanol-water mixtures, (d) Emission spectra of the oligomeric Au(I)-thiolate complex in different ethanol-water mixtures. Adapted from Ref. [143] with permission from American Chemical Society.

Liu's group has synthesized several mono-, di-, tri-, and tetra-nuclear gold(I) pentafluorobenzene derivatives (**52-55** and **62**) that have also been reported to exhibit AIE [141, 144] (Fig. 14). In the case of complex **52**, adding increasing amounts of water to an ethanol solution resulted in a PL enhancement with a chromaticity change from blue to yellowish-green. The observed emission maxima at $f_w = 40\%$ were the same as in ethanolic solution, while the PL intensity increased by an 80-fold factor. For higher water content the emission maxima shifted from blue to yellowish-green at $f_w = 52\%$ and the PL intensity showed a 38-fold increase with respect to the original ethanolic solution. The authors speculate that the PL intensity is enhanced due to aggregate formation and that at higher water fractions the complex formed closer packed aggregates, increasing the possibility of intermolecular gold–gold interactions that would lead to a new LMMCT excited state responsible for the observed colour change.

Tsutsumi and co-workers have reported a series of new cyclic trinuclear Au(I) complexes (**56-61**) with alkoxy side chains of various lengths that were non-emissive in solution, while some

of them were in crystalline form (Fig. 14) [145]. Out of the six complexes, they were able to obtain only three crystal structures (**56-58**) revealing that the emissive complexes had Au⋯Au short contacts in the range of 3.35 -3.38 Å, significantly shorter than 3.8 Å, the sum of van der Waals radii for two Au atoms. Thus, the same aurophilic interactions leading to molecular aggregation should be also responsible for the changes in the luminescence observed upon aggregation.

The synthesis of a new fluorene-based gold(I) complex (**62**) candidate for single-component WOLEDS, with a bright white emission in solid state as well as in thin films was reported in reference [146] (Fig. 14a). The complex exhibited interesting changes in its PL emission with the extent of aggregation, showing a bluish green colour in solution that changed to white when water was added with $f_w \geq 30\%$ (Fig. 14b-d). The formation of aggregates was confirmed by dynamic light scattering (DLS) experiments showing that the increasing percentage of water resulted in smaller size nano-aggregates (from 220 nm to 86 nm). This trend was interpreted to point towards changes in the extent of Au-Au interactions that would lead to new emission bands. The crystal packing of the complex exhibits many short non-bonded atomic distances compatible with weak π-π and intermolecular C–H⋯F interactions. The shortest Au⋯Au distances of 4 Å are, however, too long for efficient aurophilic interactions. The formation of aggregates for higher water content results in a change in emission to white light probably induced by the structural rearrangement involving both molecular non-covalent as well as the Au⋯Au interactions.

Further additional reports on AIE for Au(I) complexes can be found in references[147] [148].
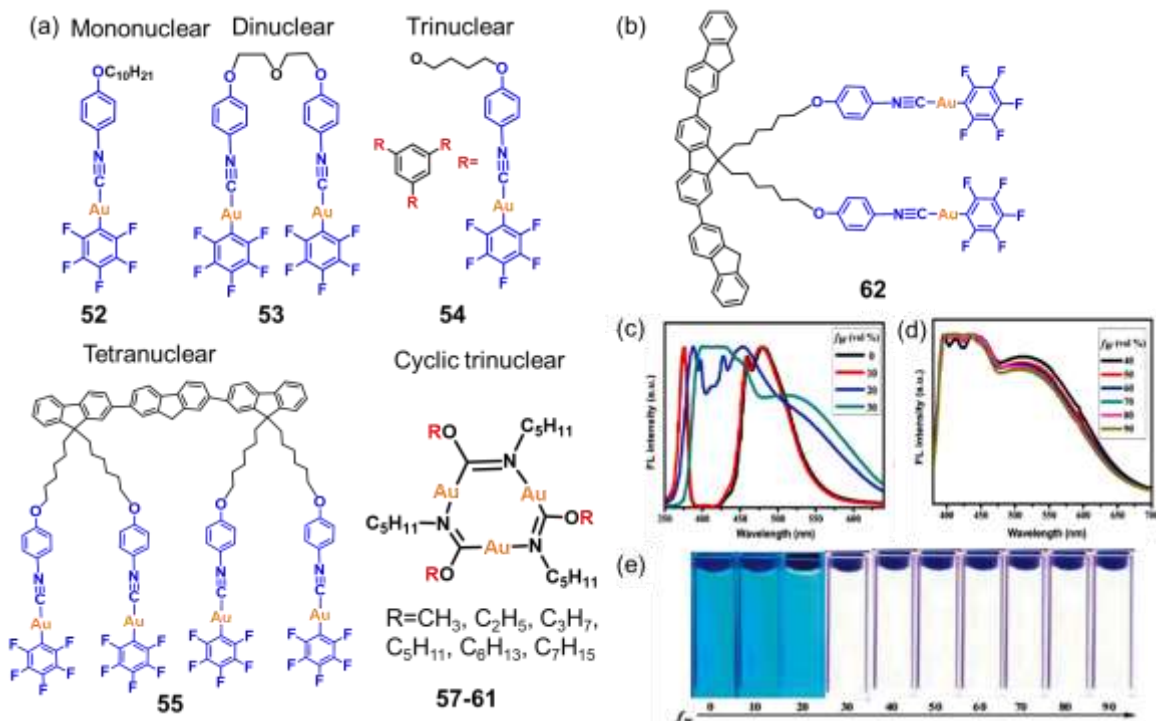
Fig. 14. (a-b) Molecular structure for different AIE-active mono-, di-, tri-, tetra-nuclear and, cyclic trinuclear Au(I) complexes (**52-62**), (c) Emission spectra of the dilute solutions of **62** (2.0 × 10⁻⁵ M) in DMF–H₂O mixtures with different volume fractions of water (0–30%) and (d) (40-90%) with λ_{exc} =365 nm, (e) Fluorescence images of **62** in different DMF-H₂O mixtures with varying water fractions under 365 nm UV irradiation. Adapted from Ref. [146] with permission from The Royal Society of Chemistry.

2.2.2 Pt (II) complexes

Luminescence of complexes with d⁸ transition metals, especially those containing Pt(II),[149] has attracted the interest of chemists since the first report on the preparation of Magnus' salt, [Pt(NH₃)₄][PtCl₄], back in 1828 [150]. Extensive optical investigations have been undertaken to understand the origin of the green colour in this complex when compared to its colourless [Pt(NH₃)₄]²⁺ and the pink [PtCl₄]²⁻ constituting ions, finding that the presence of non-covalent Pt···Pt interactions is determinant in this respect. In general, square-planar complexes of Pt(II) are able to aggregate under the effect of two types of non-covalent intermolecular interactions, namely Pt···Pt and π-π stacking interactions, that have been extensively exploited to induce changes in the photophysical properties of Pt(II) complexes upon aggregation, crystallization and exposure to vapours or mechanical stress [28, 140, 151, 152] and employed in diverse imaging applications [153], as thermochromic materials [154], or in the development of new phosphorescent organic light-emitting diodes (PHOLEDs) [155]. Recently, d⁸ transition metal

25

complexes have also shown to exhibit AIE. Some of the most relevant studies in this direction are reviewed in the following with more detail.

Chloro Pt(II) complexes with N^N^N ligands or the tpy ligand ([Pt(tpy)Cl]$^+$Cl$^-$) (**63**) (Fig. 15) were found to be non-emissive in solution. The authors speculated that this could be due to an efficient radiationless decay via a low-lying triplet state [156]. The photo physical properties of these complexes can be changed simply by modifying the environment in presence of oppositely charged polyelectrolytes, block copolymers, or formation of micelle-like aggregates, leading to a remarkable emission enhancement.

Two novel luminescent Pt(II) complexes of terpyridyl ligands,[Pt(tpy)(C≡C-C≡CH)]OTf (**64**) and [Pt(^{t}Bu$_3$-tpy)(C≡C-C≡CH)]OTf (**65**) (where tpy =6',2''-terpyridine and ^{t}Bu$_3$-tpy= 4,4',4''-tri-*tert*-butyl-2,2': 6',2''-terpyridine) were reported by Yam and co-workers (Fig. 15a) [157]. Complex **64** exhibited polymorphism, a dark-green and a red form, both of which have been structurally characterized by X-ray diffraction analysis and found to exhibit crystal-packing arrangements involving different intermolecular interactions. Short Pt···Pt distances in the range 3.4 - 3.7 Å were found in the crystals of complex **64**, but not in those of complex **65**. The emission and absorption spectra for **64** were recorded with varying diethylether fractions in acetone, resulting in an emission enhancement at λ_{max} 785 nm (arising from states with a ^{3}MMLCT character) (Fig. 15b-c). The absorption spectra with isosbestic points suggested a clean conversion of monomeric **64** to another species (Fig. 15c). A drastic change in colour from green to blue in acetone solutions was also observed for complex **64** after addition of diethyl ether, while complex **65** did not show such type of behaviour (Fig. 15d). According to the authors, aggregation resulting from direct metal-metal and π-π stacking interactions leads in this case to this special type of solvatochromism and emission enhancement.
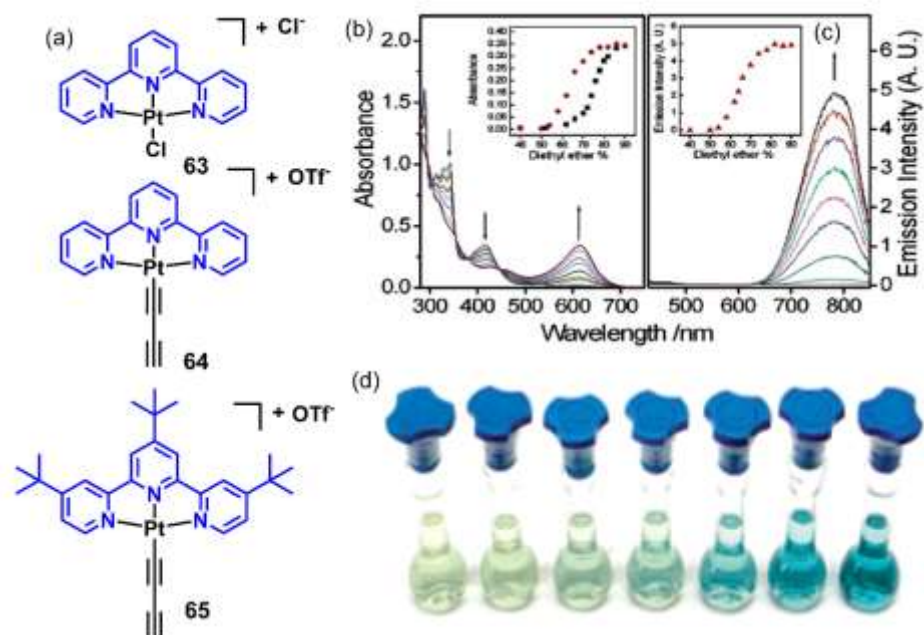
Fig. 15. (a) Chemical structure of complexes **63, 64** and **65**, (b) UV-Vis absorption changes of complex **64** in acetonitrile with increasing diethyl ether content. Inset: Plot of absorbance vs. diethyl ether composition in acetonitrile at 615 nm and in acetone at 610 nm, (c) Emission enhancement of **64** in acetone upon increasing diethyl ether content. Inset: Plot of corrected emission intensity as a function of diethyl ether composition, (d) Photograph showing the change in solution colour of complex **64** after addition of different volumes of diethyl ether in acetonitrile in the ratios, from left to right, of 64, 68, 72, 74, 76, 78, 80%. Reprinted from ref. [157] with permission from The American Chemical Society.

Connick and co-workers reported that salts of the [Pt(Me$_2$bzimpy)Cl]$^+$ complex with two different counter ions, Cl$^-$ and PF$_6^-$ (**66**) (Fig. 16a), changed their colour upon exposure to volatile solvents [158]. The chloride salt was found to change its colour from yellow to red within seconds upon exposure to methanol, chloroform, ethanol, or acetonitrile vapours, while exposures to other solvents were not having any impact on its photophysical properties (Fig. 16b). In contrast, a colour change from yellow to violet was observed for the PF$_6^-$ salt only in the case of exposure to acetonitrile vapour. For either salt, leaving vapour-exposed samples in air for several days, or heating them for several minutes restored the original colour and the vapochromic response was found to be fully reversible.

The mechanistic details of this response are not clear. The available evidence is consistent with an enhancement of intermolecular interactions leading to a decrease in Pt···Pt separation upon

27

vapour sorption, possibly resulting in a change in the orbital character of the lowest emissive state (^{3}MMLCT). Additionally, upon increasing the complex concentration in EtOH-MeOH glassy solutions the emission intensity was strongly enhanced because of aggregate formation (Fig.16 c).
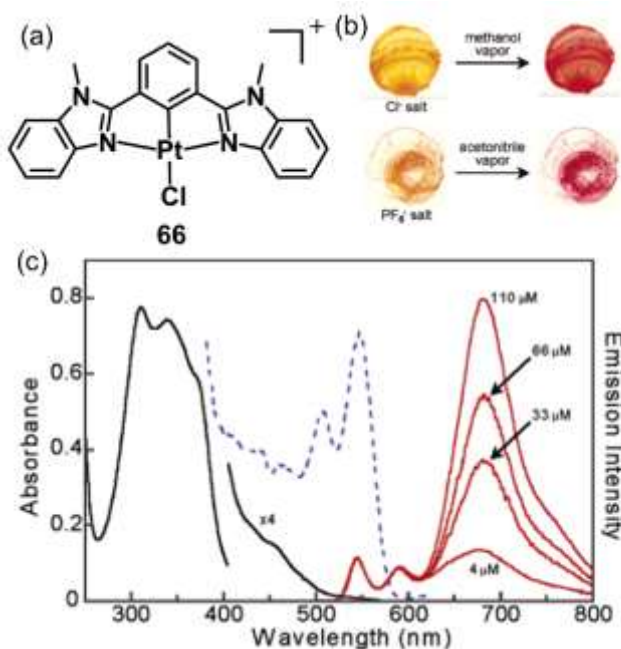

Fig. 16. (a) Chemical structure of complex **66**, (b) Response to methanol and acetonitrile vapours of complexes **66** (Cl)$^-$ and **66** (PF$_6$)$^-$, respectively, (c) UV-visible absorption spectrum of **66** (Cl)$^-$ 2.5H$_2$O in room-temperature methanol solution (black lines), and 77 K 4:1 EtOH-MeOH glassy solution emission (λ_{ex} = 400 nm; red lines) and excitation (λ_{em} = 670 nm; blue lines) spectra. Emission spectra are normalized at 545 nm. Adapted from ref. [158] with permission from The American Chemical Society.

An insignificant change in the coordination sphere and the microenvironment of the terpyridyl–Pt(II)–acetylide complex can lead to remarkable changes in both its supramolecular structure and spectroscopic properties. Based on this observation, a series of mono and binuclear organo Pt(II) complexes (**67-75**) (Fig. 17), [(^{t}Bu$_3$tpy)Pt(C≡C-1,2-C$_6$H$_4$)$_n$-C≡C-Pt(^{t}Bu$_3$tpy)][ClO$_4$]$_2$ (**67–73**, n=1, 2, 3, 4, 5, 6, 8; ^{t}Bu$_3$tpy =4,4',4''-tri-tert-butyl-2, 2': 6', 2''-terpyridine) with foldable oligo(orthophenyleneethynylene) linkers were synthesized by Che and co-workers (Fig. 17a) [159]. The low-energy absorption band of **73** was found to follow Beer-Lambert's law in the

concentration range of 10^{-4} to 10^{-5} mol L^{-1} in CH_3CN, suggesting the absence of significant aggregation in these conditions. All complexes exhibited emission in degassed solutions, in CH_3OH/CH_3CH_2OH (v/v=1:4) glassy solutions, as well as in solid state at 77 K, with lifetimes in the microsecond range and efficiencies in the range of (0.2-5.9%). The gradual increment of water in ACN solutions of complexes **69-73** resulted in a PL enhancement with a red shifted emission for **69-73.** The emission maxima of complex **71** showed red shifted emission from 567 to 670 nm in aerated H_2O/CH_3CN (Fig. 17b). The absorption spectrum showed a sharp decrease at λ=350 nm and increase in low energy absorption band at 500 nm (Fig. 17c), while complexes **67** and **68** were not showing any promising AIE. For complex **75** experiments showed the same trends as for **69-73**, *i.e.* enhanced red-shifted emission, while complex **74** showed an ACQ effect after increasing the water fraction (**74** has no angular ortho-PE ligand). Aggregate formation was confirmed by DLS and TEM images. The red shifted emission spectra in water-ACN mixtures for **69-73** and **75** are believed to have their origin in the intramolecular interactions between the [Pt($^tBu_3$tpy)] planes and the bridging ortho-PE(n) ligands. Structural data obtained from X-ray diffraction for **69-73** show that they have the same molecular interactions as complex **67** but that **69-73** can fold easily and experience additional intramolecular π-π interactions because of the ortho-PE(n) (n$\geq$ 3) chains. Hence, the aggregate formation results in a considerable RIM.

(a)

n= 1 (67), 2 (68), 3 (69), 4 (70),
5 (71), 6 (72), 8 (73)
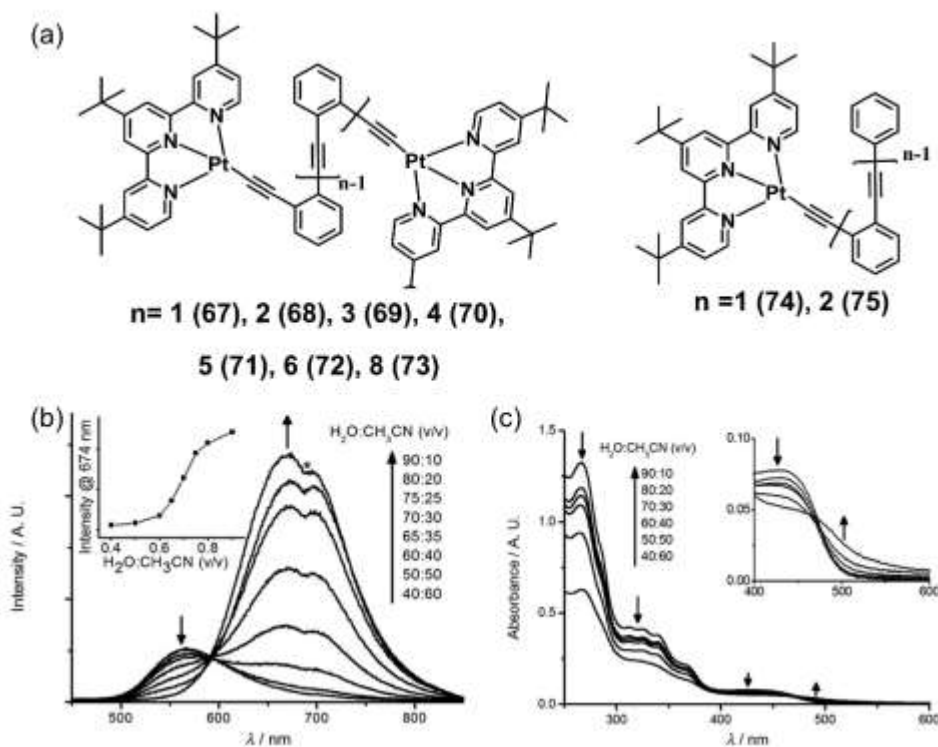
n =1 (74), 2 (75)

(b)

(c)

Fig. 17. (a) Molecular structures of complexes **67-75**. Spectra for **71** in aerated H_2O/CH_3CN mixtures upon increasing the water fraction (f_w = 40-90%), **(b)** Emission spectra (λ_{ex}=350 nm) with the inset showing the plot of emission intensity at 674 nm against water fraction, **(c)** UV/Vis absorption spectra with the inset showing the enlarged 400–600 nm region. Adapted from ref. [159]. Reprinted with permission from WILEY-VCH.

In a 2009 paper, Che and co-workers described a simple preparation of supramolecular polymers with chromonic liquid crystallinity by self-organization of cationic Pt(II) complexes in water through Pt-Pt and hydrophobic interactions (Fig. 18a) [160]. The influence of aggregation on the absorption and PL spectra of these complexes (**76-82**) was studied in water/MeOH solutions (Fig.18b-c). The methanolic solution of complexes **76** and **80** shows vibronically structured high-energy emission peaks with maxima at 525 and 480 nm, respectively. A red shifted emission with increasing water concentration was observed for these peaks. Additionally, the emission colour of complex **80** gradually changed from green to red with increasing water fractions (Fig.18c). In pure water, the emission maxima were found to be at 677 and 655 nm, respectively. Conversely, no emission was observed in water for complex **82** at 298 K. A mixture of ^{3}MLCT/^{3}ILCT excited states could be assigned for the high-energy emission band in methanolic solution, while the ^{3}MMLCT excited state seems to be responsible for the low-energy emission band in aqueous solutions. The aggregate formation in water is suggested to be induced by Pt(II)$\cdots$Pt(II) interactions. More related work of Che's group can be found in references [152, 161-164].
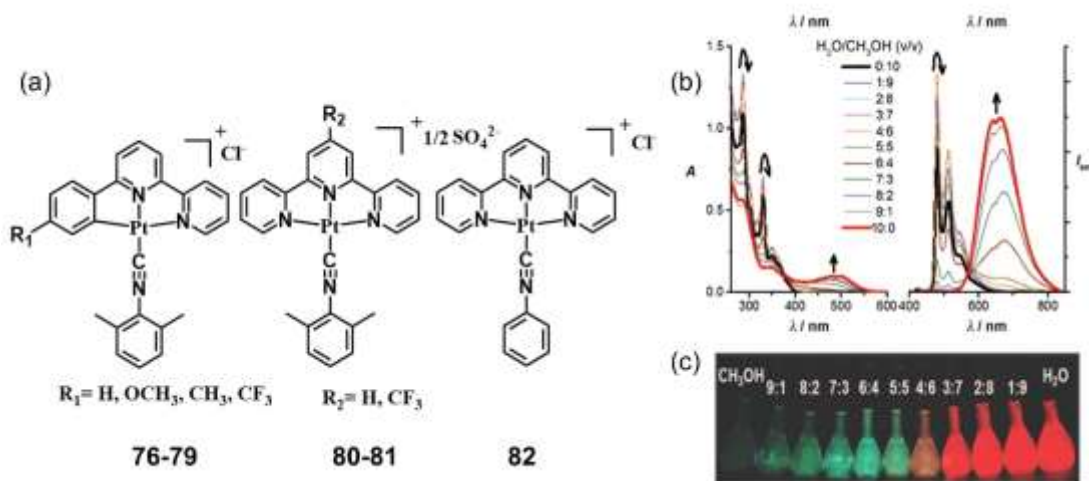
Fig. 18. (a) Molecular structure of complexes **76-82**, (b) UV/Vis absorption (left) and emission (right) (λ_{ex} = 370 nm) spectra at 298 K for complex **80** using H_2O/CH_3OH mixtures upon increasing the water percentage from 0 to 100%, (c) Photograph of the sample series of complex **80** under a 365 nm UV lamp. Adapted from ref. [160]. Reprinted with permission from WILEY-VCH.

Since supramolecular gels provide fibrous aggregates with long-range order, they could be of interest in the fields of optoelectronic devices and sensors. In this context, transition metal based gelators can display metal–metal interactions that influence their photophysical properties. The synthesis of a 2, 6-bis(tetrazolyl)pyridine complex (**83**) with alkyl pyridine as an ancillary ligand (Fig. 19) [165] that is able to self-assemble into bright nanofibers was reported in 2011 by De Cola's group. Complex **83** showed a strong luminescence in a frozen CH_2Cl_2 matrix at 77 K, as well as in thin films, while it was non-emissive in solution. The photoluminescence quantum yield was found to be up to 87% in thin films, with concentration independent colour and efficiency. The observed changes in the PLQY and the emission properties from solution to solid state were attributed to the aggregation process, facilitated by $Pt \cdots Pt$ intermolecular interactions that were suggested to generate a new, lowered energy, ^{3}MMLCT state. Finally, the bright luminescence upon aggregation could be used to monitor the assembling process with a high sensitivity (Fig. 19).
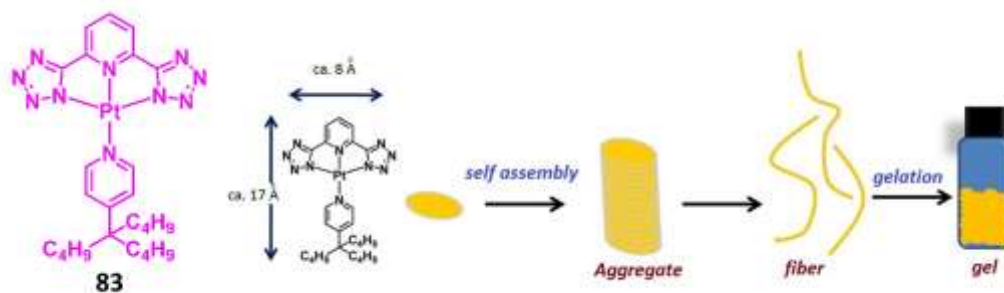
Fig. 19. Molecular structure of complex **83** and a representation of the self-assembly process, going from luminescent aggregates to fibres and gels. Adapted from ref. [165] with permission from WILEY-VCH.

Naota and co-workers investigated bis(salicylaldiminato) Pt(II) complexes (**84-92**) that were found to be strongly emissive in solid state, but not in solution (Fig. 20), finding that the solid-state quantum efficiency could be controlled with varying the length of the linker [166]. Complexes **88** and **90,** with dodeca- and tridecamethylene linkers showed a high efficiency in solid state, while **85-87**, with short linkers, were found to be non-emissive between 77 K and 298 K. The strongly bent coordination sites found in the crystal structures of these complexes were suggested to favour energy loss through non-radiative pathways.

Dimeric arrays with strong Pt···Pt interactions and a planar coordination geometry were found in the case of **88**, **89**, and **92**. Additionally, an intermolecular H-bonding network through neighbouring PEG units was found in case of **92**. These interactions (Pt···Pt and H-bonding) were suggested to suppress the mobility in the aggregate/solid state, leading to the observed strong phosphorescence. These researchers have shown in another paper that instant and precise control of phosphorescent emission can be performed by ultrasound-induced gelation of organic liquids with chiral, clothespin-shaped trans-bis(salicylaldiminato)Pt(II) complexes [167]. According to their findings, emission from the gels can be controlled by sonication time, linker length, and optical activity of the complexes.
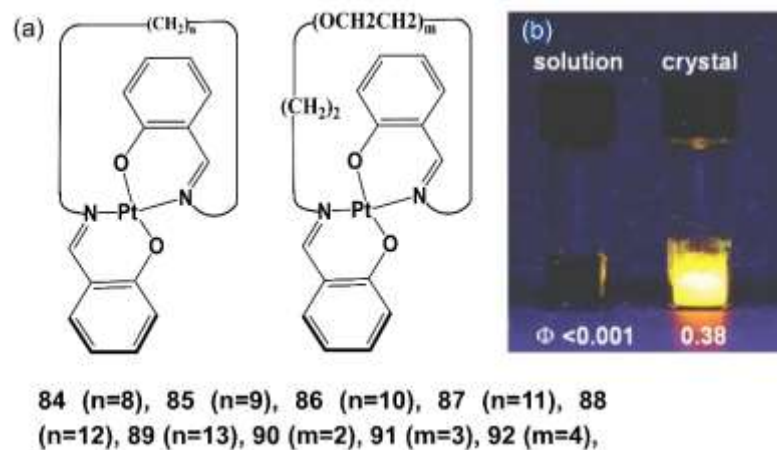
Fig. 20. (a) Molecular structure of complexes **84-92**, (b) Photograph of complex **92** in solution and crystalline states at 298 K under UV illumination (λ_{ex} = 365 nm). Adapted from ref. [166] with permission from The American Chemical Society.

In 2013, novel dinuclear alkynyl Pt(II) terpyridine complexes having an amphiphilic binaphthol bridge with two triethylene glycol monomethyl ether (TEG) chains (**93-95**) were synthesized by Leung and Yam (Fig. 21) [168]. Interestingly, for complexes **94** and **95** with hydrophilic chains of triethylene glycol monomethyl ether, a helical conformation was confirmed from the CD spectra measurement of their aqueous solution.

The UV-Vis absorption spectra of ACN solutions of complexes **94** and **95** showed a significant drop of the absorbance in the high-energy region (284-337 nm) upon gradual addition of water, which was attributed to intraligand (IL) (π -π* transitions) between the terpyridine and alkynyl ligands. A slight drop was also observed for the low-energy absorption at 449–457 nm. These results revealed that complexes **94** and **95** can undergo self-assembly through π–π stacking interactions with increasing water concentration. The addition of water to an ACN solution of complex (***rac***)-**94** leads to aggregate formation into hierarchical helices of helices, requiring a tight stabilization of the helical strands. The aggregates contain stacked helices resulting from inter- and intramolecular Pt···Pt and π–π stacking interactions. With increasing water fraction PL enhancement of the ^{3}MMLCT band was observed which further became more intense in the presence of higher water fractions (Fig. 21b-d).

The presence of supramolecular self-assembly for complex **94** in water-ACN mixtures was studied by using resonance light scattering (RLS) experiments. Increasing the water content

resulted in the enhancement of the RLS signals, indicating the formation of larger sized aggregates in the solution medium.
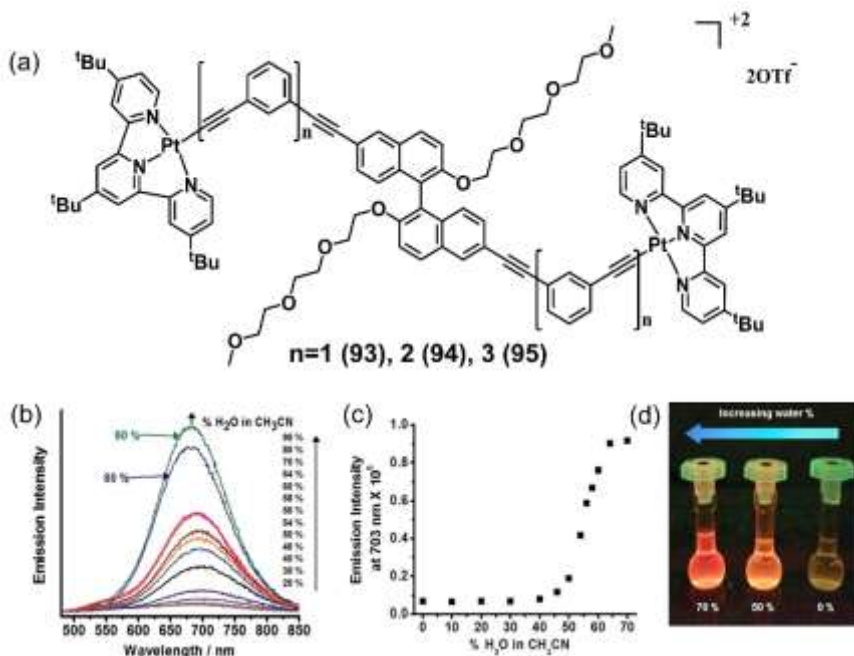

Fig. 21. (a) Molecular structure of complexes **93-95**, (b) Emission spectra of complex (rac)-**94** in CH_3CN (1.7×10^{-5} M) with increasing H_2O content from 20 to 70% at 298 K, (c) Plot of the CD intensity at 703 nm as a function of solvent compositions, (d) Photograph of complex (rac)-**94** in 0, 50 and 70% H_2O in CH_3CN under UV light irradiation (350 nm; in air). Adapted from ref. [168] with permission from The Royal Society of Chemistry.

In 2014, Bu and co-workers synthesized three chloro Pt(II) complexes (**96-98**) of 2,6-bis(benzimidazol-2'-yl)-pyridine bearing hexaethylene glycol methyl ether (HEME) , that were found to be non-emissive in dilute aqueous solution (Fig. 22a). [169]. The HEME group was strategically introduced into the complex to get a better solubility in water as well as 1-butyl-3-methylimidazolium hexafluorophosphate ($BMIMPF_6$), a typical ionic liquid. A remarkable PL enhancement was observed upon addition of hexafluorophosphate salts to these solutions (Fig. 22b-c). The low energy band (545 nm) in the UV spectra of complex **98** revealed the existence of a MMLCT transition (Fig. 23)., indicative of strong Pt···Pt and π–π stacking interactions. The addition of 0.5 wt% $BMIMPF_6$ to a dilute aqueous solution of **97** resulted in an immediate colour change, from light-yellow to red. The broad absorption band at 300–390 nm dropped

significantly in intensity, and new absorption bands that were attributed to [3]MMLCT transitions appeared at 536 and 571 nm. In case of complexes **96** and **98** the appearance of the [3]MMLCT band was not observed. Increasing the concentration of BMIMPF$_6$ lead to a PL enhancement. Aggregate formation in aqueous solutions containing 0.5 wt% BMIMPF$_6$, supported by DLS and TEM images, is due to strong Pt⋯Pt and π–π stacking interactions. Addition of other hexafluoro-phosphate salts (TMAPF$_6$, NH$_4$PF$_6$ and KPF$_6$ (TMA = tetramethylammonium) to the dilute aqueous solutions resulted also in remarkable PL enhancement, while the addition of NaClO$_4$ and NaBF$_4$ did not have much influence on the PL intensity. Finally, based on the observation that due to the presence of the common ion effect complex **98** became insoluble (aggregated) in presence of the hydrophobic PF$_6^-$ anion and this led to emission enhancement, **98** was successfully used for PF$_6^-$ detection. More recent reports on AIE for Pt(II) complexes may be found in references [170-173].
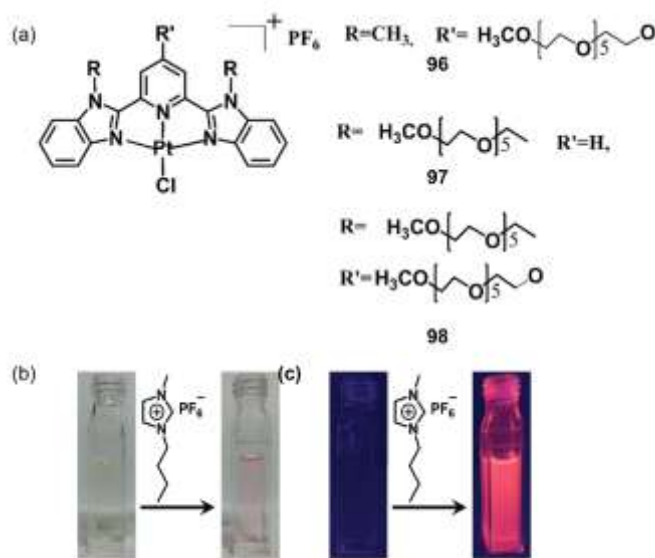

Fig. 22. (a) Molecular structure of complexes **96-98**; Photographs of **98** taken under, (b) Sunlight and, (c) UV irradiation at 365 nm before and after addition of 0.5 wt% BMIMPF$_6$. Adapted from ref. [169] with permission from The Royal Society of Chemistry.
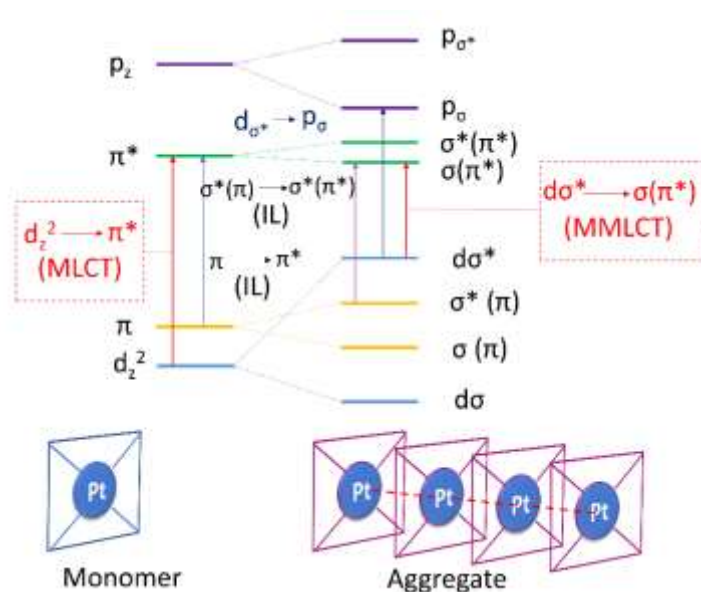
Fig. 23. Schematic representation of metal-metal interactions for a square planar d^8 metal complex leading to the formation of a MMLCT state.

2.3 Other possible mechanisms

According to Huang and his team, the formation of ^{3}MMLCT states and the hindered motion of a complex in the aggregated state cannot always explain the origin of the observed AIE. In their study, they claim that the mechanism for AIE in transition-metal complexes is more complex than that of the relatively simple organic molecules and to sustain this affirmation they present a series of Pt(II) complexes Pt(ppy)(LX), Pt(dfppy)(LX) and Pt(fiq)(LX) (**99–105)** (Fig. 24) [174] where ppy=2-phenylpyridine, dfpp=2-(2,4-difluoro-phenyl)pyridine, fiq =1-(9,9-dioctylfluoren-2-yl)isoquinoline, and LX =2-(phenyliminomethyl)-phenol (L1), 2-(naphthyliminomethyl)-phenol (L2) or 2-(propyliminomethyl)-phenol (L3) that were all found to be AIE-active. Surprisingly, a small change in the LX ligand in complexes **106-107**, where LX is 1-((phenylimino) methyl)naphthalen-2-ol, (L4) **)** (Fig. 24a), suppressed the AIE behaviour. The AIE for these complexes was studied using THF-water mixtures and tunable emission colours in crystal samples (yellow to red) were achieved.

These observations disagree with the widespread idea that internal motion is the cause for the non-emissive nature of the complexes in solution since compounds **101** and **104**, without mobile phenyl or naphthyl groups were showing the same behaviour as the rest of compounds. In a computational study, the HOMO and LUMO for these complexes were found to be mainly located on Pt and the N^O ligand and not over the ppy ligand as usual in this type of complexes,

and it was suggested that the participation of the N^O ligand and the structural distortion of the chelating six-membered cycle between Pt and the N^O ligand in the T_1 state would be responsible for the non-emissive nature of these complexes. An analysis of the crystal structures revealed also that there are no relevant Pt⋯Pt interactions present in the solid state, ruling out the possibility of a ^{3}MMLCT state. To understand the origin of AIE in this case, the structure was optimized using DFT calculations simulating the crystal state where the LUMO for complexes **99-102** was found to be localized on both the ppy and the N^O ligands, while the HOMO was localized on the ppy, the N^O ligand, and the Pt atom, predicting a strong emission in the solid state. Surprisingly, the LUMO for complex **107** was found to be localized mainly on the N^O ligand, making it non-emissive in the solid state. Based on the above findings, a restricted structural distortion in the excited state (RSDE) was suggested as a possible AIE mechanism in this case (Fig. 24b).

Fig. 24. (a) Molecular structure of complexes (**99-105**) (AIE-active) and (**106, 107**) (AIE-inactive), (b) Calculated geometries and molecular orbitals of complex **99** in different states. Adapted from ref. [174] with permission from The Royal Society of Chemistry.

Cowley et al. studied the photophysical properties of four bis(imino)acenaphthene zinc complexes [(BIAN Zn(II)] (**108-111**) with methylated aryl substituents (Fig. 25a) [175, 176]. All reported complexes are non-emissive in solution while only **108** and **109** were found to emit in the solid-state. The AIE experiment for these complexes was carried out with a DCM-hexane

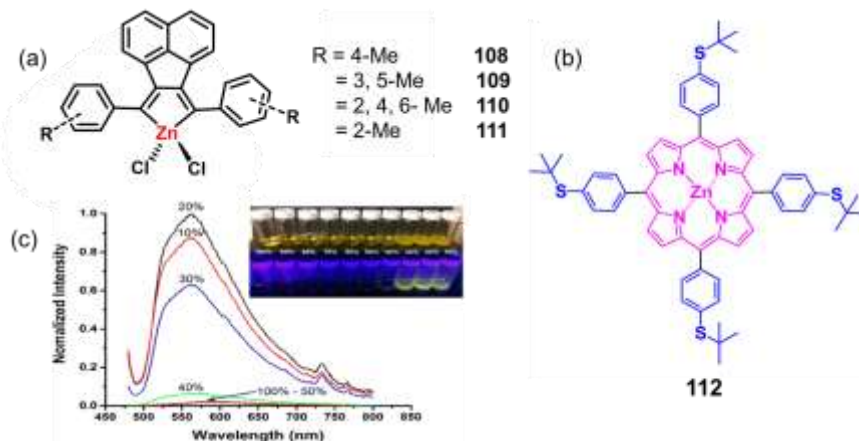mixture and the PL spectra of **108** showed a maximum enhancement in 20% DCM-hexane mixture (Fig. 25c).

Fig. 25. (a) Molecular structure of complexes **108-111**; (b) **112**; and (c) The emission spectra of **108** in different fractions of DCM-Hexane mixtures ($f_H = 0$-90%). Inset image (top) photograph complex **108** under daylight and (bottom) under 365 nm UV light. Adapted from ref. [176] with permission from American Chemical Society.

The emissive vs. non-emissive behaviour of these complexes in the solid state could be nicely correlated to differences in molecular structures and crystal-packing motifs. The average acenaphthene-aryl inter planar torsional angles in the emissive complexes **108** and **109** were 59° and 70°, respectively, while significantly larger torsion angles, 80° and 82°, were found for **110** and **111**. For the emitting complexes, **108** and **109**, strong $\pi-\pi$ stacking interactions are clearly evident in the crystal structures, resulting in a head-to-tail arrangement of two naphthalene units for **108** and a displaced $\pi-\pi$ stacking motif along with two other Bis(imino)acenaphthene (BIAN) complexes that flank this arrangement in an orthogonal manner for **109**. On the other hand, the difference in the torsional angles resulted in a less dense crystal packing for **110** and **111**. In the cases of **108** and **109**, the strong $\pi-\pi$ stacking leading to excimer formation is suggested to be responsible for the emission enhancement. TD-DFT based calculations for $\pi-\pi$ stacked dimers were presented to further substantiate this hypothesis.

In 2014, Yang and co-workers synthesized a novel porphyrin based Zn(II) complex (Zn-TSPP) **(112)** with TSPP = 5, 10, 15, 20-tetra-4′-(tert-butylthio)phenylporphyrin that was found to exhibit AIE (Fig. 25b)[177], with addition of water to THF solutions greatly enhancing the emission intensity. The absorbance spectra of Zn-TSPP showed a red shift in the Soret bands

after addition of water, confirming the formation of J-aggregates where the molecules arrange in an edge-to-edge orientation. The bulky tertiary butyl groups where suggested to block π–π stacking interactions favouring the formation of J-aggregates.

3 Applications of AIE metal complexes

3.1 Stimuli responsive AIE complexes

Stimuli-responsive luminescent materials are highly desirable for different applications such as sensors, memory storage, security inks, and biological or healthcare uses. Since in many AIE-active complexes a slight disturbance in molecular packing may lead to measurable changes in the PL emission, they are especially well suited as stimuli-responsible materials. If the emission intensity, colour or quantum yield of the complex change in the presence of external stimuli such as heat, exposure to a vapour, or mechanical forces (including shearing, crushing, grinding, stretching, and hydrostatic pressure) one speaks about thermo-, vapo- or mechanoresponsive luminescent materials, respectively. In this section we will briefly describe some of the applications of AIE systems as stimuli responsive materials that have been proposed in the literature.

3.1.1 Mechanochromic AIE complexes

An AIE-active complex, [Ir(bipy)(PPh$_3$)$_2$)(H$_2$)]Cl [**9(Cl⁻)**], developed by our group was found to exhibit mechano- as well as vapochromism (Fig. 26). The emission colour in solid-state samples changed from green (λ_{max} = 519 nm) to faint yellow (λ_{max} = 548 nm) after exposure to DCM or chloroform [101]. The mechanochromic behaviour of this complex was demonstrated by grinding its yellow form and observing a change to the green one. Applying pressure to the yellow form did, however, not change the emission colour, indicative that it is a shearing force that leads to the colour change. Further, a sample of the yellow complex was coated on filter paper and the word "BITS" was written with the help of a capillary loaded with acetone. A bright green emission was observed because of solvent/vapour induced recrystallization that was confirmed by thermogravimetric analysis (TGA), which showed a loss of one molecule of DCM. The experimental data support that the green form of the complex, with a crystalline nature, was converted into the yellow amorphous form upon exposure to DCM or chloroform vapours by intermolecular interactions of the solvent molecules with the complex.

Fig. 26. (a) Molecular structure of complex of **9 (Cl⁻)** and picture of a filter paper coated with the complex where the word 'BITS' was written by using a capillary tube loaded with acetone, (b) Colour change of complex **9 (Cl⁻)** after mechanochromic and vapochromic response. Adapted from ref. [101] with permission from the American Chemical Society.

Complex **113** (Fig. 27) was found to be non-emissive in common organic solvents, but strongly emissive in the solid state [102]. The complex was found to exhibit a reversible piezochromic luminescent (PCL) behaviour. In powder form, the complex emitted a yellow luminescence that was changed to an orange emission after grinding. The PCL behaviour of the complex was explained based on NMR spectroscopy, differential scanning calorimetry (DSC) and powder X-ray diffraction (PXRD). The PXRD data revealed that a phase change (crystalline to amorphous) upon grinding was responsible for this abnormal PCL behaviour.
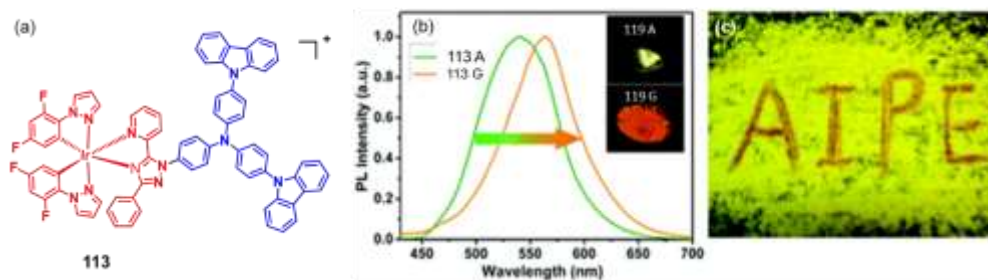

Fig. 27. (a) Molecular structure of complex **113**, (b) Emission spectra of the samples **113A** (as-prepared powder) and **113G** (ground orange-emitting powder), (c) The powder **113A** was cast on the filter paper and the letters "AIPE" were written with a spatula under UV light at room temperature. Adapted from ref. [102] with permission from The Royal Society of Chemistry.

Inspired by their previous work, Su and co-workers, synthesized three multifunctional cationic Ir(III)-based materials with AIE and PCL behaviour in a controlled manner by simply adjusting the substitution on the ancillary ligands [178]. In this report, the same cyclometalated ligands were kept and different substitutions were introduced to modify the ancillary ligand (Fig. 28). The strategic design of the ligands resulted in controlled properties and complex **114** turned out to be a PCL material, complex **115** an AIE material, while complex **16**, which has already been mentioned above, exhibited a combined PCL and AIE behaviour. DFT based calculations showed that complex **114** has a predominant ^{3}MLCT and ^{3}LLCT character while an ^{3}ILCT excited-state was predicted for compounds **115** and **16**. The PCL behaviour of **114** and **115** was attributed to crystalline–amorphous phase transformation by carefully analysing experimental data. Probably due to the presence of the terminal tert-butyl groups, complex **16** was found to be always amorphous. Its blue emitting powder changed to green emission after smearing and this green colour changed immediately to blue with a thermal stimulus (180 ^{0}C for 1 minute) and finally, exposure to DCM converted the blue and green colours to a dark colour that reverts to the blue colour after heating, showing the reversible nature of these changes (Fig. 28b).
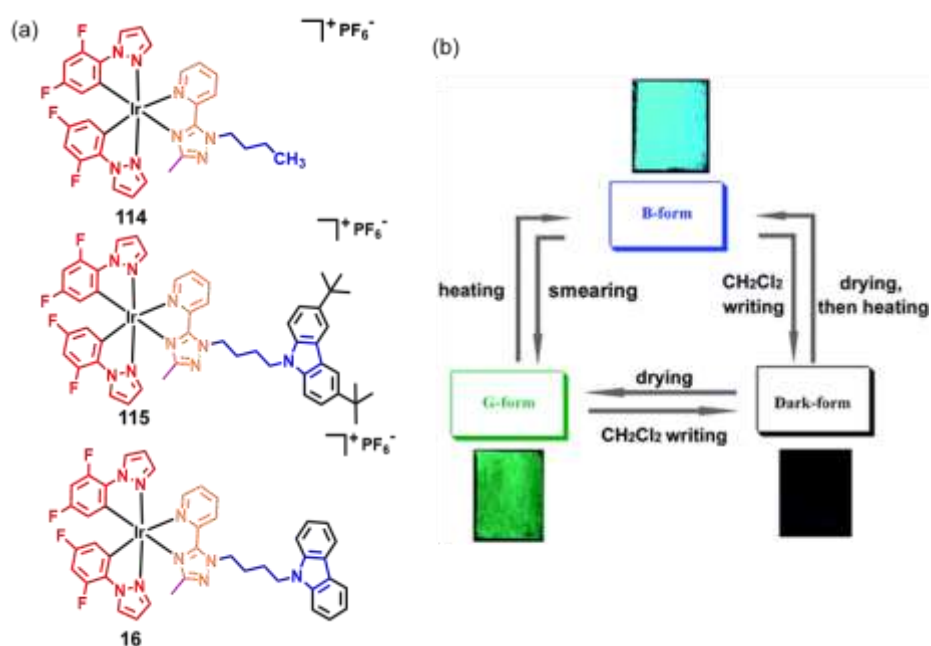

Fig. 28. (a) Molecular structure of complexes **114-115** and **16**, (b) Illustration of the multi-channel photoluminescent colour changes of complex **16**. Adapted from ref. [178] with permission from The Royal Society of Chemistry.

Recently, two heteroleptic cationic Ir(III) complexes $[(X)_2Ir(L_2)]^+PF_6^-$ where L_2 = 3,6-di-tert-butyl-9-(4-(4,5-dimethyl-2-(pyridin-2-yl)-1H-imidazol-1-yl)butyl)-9H-carbazole, X = difluorophenylpyridine (dfppy) (**116**), dimethylphenylpyridine (dmppy) (**117**), were designed and synthesized [62]. These two complexes were found to be AIE-active with a fluorescence–phosphorescence dual-emission. A pressure induced emission colour change was observed for **117** where the emission changed from green to yellow after grinding using a pestle. The green colour was fully recovered after exposure of CH_2Cl_2 atmosphere for about 30 min. These changes were attributed to piezochromic and vapochromic properties and were further supported by PXRD analysis. The green emissive complex shows intense and sharp reflection peaks that change to weak and broad peaks after grinding and changing its colour to yellow (Fig.29).
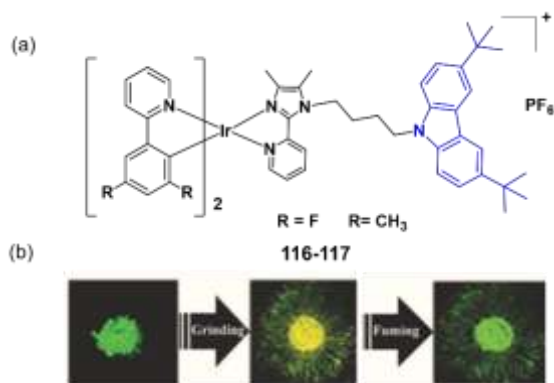
Fig. 29. (a) Molecular structure of complexes **116** and **117,** (b) Photographs obtained under UV light at 365 nm showing the effects of reversible grinding–fuming on a sample of complex **117.** Adapted from ref. [62] with permission from The Royal Society of Chemistry.

The synthesis of new Au(I) complexes based on the donor-acceptor (D-A) model **(118-120),** containing iso-cyanobenzene as the bridge (electron-acceptor) and C_6F_5–Au groups (electron-donors) (Fig. 30a) was reported by Liang et al. in 2014 [179]. The AIE of these complexes was investigated using mixtures of different solvents, tetrahydrofuran (THF), acetonitrile, acetone, dimethylformamide (DMF) and dimethylsulfoxide (DMSO) with water. A colour change from blue to yellow was observed at f_w = 60% for complex **118**. The change in the emission spectra

with respect to the polarity of solvents with increasing f_w was explained considering an intramolecular charge transfer (ICT) process, which is a common phenomenon for D-A systems. The emission colour of the complex **118** also switched between a dark (weak blue) and bright (greenish blue) state as a response to external stimuli (pressing and annealing) (Fig. 30b-g). The weak PL of an unground solid sample was intensified after grinding.

A plausible mechanism for the reversible mechanoluminescence process was suggested based on PRXD data. The unground sample showed many sharp, intense peaks which turned into weak and less defined ones after grinding, indicating a crystalline-to-metastable phase conversion. However, the intense peaks were recovered after annealing or exposure to DCM, revealing a reversible mechanoluminiscent behaviour. The authors concluded that weak π–π and intermolecular C–H···F interactions in the crystalline phase prevent the establishment of aurophilic interactions and after exposing a sample to external stimuli, these C-H···F interactions may weaken, allowing the formation of Au···Au interactions that would switch the emission on.
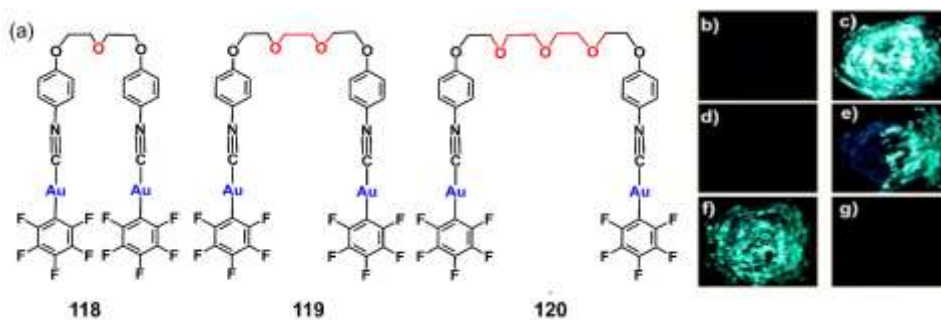
Fig. 30. (a) Molecular structure of complexes **118-120**. Photographs showing a powder sample of complex **118** under 365 nm UV light, (b) Before grinding, (c) After grinding, (d) After treatment with dichloromethane, (e) and (f) Repetition of the green emission by grinding the powder with a pestle at room temperature, (g) Annealing (at 100 ^{0}C for 30 s). Adapted from ref. [179] with permission from The Royal Society of Chemistry.

In 2015, Liu and co-workers synthesized a diisocyano-based dinuclear gold(I) complex **(121)** that resulted to be an AIE-active metal-bearing luminogen with switchable mechanochromic characteristics (Fig. 31) [180] . The AIE features were studied for mixed DMF-water solutions. In a similar fashion to compounds from a previous report [179], these complexes exhibited also a reversible mechano-luminescent behaviour. The complex, with two emission bands at 490 nm

and 523 nm, after grinding showed a new emission band at 559 nm (yellow) (Fig. 31b-c). This change, which is reversible in nature, was interpreted in similar terms as in the previous report, i.e. due to a crystalline to amorphous phase conversion. In general, the absolute fluorescence quantum efficiency for solid-state samples was found to be around 7%, but it increased to 41% in well crystallized samples, a clear example of crystallization induced emission enhancement (CIEE).
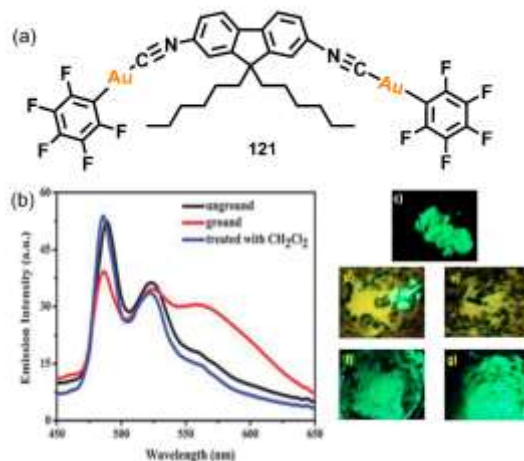

Fig. 31. (a) Molecular structure of complex **121**, (b) PL spectra of complex **121** before grinding, after grinding and after DCM exposure; Photographs showing, (c) The original sample, (d) The partially ground sample, (e) The entirely ground sample, (f) The change in emission colour after DCM exposure (g) The effect of annealing at 100 ^{0}C for 30 s. All the above images have been taken under 365 nm UV irradiation. Adapted from ref. [180] with permission from The Royal Society of Chemistry.

A new AIE-active, excimeric Pt(II) complex, [Pt(C^N)(L1)(Cl)] (**122**), [C^N =2-phenyl-pyridine; L1 =N1-tritylethane-1,2-diamine] has been reported by our group [181]. The complex showed a distinct yellow emission that turned into orange after being ground in a mortar with a pestle (Fig. 32). The mechanochromic behaviour of this complex was thoroughly studied by PXRD and DSC. The PXRD data revealed the crystalline nature of the yellow form while the orange form was found to be amorphous. This was further supported by the DSC experiment that showed an endothermic melting peak in both cases (199.9 and 170.0 ^{0}C, respectively), while a glass transition peak (61 ^{0}C) and a broad exothermic re-crystallisation peak at 100 ^{0}C was

observed for the orange sample. The yellow emissive complex was further transformed to a green-emitting form after mildly crushing it with mesostructured silica.

Fig. 32. Luminescent images of pristine complex **122** (yellow), **122** after grinding (orange), and after mixing **122** with mesoporous silica (photograph taken under 365 nm UV illumination). Adapted from ref. [181] with permission from The Royal Society of Chemistry.

3.1.2 Vapochromic AIE complexes

Two AIE-active Ir(III) complexes with molecular formulae [Ir(PPh₃)₂(1,10-phenon)(H)₂]PF₆ **10 (PF₆⁻)** and [Ir(PPh₃)₂(1,10-phenon)(H)(Cl)]PF₆ (**123**) synthesized in our group were found to have a response towards volatile organic compounds [100]. Experiments show that their maximum emission gradually shifts towards a longer wavelength with increasing solvent polarity (Fig. 33), Complex **10 (PF₆⁻)** when recrystallized from DCM emits greenish yellow light on exposure to UV radiation (Fig. 33) changing from greenish-yellow to yellow upon exposure to solvents such as acetone or acetonitrile with polarity higher than DCM. Upon exposure to solvents with lower polarity such as chloroform, benzene or 1,4-dioxane, the solid thin films emit a yellowish-green or bluish-green light (Fig. 33). Complex **123**, recrystallized from DCM emits green light and in thin-films, in an analogous way to what happens for complex **10 (PF₆⁻)** and it emits blue light upon exposure to non-polar solvents and green light in presence of polar solvents.
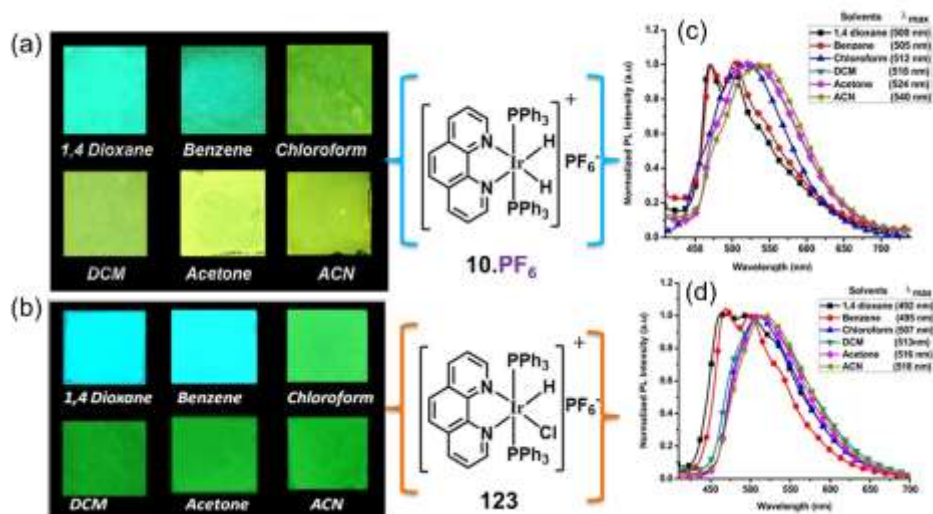
Fig. 33. Observed thin-film emission colour of (a) **10 (PF₆⁻)** (bluish-green to yellow, under 365 UV irradiation) and (b) of **123** (blue to green, under 365 UV irradiation) after systematic exposure of different VOCs (polarity increases in the order: 1,4-Dioxane, Benzene, Chloroform, DCM, Acetone, Acetonitrile). Corresponding emission spectra of thin films (c) **10 (PF₆⁻)** and (d) **123**. Adapted from ref. [100] with permission from WILEY-VCH.

Bryce et al. have synthesized an AIE-active dinuclear Ir(III) complex [Ir$_2$(ppy)$_4$ (N^O)] (where ppy =2-phenyl pyridine and N^O= t-butyl substituted Schiff base) **(20)** (Fig. 34) with piezochromic luminescence and vapochromism [61]. Its crystal structure revealed the existence of intramolecular π-π interactions between the bridging phenyl ring and the phenyl rings of phenylpyridine which are easily modified by thoroughly grinding for 30s, resulting in an emission colour change from orange to red and a dramatic 480-fold decrease in the PL quantum yield. The emission colour was fully recovered after exposure to DCM. This behaviour was further utilized to fabricate a device for detecting volatile organic compounds. A warning signal composed of a ground sample emitting weak red phosphorescence was carefully spread on a filter paper using a porcelain pestle (Fig. 34). The emission of this warning signal was switched on (weak red to orange) after exposing to different VOCs. Polar VOCs such as CHCl$_3$ and MeOH showed turn-on response times of 10 and 30s, respectively. Upon exposure to n-hexane, however, the signal did not show any change.
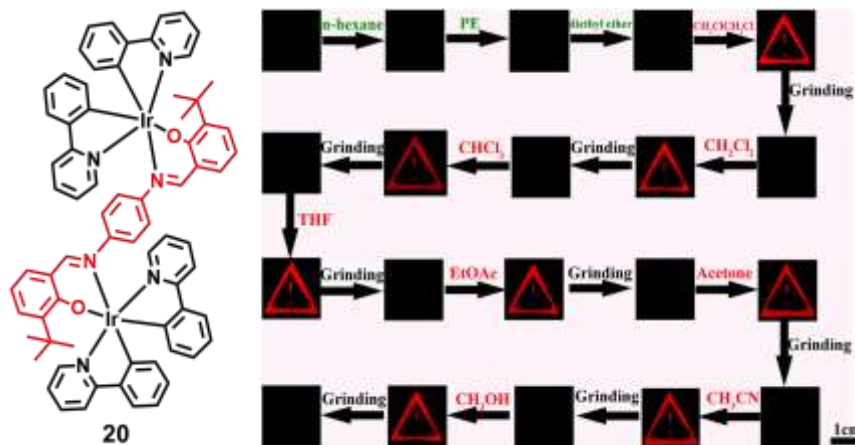
Fig. 34. Photographic images under illumination with 365 nm UV light of the monitoring of VOCs by **20** after exposure to different VOCs and grinding. Adapted from ref. [61]. with permission from The Royal Society of Chemistry.

3.1.3 Thermochromic AIE complexes

Another way of obtaining a colour change in a compound is by changing temperature. In a recent article, Liu and co-workers report on the thermochromic behaviour of a new gold complex with AIE. To study the AIE of complex **52** (Fig. 35a), photoluminescence and UV spectra were studied in EtOH–H_2O mixtures with various water contents finding that the PL intensity was not only significantly enhanced with the addition of water, but the emission color also changed from blue to yellowish-green. After gentle heating (T > 55 ^{0}C) a powder sample of **52** showed a similar reversible colour change (Fig. 35b) demonstrating the thermochromic behaviour of this complex [144]. The changes observed in the luminescence were explained based on molecular packing. The Au-Au distances in the crystal structure were found to lie in the range of 3.8-4.8 Å, well above the range of typical aurophilic interactions (Au-Au = 2.7–3.3 Å) (Fig. 35c). These Au-Au distances are however suggested to shorten in an amorphous phase formed after heating. After cooling the sample, the system would return to the more stable crystalline state. The colour change is supposed to arise from these aurophilic interactions in the amorphous phase, which may be responsible for the new ligand-to-metal–metal charge transfer (LMMCT) excited state [$C_6F_5 \rightarrow Au\cdots Au$].
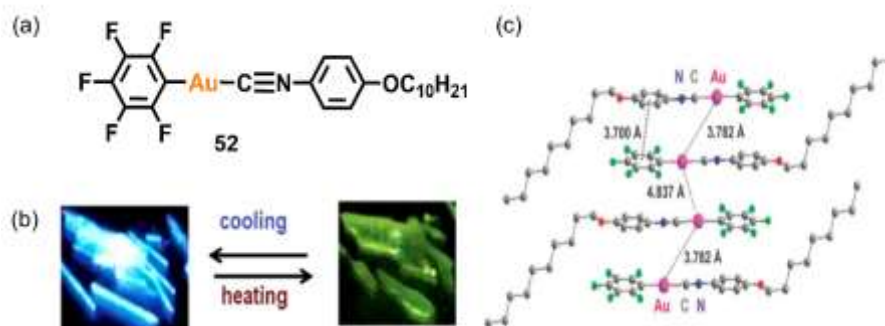
47

Fig. 35. (a) Molecular structure of complex **52**, (b) Images of the compound before and after heating under 365 nm UV illumination, (c) The packing diagram of **52**. Adapted from ref. [144] with permission from The Royal Society of Chemistry.

3.1.4 Aggregation induced electrochemiluminescence

In contrast to photoluminescence (PL), in electrochemiluminescence (ECL) [182-184] an electronically excited state is generated electrochemically at an electrode surface and controlled by the application of a potential. For many applications ECL is clearly superior to PL, especially due to its extremely low detection limit and it is currently evolving towards one of the most relevant detection methods for bioassays. Despite this, almost all current applications of ECL use the luminescent $Ru(bpy)_3^{2+}$ label (where bpy = 2,2′-bipyridine) [185, 186] and there is a growing interest in the development of other emitters, notably those based on Ir(III) or Pt(II) because of their colour tunability and higher quantum yields. The attempts to develop new ECL emitters has reached for the moment a limited success mainly due to quenching by dioxygen and the interaction with the environment that strongly quenches the long-lived excited state of the metal complexes. In this respect, the recent discovery of aggregation induced ECL in Pt(II) and Ir(III) complexes might open the way to the development of new ECL labels free from the aforementioned problems [187, 188].

The first AIE-active electrochemiluminescent Pt(II) complex, **124** (Fig. 36) was developed by the group of de Cola by combining the tridentate 2,6-bis(3-(trifluoromethyl)-1H-1,2,4-triazol-5-yl)pyridine ligand with a 4-amino pyridine substitute with two triethylene glycols in a square planar Pt(II) complex [187]. The combination in a same complex of a hydrophilic ancillary ligand with the hydrophobic character of the main chelate leads to an amphiphilic compound with a marked tendency to self-assemble in water into discrete aggregates with Pt⋯Pt contacts shorter than 3.5 Å. While in dilute DCM solution the complex has a quite low emission quantum

48

yield (1%), in aqueous media, the resulting solutions show a strongly red-shifted emission with a remarkable 72% quantum yield. Interestingly, **124** showed an intense ECL upon aggregation via a co-reactant pathway using both TPrA and oxalate, both in the solid state and in solution, where the efficiency of **124** was found to exceed that of Ru(bpy)$_3^{2+}$ by 20%.

Shortly after this first article on aggregation induced ECL, Gao et al. reported the synthesis and characterization of an Ir(III) complex, **125** showing aggregation induced electroluminescence (AI-ECL) (Fig 36) [188]. In this complex, [Ir(tpy)(bbbi)], where tpy = 2,2′:6′,2″-terpyridine and bbbiH$_3$= 1,3-bis(1H-benzimidazol-2-yl) benzene, the two tridentate ligands, *i.e.*, tpy and bbbi^{3-}, chelate a central octahedrally coordinated Ir(III) ion through N^N^N and N^C^N coordination modes, respectively. Both ligands are planar and aromatic and facilitate the formation of intermolecular π−π-stacking interactions. Moreover, complex **125** contains non-coordinated imidazole N atoms that can engage in intermolecular hydrogen-bonding interactions. In the crystal structure, the planes of the two ligands are almost orthogonal to each other minimizing steric hindrance. Neighbouring [Ir(tpy)(bbbi)] complexes form chains along through two types of π−π-stacking interactions and edge-on C−H⋯π interactions that provide an effective restriction of internal motion (the low energy vibration mode of the two rigid ligands changing the dihedral angle between their planes) and explain the AIE effect observed for **125**, both in the crystals as in DMSO-H$_2$O mixtures with f_w = 90% where **125** formed monodisperse nanoparticles with an average hydrodynamic size of 120 nm.
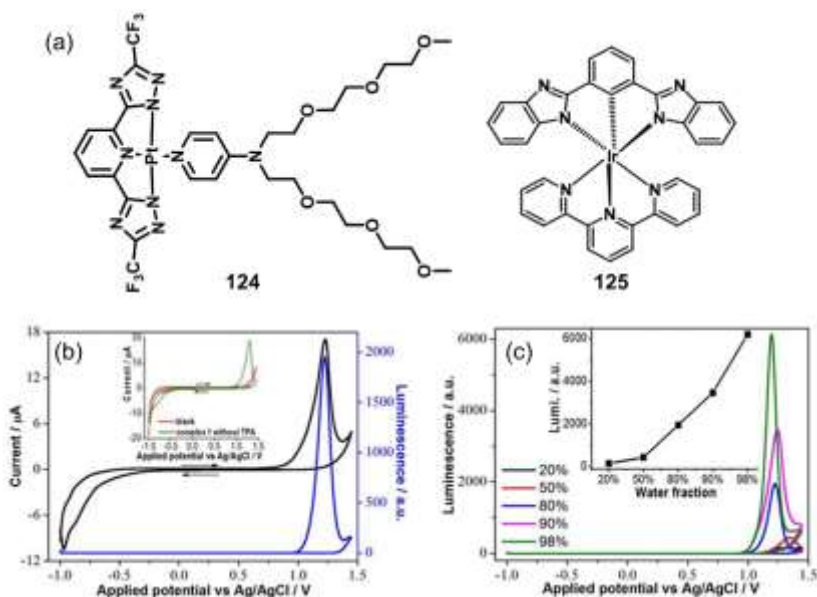

Fig. 36. (a) Molecular structure of the aggregation induced ECL complexes, **124-125**, (b) Cyclic voltammogram (dark line) and ECL trace (blue line) of complex **125** (c = 200 µM) in a

DMSO−H$_2$O (20/80, v/v) mixture containing 1 mM TPA, 100 mM NaCl, and 10 mM PBS (pH 7.4), (c) ECL intensity changes of complex **125** (c = 200 μM) upon variation of the H$_2$O fraction of a DMSO−H$_2$O mixture. The scan rate was 0.1 V/s. Adapted from ref. [188] with permission from American Chemical Society.

The cyclic voltammetry (CV) and ECL of complex **125** was measured in a DMSO/H$_2$O mixture (f_w = 80%) containing 1 mM tripropylamine (TPA) as the coreactant and 100 mM NaCl and 10 mM phosphate-buffered saline solution (PBS; pH 7.4) as supporting electrolytes. During the potential scanning process, a strong ECL emission with a peak at 1.23 V (Fig. 36b) was observed. ECL spectra were also obtained in a series of aqueous electrolytes with different amounts of DMSO and H$_2$O finding a ∼39-fold enhanced luminescence for **125** when the f_w increased from 20% to 98% (Fig. 36c) confirming the AI-ECL behaviour for **125** for which no ECL was observed in pure DMSO. In a further experiment, in which bovine serum albumin (BSA) was added to the medium, **125** showed a gradual increase in the ECL intensity because of the binding of BSA to the surface of the nanoaggregates showing that Ir(III) complexes such as **125** exhibiting strong AI-ECL signals may lead to the development of new AI-ECL-based biosensors and food analysis methods.

3.2 Bioimaging using AIE-active metal complexes

The development of new chemical technologies for life sciences and pathology applications are compulsory to address problems that cannot be solved by actual methods [15, 17, 18, 189-193]. One of the most suitable and successful ways to study the details in the interior of a cell is by bioimaging techniques using fluorescent dyes as labels that offer an exceptional and attractive approach for visualizing morphological details with sub-cellular resolution that cannot be resolved by ultrasound or magnetic resonance imaging (MRI) [194, 195]. Most of the fluorescent probes used nowadays are still organic compounds that have limitations such as easy photobleaching, small Stokes shifts and difficulty to filter from the auto-fluorescence emitted by certain organisms [196-198]. On the contrary, phosphorescent transition-metal complexes with MLCT luminescence exhibit not only larger Stokes shifts, but also much longer lifetimes as well as a higher stability, making them better candidates for new bioimaging probes. However, for most of these probes if the emitter concentration is too high, aggregates form, causing ACQ that reduces the luminescence intensity, a problem that can be tackled by using AIE-active emitters [18, 59, 199-201].

Recently, an Ir(III) complex **8**, was encapsulated in a micellar structure with polyethylene glycol–polylactic acid (PEG–PLA), a biodegradable polymer [99]. The micelles of PEG–PLA with encapsulated AIE-active Ir(III) complex were used as in vitro cellular imaging probes for biomedical applications being able to successfully label the cytoplasm and the cell surface of HeLa cells (Fig. 37a). The cytotoxicity of the Ir(III) complex **8** was investigated by the conventional MTT assay showing a >80% survival of the cells in all tested concentrations (Fig. 37b) suggesting that photoluminescent PEG-PLA particles have a low toxicity and could be used as cell imaging probes under in vitro conditions.
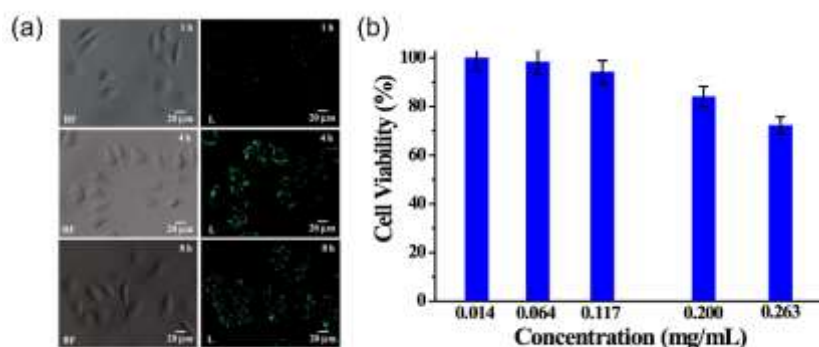
Fig. 37. (a) Bright field (BF) and luminescence (L) image of HeLa cells labelled with Ir complex **8** encapsulated PEG-PLA particles. Cells are incubated with particles for 1, 4 and 8 hours and then washed cells are imaged under a microscope, (b) Viability of HeLa cells in presence of Ir(III) complex **8** encapsulated PEG-PLA nanoparticles. Adapted from ref. [99] with permission from the Royal Society of Chemistry.

A series of mitochondria targeted AIE-active complexes (**126-128**) were synthesized by Chao and co-workers who recognized these complexes as two-photon absorbing (TPA) as well as photodynamic therapy (PDT) agents [202]. The complexes were able to generate singlet oxygen in different water-DMSO mixtures with a maximum $^1O_2$ emission intensity at $f_w = 90\%$. This singlet oxygen generation in presence of nanoaggregates was further supported by the help of a reactive oxygen species (ROS) indicator, 3-diphenylisobenzo-furan (DPBF). The lipophilicity ($logP_{o/w} = 1.42$) of complex **126** facilitated the cellular uptake and successfully stained the mitochondria membranes of cancerous cells. The cellular uptake of complex **126** followed by an

endocytic pathway, was confirmed by confocal laser scanning microscopy (CLSM). The toxicity of these complexes was measured in presence of and absence of light, resulting in an increased cytotoxicity after photon excitation. The potentiality of complex **126** for dual TPA-PDT was tested, finding a better photocytotoxicity towards HeLa cells than L02 ones after selectively accumulating in the mitochondria (Fig. 38).
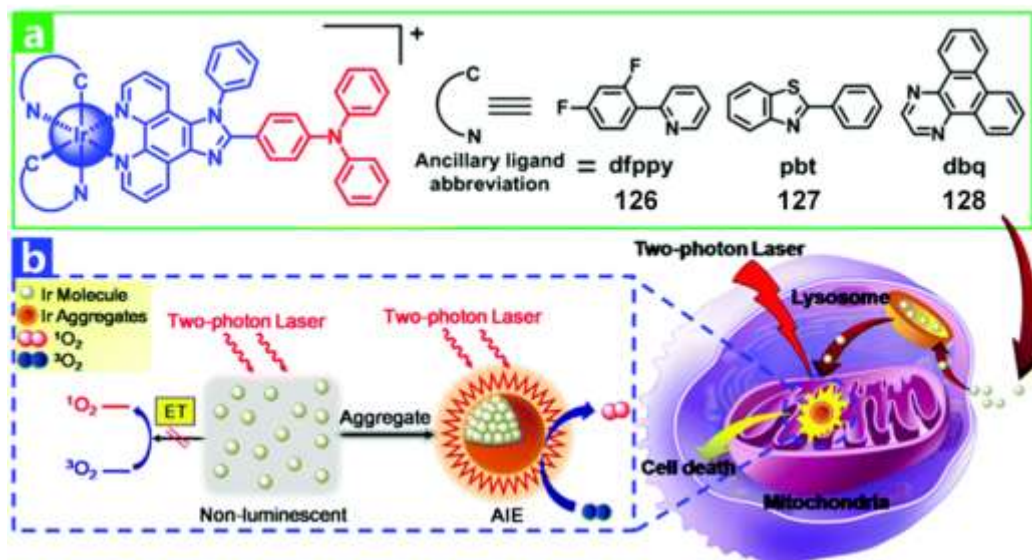
Fig. 38. (a) Molecular structure of complexes **126-128**, (b) Scheme showing the complexes acting as dual two-photon absorbing (TPA) photodynamic therapy (PDT) agents. Adapted from ref. [202] with permission from the Royal Society of Chemistry.

In another report Chao and co-workers developed two AIE-active Ir(III) complexes **129-130** for mitochondria-targeted two-photon PDT in monolayer cells and multicellular tumor spheroids (MCTSs) [203]. The $^1O_2$ generation capability of these complexes was better in aggregate state than in solution. The complexes were shown to easily aggregate in the cell and selectively target mitochondria of cancerous cells (HeLa) over normal ones (human hepatic L02). Confocal laser scanning microscopy (CLSM) was further used to monitor the cellular uptake, localization and mitochondria damaging process under one- and two-photon light irradiation (Fig. 39). Some recent interesting contributions showing more possible uses for Ir(III) based complexes in the fields of data protection and real-time monitoring of mitophagy in living cells can be found in references [204, 205].
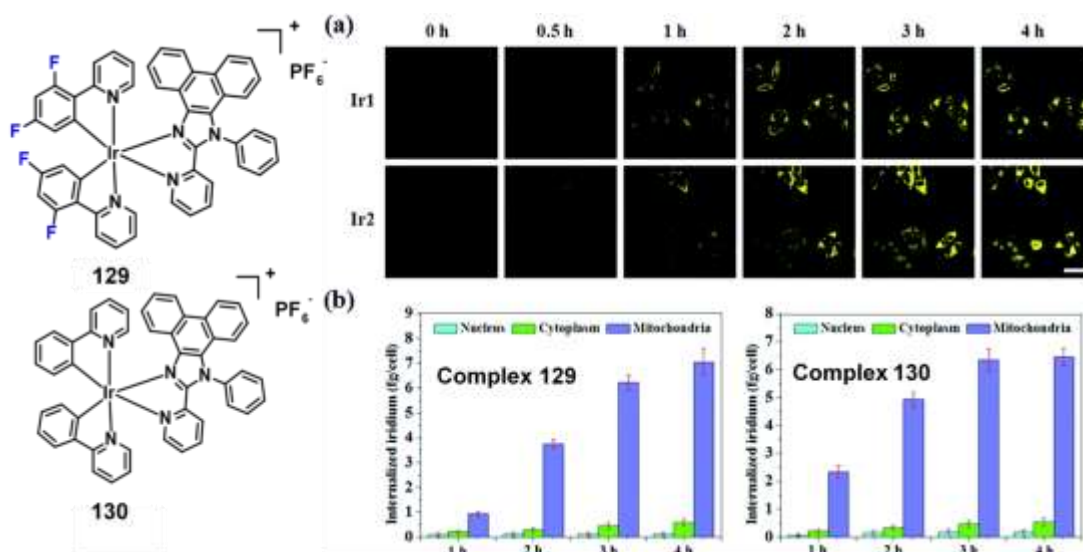
Fig. 39. Real-time uptake monitoring of **129** and **130** (1 μM, λex = 740 nm, λem = 550 ± 20 nm) in HeLa cells at incubation times of 0–4 h. Scale: 50 μm, (b) The internalized iridium of the HeLa cells was quantified by ICP-MS with different incubation times.Adapted from ref. [203] with permission from the Royal Society of Chemistry.

Cancer theranostics [126, 204-206] is a recent idea, introduced in 2010, in which the integration of therapeutic and diagnostic agents provides a powerful means for simultaneous real time monitoring of therapeutic responses allowing a personalized onco-tratment that can be performed at the appropriate time. In the current clinical scenario, the imaging part of any theranosic approach is restricted to MRI, PET and CT. Although these techniques have widespread applications, it is sometimes difficult to distinguish clearly between normal and malignant tissues using these methods, and the development of new theranostic technologies based on luminescent materials is certainly a promising avenue for the coming years.

Following this idea, our group has recently developed a new cytotoxic AIE-active Pt(II) complex, bis(diphenylphosphino)methane phenylpyridine Pt(II) chloride, referred henceforth as BMPP-Pt (**131**) with promising features for the development of new theranostic applications [207]. In the initial experiments, **131** has been found to exhibit a strong fluorescence intensity and an interesting AIE behaviour in DCM/hexane mixtures. Since it is also highly emissive in the solid state and has an amphiphillic nature, it can be considered for bioimaging, which

53

combined with its potent cytotoxic activity makes it ideal for the formulation of new theranostic modalities. As the water solubility of **131** is quite poor, to improve its cellular delivery, **131** was encapsulated into mesoporous silica nanoparticles (Fig. 40) (named Pt-MSNPs in the following). The **131** encapsulated MSNPs were further modified by conjugating them with an aptamer against an Epithelial Cellular Adhesion Molecule (EpCAM) on their surface for cancer cell targeting. To conjugate with the aptamer, initially the surface of Pt-MSNPs was modified with glycidoxypropyltrimethoxysilane (GOPS) that resulted in Pt-MSNP-GOPS and then the anti-EpCAM aptamer was added to the aqueous solution of Pt-MSNP-GOPS, incubated for one hour and washed with phosphate buffer to produce the anti-EpCAM aptamer conjugated **131** loaded MSNPs.

Pt-MSNPs, Pt-MSNP-GOPS and Pt-MSNP-E were found to show green emission in water. To confirm the internalization of the AIE-active **131** complex, we exposed Huh7 liver cancer cells to free **131** for 24 h. Confocal microscopy and flow cytometric analysis revealed that these complexes are internalized, though the fluorescence signal was weak. Thereafter, to evaluate whether encapsulation of **131** into MSNPs can enhance their cellular internalization properties, Huh7 liver cancer cells were treated with **131** and Pt-MSNPs and were monitored for their relative fluorescence in comparison with free **131** complexes.
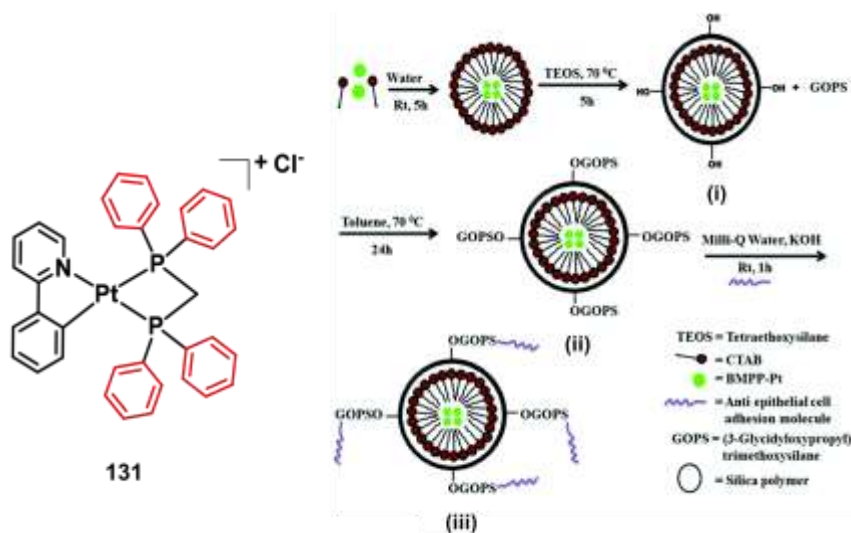
Fig. 40. (i) Preparation of **131** loaded mesoporous silica nanoparticles (MSNPs), (ii) Modification of the MSNPs with GOPS and (iii) conjugation of an anti-EpCAM aptamer with the GOPS modified MSNPs. Adapted from ref. [207] with permission from the Royal Society of Chemistry.

The cytotoxic potential of **131** was evaluated in the Huh7 cells through MTT assays. Since encapsulation of **131** into MSNPs enhances their cellular uptake, we compared the cytotoxic potential of free **131** to that of MSNP encapsulated **131**. Both showed a considerable cytotoxic effect while blank MSNPs, on the contrary, showed only a very low level of cell death, even at a very high concentration. Interestingly, in addition to its effective internalization when compared to the Pt-MSNP complex, the Pt-MSNP-E complexes showed significantly better cytotoxicity in Huh7 cells indicating that anti-EpCAM aptamer conjugation of MSNPs was facilitating the NP entry through an appropriate channel.

3.3 AIE metal complexes for sensing applications

Over the last 50 years there has been an intense research in the development of sensing techniques for different anions and cations playing a significant role in a wide range of industrial, chemical, and most importantly, for biological processes [208-215]. A special interest has been focused in the detection of highly toxic ions such as Hg^{2+}, Cd^{2+}, As^{2+}, Pd^{2+}, CN^-, or SCN^- [20, 22, 28, 96, 216-223].

Systems where the addition of analytes (cations or anions) to some probe molecules results in a drastic change in one or more properties of the system, such as emission, absorption, or redox potential characteristics are known as chemosensors. Among many detection techniques, the detection of luminescence is considered as one of the most promising tools for sensing applications because of its high sensitivity, easy visualization, and short response times. A chemosensor, generally consists of two units, *i.e.* a receptor unit and a signalling unit [26]. After selective binding of the analyte to the receptor, the signalling unit produces the effective changes (turn-on, turn-off or a ratiometric change) in the optical properties (Fig. 41). In this case, heavy metal-based complexes with phosphorescent emission are, in general, considered to be superior to fluorescent emitters because of their long-lived lifetimes and higher efficiencies. In recent times, the use of phosphorescent Pt(II), Ru(II), Re(I), Ir(III), Cu(I), Au(I) and Os(II)-based complexes [12, 26, 27, 224] as chemosensors has attracted a great deal of attention by several

researchers and many Ir(III) based complexes were successfully used for the detection of various analytes [12, 26].
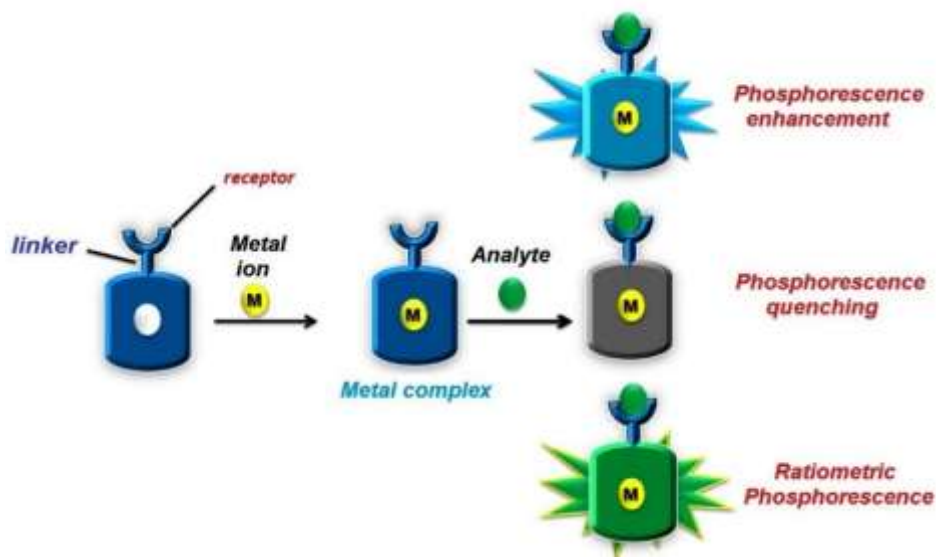
Fig. 41. A schematic representation of the "Receptor-signalling unit" approach for the design of phosphorescent chemosensors and possible varying phosphorescence signal responses. Adapted from Ref. [26] with permission from The Royal Society of Chemistry.

3.3.1 Metal cation sensing

The toxicity of mercury and its derivatives are known to pose a serious environmental threat. The most common and toxic mercury (II) species easily reaches humans or animals via the food chain and its detection is essential for both human health and environmental preservation. In our group we have designed and synthesized an AIE-active chemodosimeter showing a superb response for Hg(II) in comparison to other metal ions such as Mg^{2+}, K^+, Ni^{2+}, Al^{3+}, Cd^{2+}, Co^{2+}, Pb^{2+}, Bi^{2+}, Fe^{2+}, Ag^{+1}, Cu^{2+}, Au^+ or Zn^{+2}. The AIE-active Ir(III) complex **132** was purposely synthesized with an ancillary appended diphosphine ligand where one of the P atoms was coordinated to the Ir centre and the other P atom was left free to co-ordinate with Hg^{+2} (Fig. 42) [97]. The limit of detection was estimated to be around 170 nM, a reasonably good value if compared with many other reported Ir(III) based Hg^{2+} chemodosimeters.

Fig. 42. (a) Molecular structure of complex **132**, (b) The luminescence spectral changes of complex **138** ($f_w = 70\%$ with $[M] = 10^{-5}$ mol L^{-1}) upon increasing addition of Hg^{2+} ions (from 0.0 to 14.0 μM) (nitrate salt). DMF–H$_2$O (3:7 v/v). $\lambda_{ex} = 380$ nm, (c) The plot of I$_{463}$*vs.* the concentration of Hg^{2+}; inset, the linear relationship of I$_{463}$*vs.* the concentration of Hg^{2+} in the range of 0.0–6.0 μM, (d) pho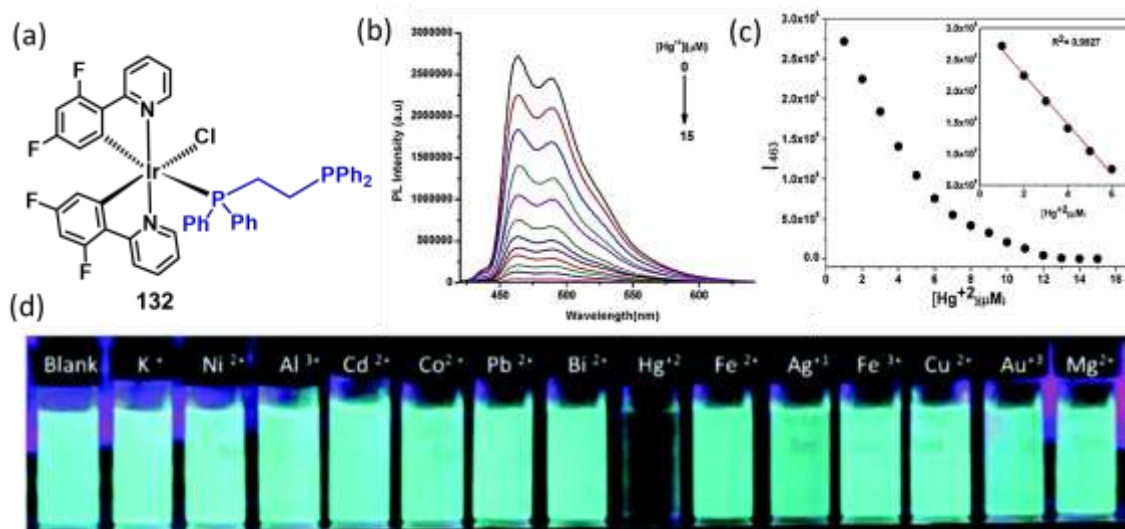tograph of complex **132** when dispersed at $f_w = 70\%$ with $[M] = 10^{-5}$ mol L^{-1}, by adding 4 equivalent of metal ions. From left to right: (i), blank; (ii), K$^+$; (iii), Ni^{+2}; (iv), Al^{+3}; (v), Cd^{+2} ; (vi), Co^{+2}; (vii), Pb^{+2}; (viii), Bi^{+2}; (ix), Hg^{+2}; (x), Fe^{+2}; (xi), Ag$^+$; (xii),Cu^{+2}; (xiii), Fe^{+3}; (xiv), Au; and (xv), Mg^{+2} irradiated with ultraviolet light at 365 nm. Adapted from ref. [97] with permission from the Royal Society of Chemistry.

The copper ion (Cu^{2+}) plays a vital role in human health with many diseases such as Alzheimer's, Menkes', Wilson's, and prion diseases related to its presence. In 2013, Chen and co-workers synthesised two cationic cyclometallated Ir(III) complexes (**133-134**) with 2,2'-bipyridine-acylhydrazone where ppy was used as the chromophoric ligand [225] . These complexes showed a very weak emission in common organic solvents in the concentration range 20 μM-20 mM, while a strong red emission was found for solid samples (Fig. 43). Additionally, complex **133** showed a 35-fold increase in its PL intensity after addition of 100 μM Cu^{+2} to its 10 μM solution, opening the possibility of using it as a potential switch-on phosphorescent sensor for this cation. The selectivity and interference experiments were performed in presence of several other metal ions including Ag$^+$, Ca^{2+}, Cd^{2+}, Fe^{3+}, Hg^{2+}, Mg^{2+}, Mn^{2+}, Ni^{2+}, Co^{2+}, and Zn^{2+} showing no obvious changes except for Fe^{3+} that quenched the emission. The possible mechanism of Cu^{2+}

detection was proved by addition of excess $Cu(ClO_4)_2.6H_2O$ after which two complexes, the hydrolyzed product and the result of oxidative cyclization, were obtained, finding that the oxidative cyclization of acylhydrazone was responsible for Cu^{2+} detection in the system (Fig. 43).
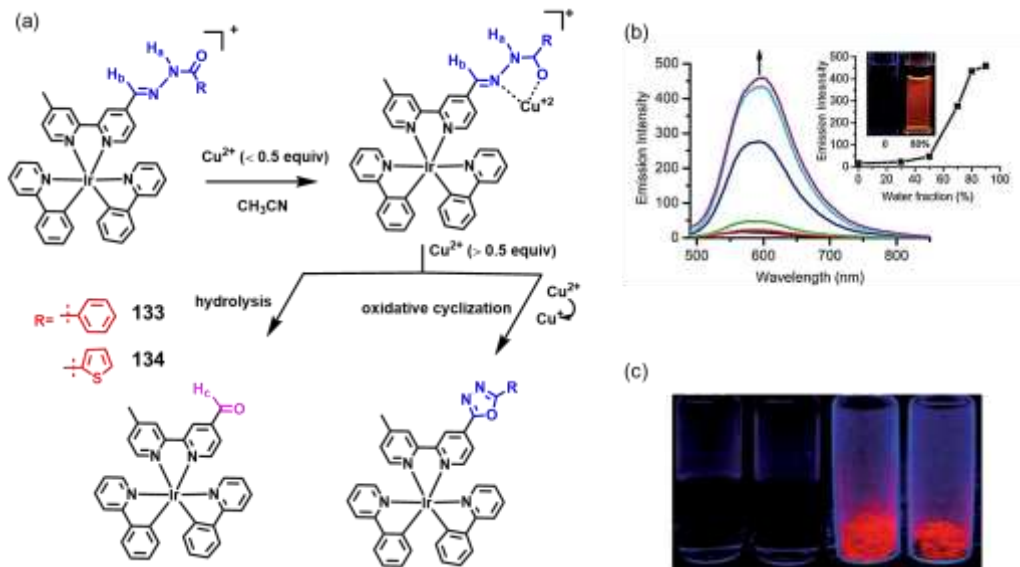
Fig. 43. (a) Molecular structure of complexes **133** and **134** and sensing mechanism, (b) Emission spectra of **133** in acetonitrile–water mixture (f_w = 0-80%), Inset: intensity change at 593 nm versus water fraction of acetonitrile–water mixture and photographic image of **133** in acetonitrile–water with water contents of 0 and 80% under UV light irradiation at 365 nm, (c) Photograph of complexes **133** and **134** in CH_3CN solution (left) and in the solid state (right) under UV light irradiation at 365 nm. Adapted from ref. [225] with permission from the Royal Society of Chemistry.

Ca^{2+} is very much important for the human body, playing a vital role in regulating the heart's function, intracellular signalling, enzyme function, the transmission of nervous system signals, hormonal secretion, blood clotting, regulating muscle functioning, as well as the strengthening of bones and teeth. According to the Institute of Medicine of the National Academy, the daily uptake of calcium should be around 1.0 g /daily, thus the detection of Ca^{2+} ion in food and different media is highly desirable. Pei and co-workers developed a low cost, fast responsive AIE-active Au(I)–thiolate complex **135** with a good affinity for Ca^{2+}. While the oligomer

complexes are not emissive in solution, addition of Ca^{2+} ions results in an aggregation that induces an AIE response [226]. A 0.8 mM detection limit was found for Ca^{2+} concentrations in the range from 0 to 400 mM, with the 100 mM concentration easily detectable by naked eye inspection, facilitating the detection of Ca^{2+} in drinking water, whole milk and serum (Fig. 44).

Fig. 44. (a) A schematic representation of the detection of Ca^{2+} based on the Ca^{2+} induced AIE property of Au(I)–cysteine complexes **135**, (b) Digital photographs of Au(I)–cysteine complexes in the absence and presence of Ca^{2+} under a portable UV light; (c) Rayleigh scattering test with a red laser pointer. Adapted from ref. [226] with permission from the Royal Society of Chemistry.

3.3.2 Explosive sensing

Nitroaromatics such as trinitrotoluene (TNT), 2,4-dinitrophenol (2,4-DNP), or picric acid (PA) are well-known explosive materials, and a convenient way to detect them is important for security related technologies. Recently, two AIE-active phosphorescent complexes, [Ir(ppy)(PPh$_3$)$_2$(H)Cl)] (**8**) and [Ir(o-CHOppy)(PPh$_3$)$_2$(H)Cl)] (**136**) have been found to be highly sensitive for the detection of picric acid (PA), with detection limits of 65 nM and 264 nM for **8** and **136**, respectively (Fig. 45). The maximum K_{sv} values for PA were 1.90 x $10^5\,M^{-1}$ and 1.00 x $10^5\,M^{-1}$ for **8** and **136**, respectively, indicating that these complexes are super-sensitive for

explosive detection. In addition, **8** has been successfully employed for selective detection of PA [227].
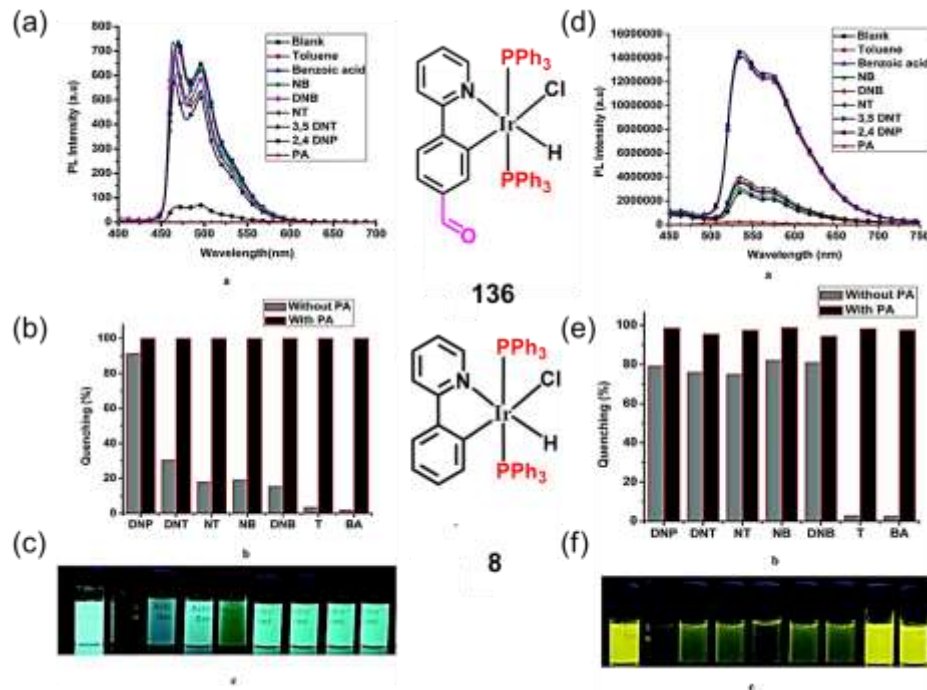
Fig. 45. (a-d) PL spectra of **136** (right) and **8** (left) with c $=10^{-5}$ mol L^{-1} at $f_w = 90\%$ (in water/THF) upon the addition of 5 equivalents of different nitro based explosive /non-explosive compounds, (b-e) Column diagrams of the relative PL intensity of **136** (right) and **8** (left) with different explosive/non-explosive compounds at 535 nm (**136**) and 470 nm (**8**). Grey bars represent the addition of various explosive/non-explosive compounds to each complex and black bars represent the subsequent addition of PA (5 equivalents) to the abovementioned solutions [1 + explosive/non-explosive compounds + PA], (c-f) Image of **136** (right) and **8** (left) when dispersed at $f_w = 90\%$ with c $= 10^{-5}$ mol L^{-1}, with addition of 5 equivalents of each of the explosive /non explosive compounds, respectively; from left to right: (i) blank; (ii) PA; (iii) 3,5-DNT; (iv) NT; (v) 2,4-DNP; (vi) 1,3-DNB; (vii) NB; (viii) T; (ix) BA. Adapted from ref. [227] with permission from the Royal Society of Chemistry.

Recently, two new AIE-active Ir(III) complexes **(137-138)** were specifically designed for selective detection of nitro explosives [228]. While **137** was utilized for selective detection of picric acid, **138** was synthesized to perform a controlled experiment in presence of a nitro explosive. Complex **137** was found to be non-emissive in an organic medium, but highly

emissive in the solid state. The PL intensity, 90 times higher at $f_w = 90\%$ than in pure acetone, was almost completely quenched by addition of 5 ppm of picric acid. The selectivity test was performed in presence of (i) different nitro explosives such as TNT, 2,4-dinitroluene (2,4-DNT), 2,6-dintritoluene (2,6-DNT),1,3-dinitrobenzene (1,3-DNB), nitrobenzene (NB), 2-nitrotoluene (oNT), and 3-nitrotoluene (mNT) and (ii) at different pH, as well as in the presence of various anions and cations (Fig. 46). The experiments indicated the selective detection of PA without any interference. The selective detection of PA by complex **137** was explained based on an energy transfer (ET) mechanism, while the sensing of other nitro explosives by complex **138** was explained based on the basis of a photo induced electron transfer (PET) mechanism.
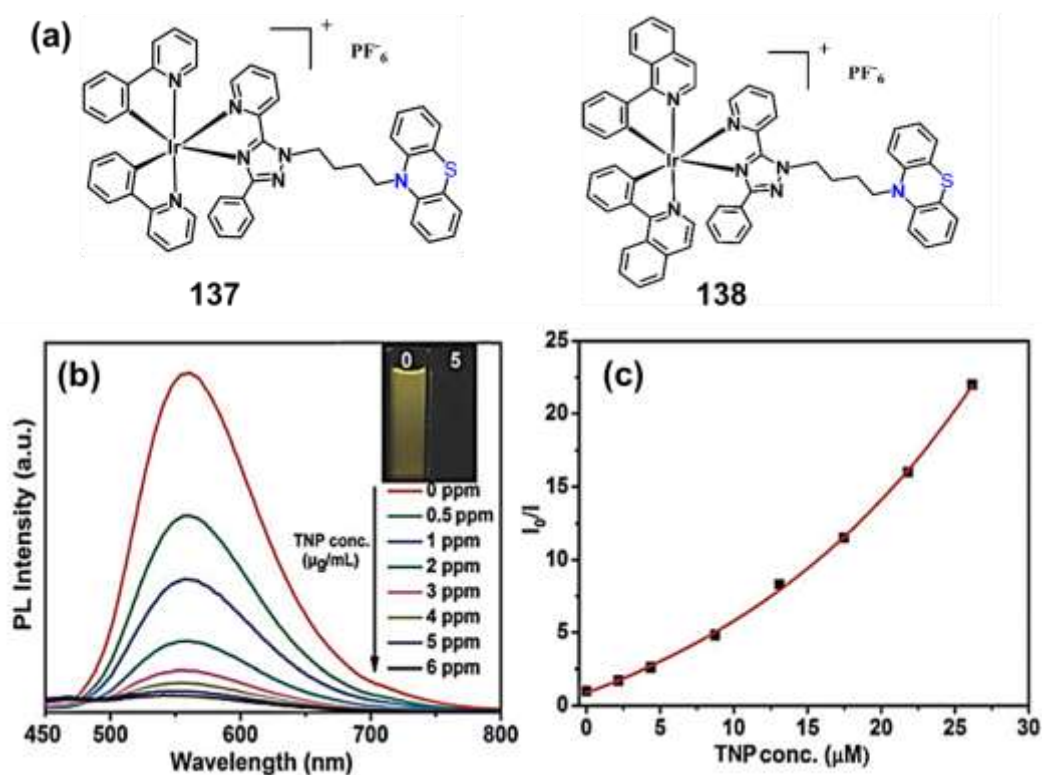
Fig. 46. (a) Molecular structure of complexes **137** and **138**, (b) PL spectra of complex **137** in acetone-water (v/v = 1:9) containing different amounts of TNP, (c) Corresponding Stern–Volmer plots of TNP (nitro-explosive power of 2,4,6-trinitrophenol). Adapted from ref. [228] with permission from the Royal Society of Chemistry.

In 2014, Reddy and co-workers synthesized complex **139**, an Ir(III) bis(2-(2,4-difluorophenyl)pyridinato-N,C2')(2-(2-pyridyl)benzimidazolato-N,N') complex, [FIrPyBiz] (Fig. 47) [229] that was successfully used for detection of TNT in the vapour and solid phases,

as well as in aqueous media. Complex **139** was found to exhibit an AIE behavior in acetone–water mixtures with the PL intensity at $f_w = 70\%$ being almost 128 times higher than in solution. On the other hand, a bright greenish-yellow emission was observed in the solid state with a quantum yield of 7.4% in air at an ambient temperature. AIE was attributed without further proof to the excimeric interactions between the cyclometalating ligands of adjacent complexes, resulting in a switch from a non-emissive ^3LX excited state to an emissive ^3MLLCT transition. Detection of TNT was carried out using a 70% water-acetone mixture for which a detection limit of 9.08 mg mL^{-1} (Fig. 47) was found.
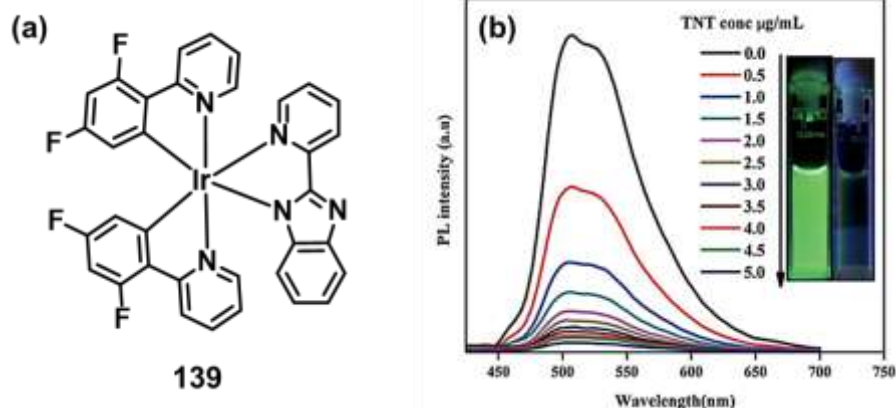
Fig. 47. (a) Molecular structure of complex **139**; (b) Phosphorescence spectra of **139** in acetone-water (30: 70%) mixtures containing different amounts of TNT (λ_{ex} = 365 nm). Adapted from ref. [229] with permission from the Royal Society of Chemistry.

It is possible to develop a portable sensor made from AIE-active complexes (**8, 136** and **140**) for the rapid on-site detection of explosives. Our group among others, demonstrated a simple method to detect explosive such as picric acid or TNT using a filter paper soaked in an AIE-active complex solution, which showed a turn-off response even at low concentration levels (Fig. 48) [227, 230]. A filter paper soaked with acetonitrile solution of complex **140** showed selective detection for TNT at 5 ppm level.
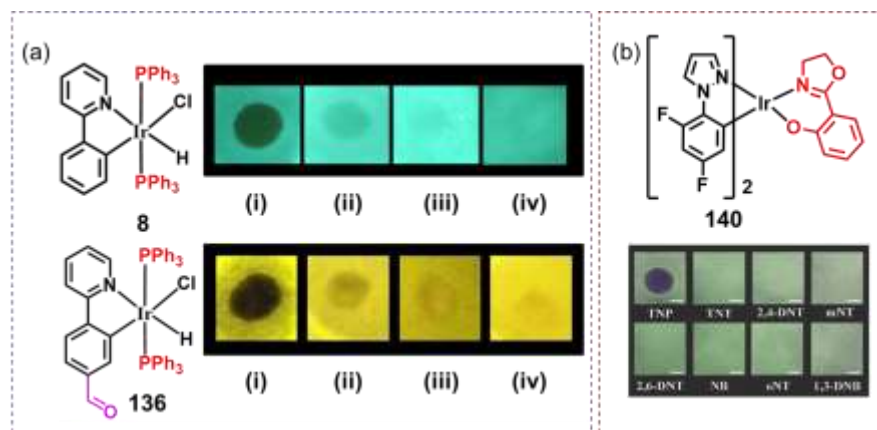
Fig. 48. (a) Portable sensors made from AIE-active Ir(III) complexes (**8** and **136**). Luminescent images of paper plates impregnated by **8** and **136** against different concentrations of PA (i) 10^{-3} M; (ii); 10^{-6} M; (iii) 10^{-9} M; (iv) 10^{-12} M and their response in presence of explosives. (b) Luminescent photographs of filter papers impregnated with complex **140** against 5 ppm of different nitro-aromatic compounds. All photographs were taken under 365 nm UV illumination. Adapted from ref. [227 and 230] with permission from the Royal Society of Chemistry.

3.3.3 Gas sensing: CO_2 and O_2 detection

The accurate determination of the presence of gases such as CO_2 and O_2 in biological tissues or cells is of a great importance in medical diagnosis, and the development of new AIE materials for sensing purposes in this field represents a promising avenue. In this sense, complexes exhibiting dual luminescence are specially interesting for developing this type of applications in which switching the luminescence by applying external stimuli is a key factor. Kasha's rule, according to which photon emission occurs only from the lowest excited state, gives however, a hint on the reasons on why it is difficult to develop single component dual-emissive small-molecular luminophores, that is, complexes with simultaneous emission from two different excited states. Such compounds must satisfy two basic requirements: the presence of a rich manifold of low-lying excited states and a limited electronic communication between them to allow radiative decays from two different states. In the literature there are a few mentions to Ir(III) complexes with a dual emission [231-234] but to the best of our knowledge, only two reports of dual emitting AIE-active complexes used for gas sensing purposes have been reported.

In the first paper, [94] we described the synthesis of four new Ir(III) complexes **141-144** by

aliphatic C-H activation of a Schiff base (Fig. 49). All four complexes were found to exhibit an intense AIE effect and, remarkably, in complex **144** substitution at the Schiff base to introduce an electron-donating diphenylamine group modifies dramatically its electronic structure leading to a dual emitter which is also AIE-active.
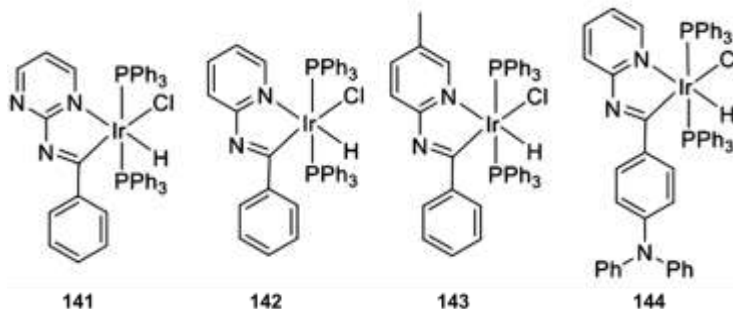
Fig. 49. Molecular structure of complexes **141-144.**

Comparing the absorption spectra of compounds **141-144** it is evident that **144** exhibits a very different behavior, with a rather intense absorption band around 400 nm that is not observed for the other three complexes (Fig. 50). A computational analysis shows that this band is due to a HOMO to LUMO transition with a strong ILCT character due to the donor nature of the diphenylamine substitution in the Schiff base (Fig. 50a). This emission band (Fig. 50c) has a strong solvatochromic behavior while the other, strongly structured one, appearing between 525-700 nm, is very similar to those observed for the other three compounds. The computational study, together with the evidences from the solvatochromic behavior and the measurements of lifetime data strongly support the dual emissive nature of complex **144**. Interestingly, the two emission bands have quite distinct features, with the solvatochromic band at lower wavelengths corresponding to fluorescence and the other one to phosphorescence. Although several examples of dual phosphorescence for Ir(III) complexes have been described previously [235, 236], this is, to the best of our knowledge, the first case of an Ir complex showing simultaneous fluorescence and phosphorescence, with a solvatochromic behavior (from blue to yellow) due to changes in the fluorescence band. The AIE properties of **144** were confirmed for solutions in different solvents such as THF, ACN or DMSO by gradual addition of water to them. An interesting feature was observed in THF/water solutions, where the sudden increase in intensity at f_W around 80% implies also a strong change in the emission colour of the solution.
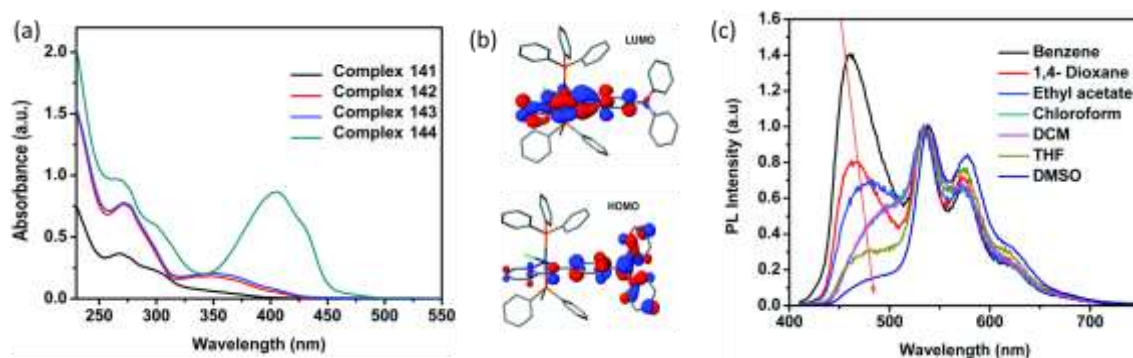
Fig. 50. UV-VIS absorption spectra of **141-144** (c= 10^{-5} M) recorded in degassed DCM at room temperature, (b) HOMO and LUMO of the optimized ground state of **144** at the B3LYP/LANL2DZ,6-31G(d) level. Hydrogen atoms have been omitted for the sake of clarity, (c) Emission spectra of **144** in different solvents. Adapted from ref. [94] with permission from the Royal Society of Chemistry.

The luminescent properties and the AIE behavior of **144** have been exploited to design a CO_2 sensing system. After reaction with diethyl amine the complex yielded a viscous carbamate ionic liquid (CIL). When it was dissolved in diethyl amine (DEA) and purged with CO_2 bubbles for 10 min, the initially non-emissive complex solution in DEA developed a perceptible emission. This change in the emission features was attributed to RIM, where the viscous CIL was able to restrict the rotation of triphenyl phosphine groups blocking the non-radiative deexcitation. Further, to study the response towards CO_2, different amounts of CO_2 were passed through a solution of complex **144** in DEA at a fixed rate and time. The emission was enhanced after gradual addition of CO_2 in the system, yielding a linear relation between emission intensity and CO_2 concentration, and hence, providing a straightforward way to quantify the CO_2 absorption (Fig. 51) [94].
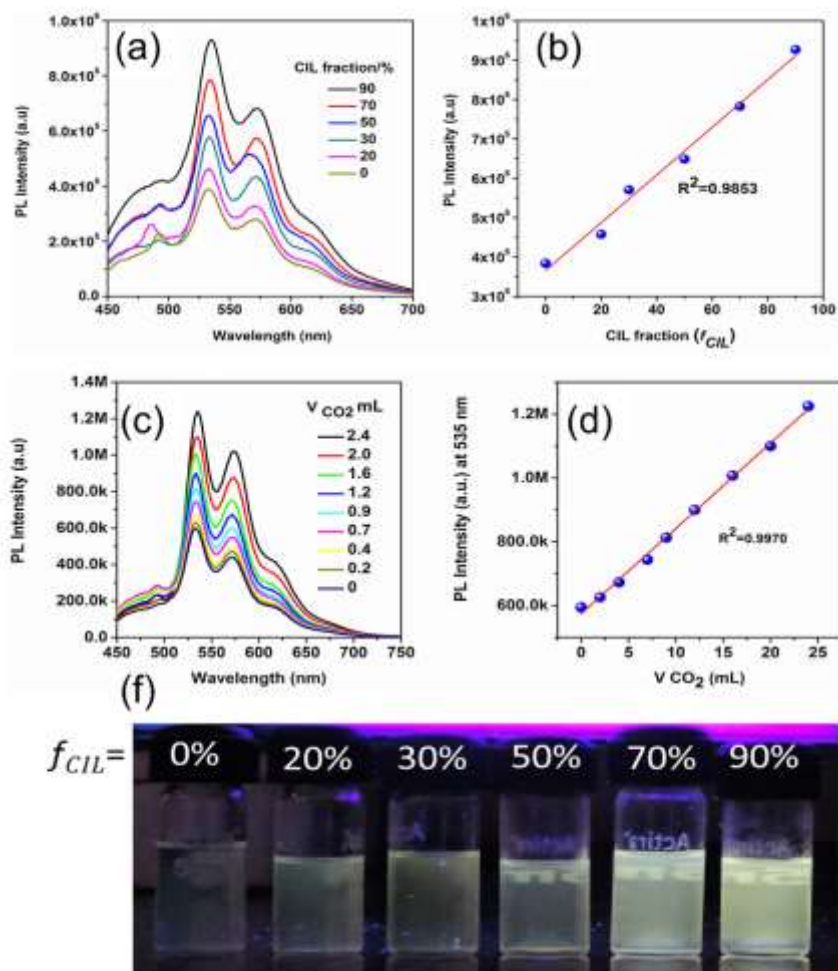
Fig. 51. (a) Emission spectra of **144** in DEA with different fractions of CIL ($f_{CIL} = 0$–90%). (b) Maximum emission intensity with respect to CIL, (c) PL spectra of **144** in DPA with different volumes of CO_2 showing a gradual PL intensity enhancement (d) PL intensity vs. increasing volume of CO_2 showing a linear relation with $R^2 = 0.9970$, (e) Photographs of **144** in DEA/CIL mixtures taken under UV illumination. Adapted from ref. [94] with permission from the Royal Society of Chemistry.

The accurate determination of the oxygen levels in biological tissues or cells is of a great importance in medical diagnosis, it is however an extremely difficult task since oxygen concentration in healthy tissues should be kept within a certain narrow range of concentrations and both hypoxia (insufficient oxygen supply) and hyperoxia (excessive oxygen supply) suppose a risk [208, 237, 238]. From the chemical point of view, it is relatively simple to devise molecules for sensors in hypoxic conditions, but single molecules with adequate responses for both hypoxia and hyperoxia have been proven to be quite elusive. Current sensors for oxygen in biological

66

samples can be classified into two broad families, that is, fluorescent organic dyes and phosphorescent transition metal complexes. Organic dyes are designed to provide an irreversible response to specific reductases in hypoxic environments, giving rise to a detectable change in their fluorescence. On the other hand, transition metal complexes used in oxygen detection rely on an effective quenching of the complexes' phosphorescence from the triplet state by oxygen via energy transfer. Both types of probes have been found to exhibit a fast and reliable luminescent response in hypoxic environments, but the sensing sensitivity is found to dramatically drop down for higher oxygen concentrations [94, 208]. In a recent publication [237], Zhang et al. have taken advantage of the dual phosphoresence exhibited by new AIE-active Ir(III) complex containing aminomethyl substituted phenylpyridine ligand **145** to develop a single molecule based system for O_2 sensing in biological samples able to work both in hypoxia and hyperoxia conditions.

Ir(III) polypyridine complexes with two types of ligands may exhibit intense phosphorescence from triplet metal/ligand to ligand charge transfer (^{3}MLLCT) or intra-ligand (^{3}IL) excited states, depending on the electronic structures of the chosen ligands. Incorporation of functional groups such as amino groups with unconjugated lone pair electrons that give rise to additional transitions to π^* MOs that may interrupt the internal conversion of the excited lowest state producing a dual phosphorescence from two independent states. This approach has been followed in refs [236, 237] by synthesizing a series of new Ir(III) complexes containing aminomethyl substituted phenylpyridine ligands for O_2 sensing purposes (**Fig. 52)**.
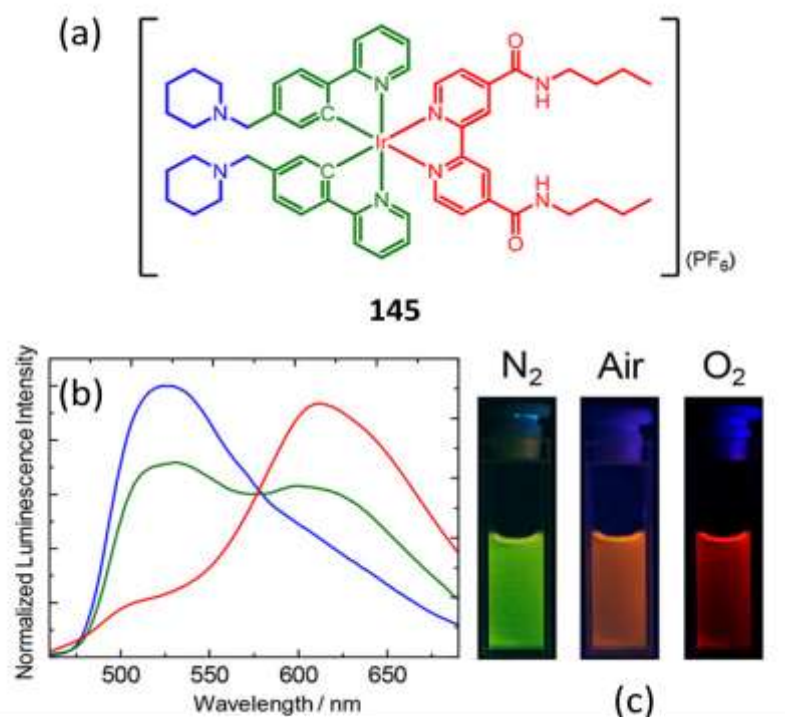
Fig. 52. (a) Molecular structure of complex **145** and (b) its photoluminescence spectra in PBS/CH$_3$OH (9:1, v/v) under N$_2$ (blue), air (green), and O$_2$ (red) atmospheres and (c) the corresponding photographs upon excitation by a UV lamp. Adapted from ref. [237] with permission from the American Chemical Society.

In the absence of oxygen, the photoluminescence spectrum of complex **145** (Fig. 53) shows a well-resolved dual emission composed of a vibronically structured high-energy (HE) band in the blue-green region and a structureless low-energy (LE) emission band in the yellow to orange-red region that have been assigned to ^{3}IL and ^{3}MLLCT excited states, respectively. According to the authors [236] the dual emissive character is observed for complexes with an ^{3}NLCT state arising from excitations of lone pair electrons to π* MOs (Fig. 53). In compounds where the ^{3}NLCT state has energy intermediate between the ^{3}IL and ^{3}MLLCT states it is suggested to interrupt the internal conversion that would usually take place from the high energy ^{3}IL state to the low energy ^{3}MLLCT state, giving thus rise to the observed dual phosphorescence.
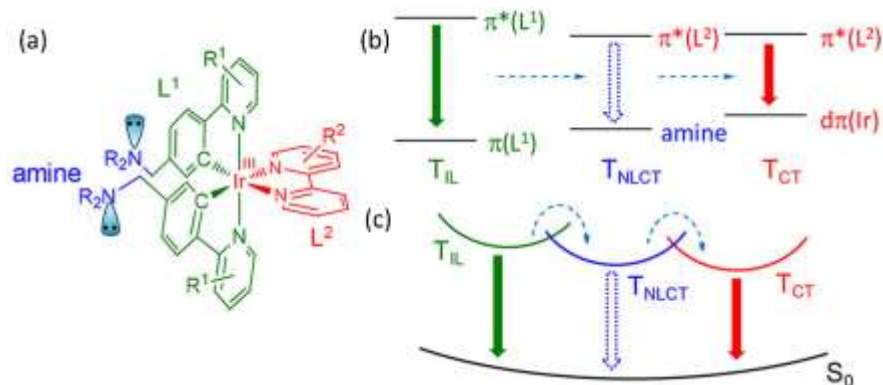
Fig. 53. (a) Structure skeleton of a potential dual phosphorescent Ir(III) complex. (b) Energy diagrams showing the states involved in IL, NLCT, and CT transitions. (b) Energy diagrams for ground and excited states showing that the NLCT state interrupts the internal conversion, resulting in dual phosphorescence from both ^{3}CT and ^{3}IL states. Adapted from ref. [237] with permission from the American Chemical Society.

As shown in Fig. 52 complex **145** exhibits an easy detectable change in emission colour from green in hypoxic conditions to red in excess O_2 concentrations. The mechanism behind this colour change relies on the different quenching efficiencies by oxygen for the two different emissions. As mentioned in a previous section, the high energy (HE) and low energy (LE) emission bands in the spectrum of complex **145** (Fig. 52) can be assigned to emission from ^{3}IL and ^{3}MLLCT excited states, respectively. The lifetimes of these two states are quite different: for complex **145** in the presence of air they were 0.36 μs and 36 ns, respectively.

According to the Stern-Vollmer equation:

$$\frac{I_0}{I} = \frac{\tau_0}{\tau} = 1 + k_q \tau_0 \left[O_2 \right]$$

where I_0 and I are respectively the intensities in the presence and absence of oxygen, τ_0 and τ are the corresponding lifetimes, and k_q is the quenching rate. The quenching efficiency or Stern-Volmer constant, $K_{SV} = \tau_0 k_q$, is proportional to the phosphorescence lifetime, indicating that a longer excited-state lifetime will favor non-radiative quenching. In the presence of air, complex **145** emits a yellow luminescence that is turned into green or red when either N_2 or O_2 are bubbled into the sample, respectively. Taking into account the large difference between the measured lifetimes of the two emitting states these changes can be explained considering that upon

69

bubbling N_2 or pure O_2, the lifetime of the HE state was correspondingly elongated or shortened, while that of the LE one was negligibly altered. This changed dramatically the quenching efficiency of the HE state so that in an hypoxic environment the spectrum is dominated by the HE band while in an hyperoxic environment it corresponds basically to the LE band.

The highly sensitive phosphorescence spectrum of complex **145** toward O_2 and its AIE-active nature, which lead to an enhancement of the emission in aggregated media, were shown to provide an excellent means for detection of both hypoxia and hyperoxia in living cells and biological tissues. Additionally, complex **145** was employed for O_2 monitoring in zebrafish. The complex (10μM, 50pL) was injected into 4- day-old zebrafish at the head. Upon photoexcitation, the whole zebrafish was intensely emissive, although long-lived phosphorescence signals were found only in the head region. The response of these signals toward different concentrations of O_2 was analysed. Bubbling either 5% or 50% O_2 into the culture media of the zebrafish did not cause any noticeable effect on the LE red phosphorescence signal, but enhanced or quenched, respectively, the green HE phosphorescence, demonstrating the sensitive profile response toward in vivo hypoxia and hyperoxia conditions.

3.4 AIE metal complexes for OLEDs

AIE materials with high quantum efficiencies have had a significant role in the development of future display technologies, i.e. OLEDs [5, 6, 10, 239-243] Efficient solid-state emitting materials are promising candidates for OLEDs. The research area of AIE-active metal complexes for display technologies is still limited. Ir(III) complexes with attractive emission features show often a weak emission in solid state because of triplet-triplet annihilation processes and for this reason AIE metal complexes that could circumvent this problem are nowadays actively sought for.

In 2011, You and co-workers synthesized two strongly emissive solid-state complexes, Ir(tfmppy)$_2$ (tpip) (**146**, tfmppy = 4-trifluoromethylphenylpyridine, tpip=tetraphe-nylimido-diphosphinate) and Ir(dfppy)$_2$(tpip) (**147**, dfppy = 4,6-difluorophenylpyridine) [244] (Fig. 54). The ancillary ligand Htpip (tetraphenylimidodiphosphinate acid) was purposely used to alter the lifetime as well as the emission wavelength. These two complexes were stable up to 361 and 411°C, respectively. The EL efficiency of complex **147** was evaluated using it as guest material in a **147**: mCP (20 nm, 10 wt%)/ TPBi (40 nm)/LiF (1 nm)/Al (100 nm) structure, with the device

showing a maximum luminance of 38 963 cd.m^{-2} at a voltage of 11.5 V and only a 6.7% efficiency roll-off from 100 to 1000 cd m^{-2}.
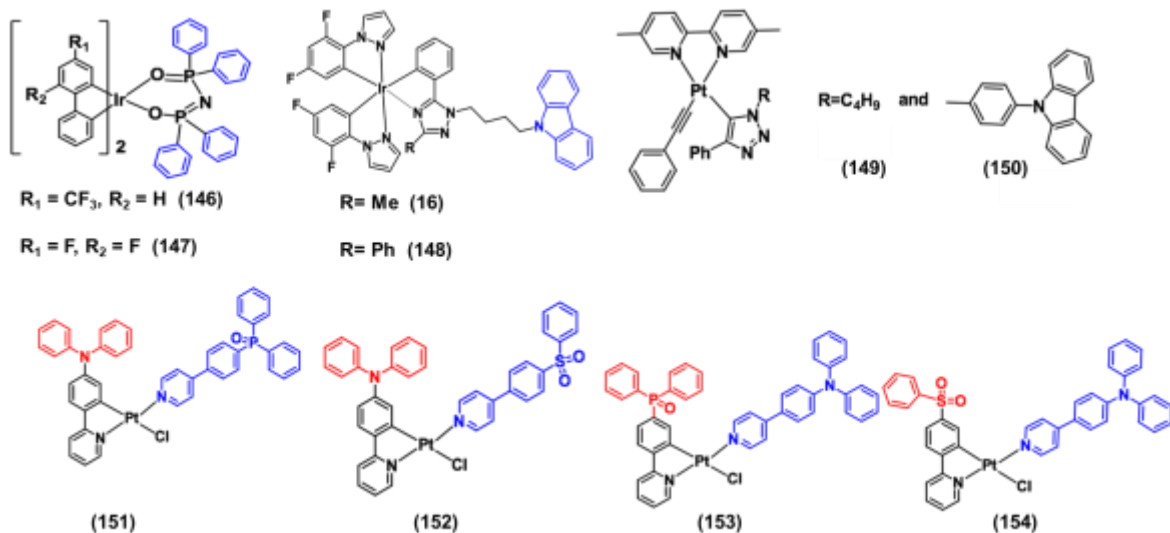
Fig. 54. Molecular structures of complexes **146-154**.

Recently, Su and co-workers have fabricated a non-doped OLED using AIE-active Ir(III) complexes **16** with Commission Internationale de l'Eclairage (CIE) coordinates of (0.29, 0.48) using a solution process (Fig. 54) [245]. The device achieved a maximum current efficiency (η_c) of 25.7 cd A^{-1} and 7.6% external quantum efficiency (η_{ext}) using the configuration glass/indium tin oxide (ITO)/PEDOT:PSS/**16**: BMIMPF 6 (5:1)/Al, where PEDOT:PSS is poly(3,4-ethylenedioxythiophene):poly(styrenesulfonate) and is inserted to facilitate the hole injection. Additionally, the 1-butyl-3-methyl-imidazolium hexafluorophosphate (BMIMPF$_6$) was added into the emitting layer to improve the turn on voltage and response time of the device. Another AIE-active Ir(III) complex (**148**) with phenyl substitution was also used for non-doped OLED showed high device performance with a η_c = 13.1 cd A^{-1} and a η_{ext} of 4.2%, respectively.

The J-aggregation behavior of IrPPy(PPh$_3$)$_2$(H)(Cl) (**8**) was utilized by our group to develop an innovative technique to fabricate an EL device by utilizing its aggregation properties (Fig. 55) [93]. The OLED was fabricated at the air–water interface using the Langmuir–Blodgett (LB) technique with the device containing a multilayer LB film (15-monolayer) of supramolecular wires as active component, a bathophenanthroline (BPhen) electron transport layer, and a N,N-di(naphthalene1-yl)-N,N′-diphenylbenzidine (NPD) hole transport layer. With a threshold

voltage of 3 V the device exhibited a luminance of ~ 260 Cd m^{-2} at 13 V with an 0.35% external quantum efficiency.
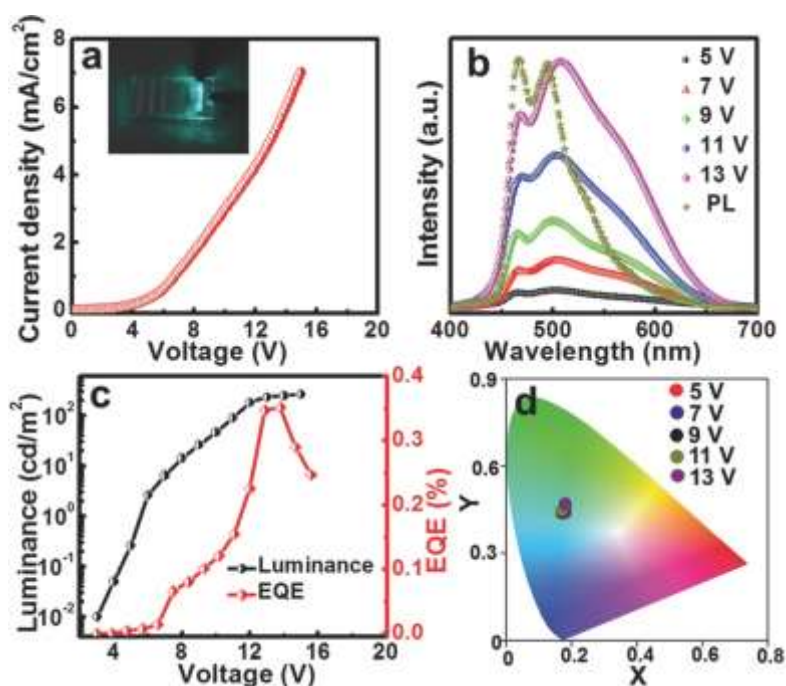
Fig. 55. (a) Current density versus voltage curve of the LED. Inset shows the photograph of working LED for complex 8. (b) Bias-dependent EL spectra of the device along with the solid-state PL spectrum. (c) Luminance versus voltage (black dotted line) and external quantum efficiency versus voltage (red square line) characteristics of LED. (d) Calculated CIE chromaticity coordinates of the emissive colors under different bias voltages. The bias voltages are shown in the inset. Adapted from ref. [93] with permission from WILEY-VCH.

Besides Ir(III) complexes, Pt(II) compounds are also considered as suitable candidates for flat panel displays and many phosphorescent Pt(II) complexes have been successfully applied as emission layers in OLED fabrication because of their efficient intersystem crossing (ISC), high phosphorescent quantum yields, relatively short triplet state lifetimes, and tunable emission colours (from blue to red) [246, 247]. In 2014, Yam's group synthesized two AIE-active unsymmetrical bipyridine−Pt (II)-alkynyl complexes (**149-150**) by using a post-click reaction (Fig.54) [248]. The photoluminescence quantum yield of complex **149** was found to increase by 24-fold in 5% doped 1,3-bis(N-carbazolyl)benzene (MCP) compared to DCM solution. The

complexes were successfully applied as dopants in phosphorescent organic light-emitting diodes (PHOLEDs) with the configuration of indium tin oxide (ITO)/poly(ethylenedioxythiophene):poly(styrene sulfonic acid) (PEDOT:PSS) (70 nm)/5% **149** or **150**:MCP (60 nm)/1,3bis[3,5-di(pyridine-3-yl)phenyl]benzene (BmPyPhB) (30 nm)/LiF (0.8 nm)/Al (100 nm). The device containing **149** showed a better performance, with a maximum current efficiency of 18.4 cd A^{-1}, a power efficiency of 8.0 Lm W^{-1} and an external quantum efficiency of up to 5.8%.

Wu and co-workers developed a series of AIE-active Pt(II)(C^N)(N-donorligand)Cl complexes (**151-154**) (Fig.54) [60] strategically designed with –SO_2Ph and –$POPh_2$ groups (for improved electron injection/ transport) and –NPh_2 (for improved hole injection/transport) of the device. PMMA films including complex **154** have a 17 times higher phosphorescence quantum yield than DCM solutions. Finally, these complexes show a good response in OLED devices fabricated with an ITO/PEDOT: PSS (45 nm)/emission layer, EML Pt x%:CBP (40 nm)/TPBi (45 nm)/LiF (1 nm)/Al (100 nm) configuration. The device with 6.0 wt% **154** was found to the best candidate with a 28.4% external efficiency, $\eta_L = 75.9$ cd A^{-1} maximal current efficiency, and $\eta_P = 62.7$ lmW^{-1} maximal power efficiency.

3.5 Miscellaneous applications of AIE-active metal complexes

Besides the more standard applications described in previous sections, AIE-active metal containing molecules have also been proposed for other somewhat surprising applications. In this closing section we describe some of these new proposals, showing the wide range of possible technological developments that might be found for new compounds with an effective AIE.
Using the piezochromic and vapochromic properties of complex **117**, an innovative technology for information encryption and decryption was designed. To demonstrate the viability of such an application a filter paper was soaked in a CH_2Cl_2 solution of (E)-4-sulphonic-40-dimethylaminoazastilbene (SDMAB) dye for 1h [62]. The soaked paper, showing a yellow colour under 356 nm UV excitation, was used as background. A rubber stamp with letters "NJ TECH" was dipped into solution of complex **117** and stamped on the filter paper on which the letters were not visible (encryption process). In the decryption stage, 10 min exposure to DCM can turn on the emission to green and the "NJ TECH" can be easily read (Fig. 56e).
Reference [104] describes a dual level anti-counterfeit application based on AIE-active complex **19,** which was found to have an excellent PCL performance. Their authors used a fluorescent

(MASK) Schiff base with a similar emission around 610 nm as complex **19**. After mechanical grinding the MASK along with the complex, resulted in a product (G) with an emission colour that was undistinguishable from that of MASK under 365 nm UV. The authors made flower-shaped orange anti-counterfeit trademark containing a central 'stamen' made of MASK and a 'petal' made of G (Fig. 56 b-c). The first level of the anti-counterfeit system was presented by exposing the device to DCM. As a result, the emission of the 'petal' changed from orange (G) to yellow (D). The second level was demonstrated by regenerating the original colour of G after grinding. A data encryption/decryption device was successfully designed where G was used as cryptographic ink and MASK as a control reagent. The characters "NENU" were written on the filter paper by using MASK, then the letters "AIPE" were spread over it. The word "AIEP" can then be made visible under 356 nm irradiation after exposure to DCM (Fig. 56d).

Recently, Liu and co-workers synthesized an AIE-active complex **155** with dual emission (λ_{max} = 362 nm, Φ = 0.16 and λ_{max} = 494 nm, Φ = 0.59) that was further employed for visualization of latent finger-marks (LFs), demonstrating the possible application of complex **155** in criminal investigations [249]. For this purpose, the aggregate of complex **155** (f_w = 90%, 1.0×10^{-4} mol/L) was used to visualize the sebaceous finger-marks on a surface. The finger marks were carefully washed with an ethanol-water mixture and after drying at room temperature, the images were captured using a camera under 365 nm UV excitation as shown in (Fig. 56f-h).
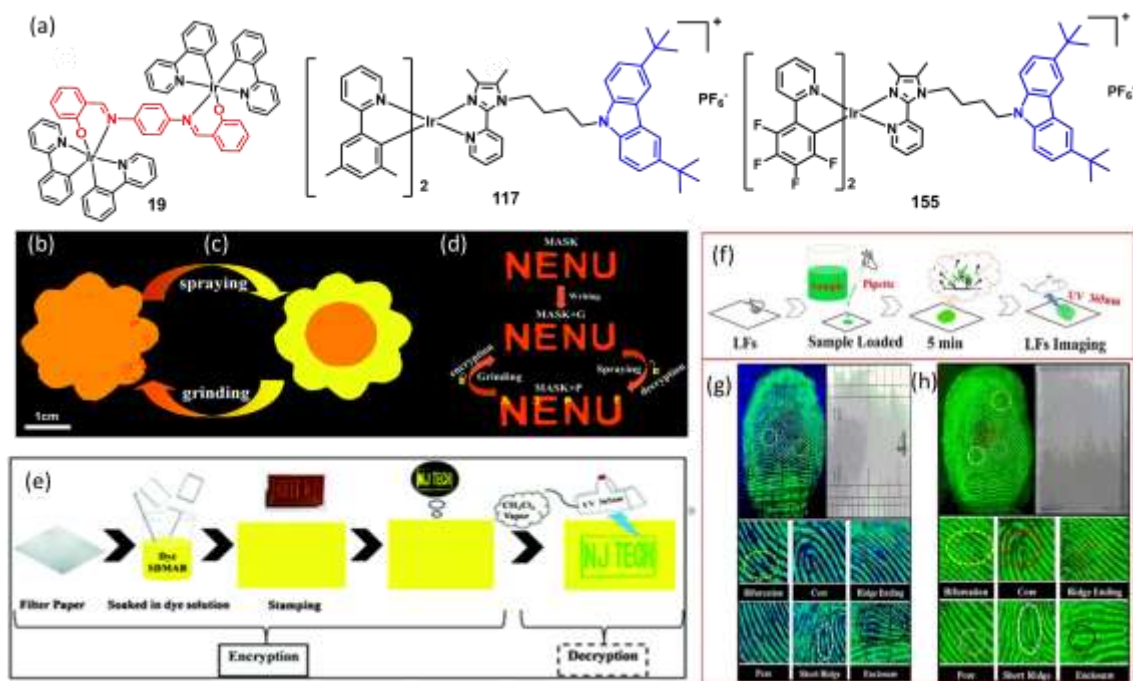
Fig. 56. (a) Molecular structure of complexes **19**, **117** and **155**; Photographic images of **19** (b) first-level anti-counterfeit trademark, (c) Second-level anti-counterfeit trademark and (d) Information encryption and decryption devices. Note the appearance of the word 'AIPE' in yellow letters within the bottom 'NENU'. Adapted from ref. [104] with permission from the Royal Society of Chemistry. (e) Data encryption and decryption process using complex **117**. Adapted from ref. [62]. with permission from the Royal Society of Chemistry, (f) Procedures and photographs of latent finger-marks (LFs) detection v using AIE-active complex **155**. LFs images on (g) stainless steel and (h) glass under 365 nm UV irradiation. Adapted from ref. [249] with permission from Elsevier.

4. Conclusions

Aggregation Induced Emission (AIE) is observed for some luminescent molecules which are poorly emissive in solution but produce an extraordinary bright emission upon aggregation. The synthesis in recent years of numerous AIE-active molecules has offered a great opportunity to study the photo-physical properties of such compounds unravelling the subtle mechanistic pathways that lead to this phenomenon. Furthermore, the AIE-active molecules have proved their great potentiality in many important and relevant applications where luminescence from solid samples or thin films is highly desirable *e.g.*, optoelectronics, bio-imaging, chemo-sensing and multi-stimuli responsive materials. After the initial bloom of new organic AIE fluorophores,

75

the scientific community steps up for the development of new transition metal based AIEgens, opening the field of applications to phosphorescent luminogens. The first AIE-active Pt(II) and Re(I) based metal complexes were reported in 2002. Since then, scientists worldwide began to explore this path with complexes including other metal ions. Heavy metal complexes containing Ir(III), Pt(II), Os(II) or Au(I) which have been known as efficient phosphorescent materials with high quantum yields, long triplet state life times and large Stokes' shifts provided a direction for further expansion in the family of AIE-active compounds.

The most fruitful concept in the development of new AIE systems has been that of restriction of intramolecular motion (RIM), encompassing the earlier suggestions of restriction of intramolecular rotations (RIR) and restriction of intramolecular vibrations (RIV). Following the ideas behind the RIM mechanism, propeller-shaped and shell-like molecular fragments have been incorporated to luminescent cores in order to quench the emission for isolated molecules in solution while preventing the formation of detrimental species such as excimers upon aggregation that could lead to the well-known ACQ effect. A fruitful strategy to translate these ideas from organic molecules to transition metal complexes has been the inclusion of highly flexible ancillary PPh$_3$ ligands containing rotatable phenyl rings in Ir(III) complexes to obtain highly efficient phosphorescent AIEgens

In this review, we have tried to cover all AIE systems containing d-block metals such as Au(I), Ir(III), Pt(II), Os(IV), Pd(II), Zn(II), Cu(I), Re(I), Ru(II). The studied Au(I) complexes exhibit metallophilic interactions and strong π-π stacking along with a few other interactions that lead to an effective metal-metal induced RIM upon aggregation. These AIE-Au complexes have been mainly studied because of their mechanochromism and/or vapochromism as well as in the fabrication of white OLEDs. Similarly, in the case of Pt(II) complexes, the AIE property is strongly related to the formation of strong MMLCT or MLLCT excited states, absent in the isolated molecules in solution. For other metals, the simplest methodology to induce AIE is to incorporate bulky rotor groups to provide an effective RIM upon aggregation. Most of the Ir(III), Cu(II), Zn(II), Os(IV) and Pd(II) AIE-active luminophores were decorated by rotor groups resulting in a remarkable emission enhancement in aggregates. An interesting feature of Ir-AIE systems is the possibility of easily tuning the emission wavelength of the AIE from blue to red by systematic variation of the chromophoric ligands. The tunable phosphorescent emission at room temperature with long luminescence lifetimes, of several microseconds, makes more abundant elements with d^{10} electronic configuration such as Zn(II) and Cu(I) active competitors

76

of costly metals such as Ir(III), Pt(II), Os(II), Re(I) or Ru(II). The application of AIE-Cu(I) complexes in bio-imaging, for instance, has drawn an immense interest in the scientific community. The multi-stimuli response indicates the vast potentiality of Zn(II)-AIE systems which can be explored for other applications such as bio-imaging or the fabrication of optoelectronic devices. The polypyridyl complexes of Ru(II) have been extensively studied and used as DNA structural probes or new therapeutic agents, although the development of Ru(II)-AIE systems remains almost untouched, opening an opportunity for research groups to design and synthesize new complexes. In a similar way Re(I) complexes with long alkyl chains exhibiting AIE properties have been used for explosive sensing and the emission enhancement of Re(I) AIE complexes after formation of micelles or vesicles has been used in mimicking biological systems and drug delivery. The inclusion of a N,N-bidentate ligand with bulky groups and ligands with propeller-shaped structures has been proved to be an effective strategy for introducing the AIE property in the system.

Finally, the development of new metal based new AIE systems is highly desirable for many applications *e.g.*, biomolecular sensing, biological imaging, chemical sensing (explosives, ions, pH, gases, peroxides, fingerprints, viscosity etc.), as stimuli responsive materials, (force, heat, vapour, etc), or in optoelectronic systems (*e.g.*, light-emitting diodes, organic field-effect transistors, optical waveguides, etc.). The simplicity and the promising applications of the AIE systems, will undoubtedly encourage scientists to develop new transition metal based AIE-active complexes which will not only enlarge the number of these systems, but will certainly play a major role in various state-of the art technological applications.

Acknowledgements

References

[1] G. Li, T. Fleetham, E. Turner, X.-C. Hang, J. Li, Highly Efficient and Stable Narrow-Band Phosphorescent Emitters for OLED Applications, Advanced Optical Materials, 3 (2015) 390-397.

[2] J. Jayabharathi, V. Thanikachalam, R. Sathishkumar, Highly phosphorescent green emitting iridium(iii) complexes for application in OLEDs, New Journal of Chemistry, 39 (2015) 235-245.

[3] W.Z. Yuan, Y. Gong, S. Chen, X.Y. Shen, J.W.Y. Lam, P. Lu, Y. Lu, Z. Wang, R. Hu, N. Xie, H.S. Kwok, Y. Zhang, J.Z. Sun, B.Z. Tang, Efficient Solid Emitters with Aggregation-Induced Emission and Intramolecular Charge Transfer Characteristics: Molecular Design, Synthesis, Photophysical Behaviors, and OLED Application, Chemistry of Materials, 24 (2012) 1518-1528.

[4] H. Sasabe, J. Kido, Multifunctional Materials in High-Performance OLEDs: Challenges for Solid-State Lighting, Chemistry of Materials, 23 (2011) 621-630.

[5] Y. Chi, P.-T. Chou, Transition-metal phosphors with cyclometalating ligands: fundamentals and applications, Chemical Society Reviews, 39 (2010) 638-655.

[6] Y. You, S.Y. Park, Phosphorescent iridium(iii) complexes: toward high phosphorescence quantum efficiency through ligand control, Dalton Transactions, (2009) 1267-1282.

[7] W.-Y. Wong, C.-L. Ho, Functional metallophosphors for effective charge carrier injection/transport: new robust OLED materials with emerging applications, Journal of Materials Chemistry, 19 (2009) 4457-4482.

[8] W.-Y. Wong, C.-L. Ho, Heavy metal organometallic electrophosphors derived from multi-component chromophores, Coordination Chemistry Reviews, 253 (2009) 1709-1758.

[9] A.F. Rausch, M.E. Thompson, H. Yersin, Matrix Effects on the Triplet State of the OLED Emitter Ir(4,6-dFppy)2(pic) (FIrpic): Investigations by High-Resolution Optical Spectroscopy, Inorganic Chemistry, 48 (2009) 1928-1937.

[10] H. Yersin, Highly efficient OLEDs with phosphorescent materials, John Wiley & Sons, 2008.

[11] L. Cao, R. Zhang, W. Zhang, Z. Du, C. Liu, Z. Ye, B. Song, J. Yuan, A ruthenium(II) complex-based lysosome-targetable multisignal chemosensor for in vivo detection of hypochlorous acid, Biomaterials, 68 (2015) 21-31.

[12] Y. You, Phosphorescence bioimaging using cyclometalated Ir(III) complexes, Current Opinion in Chemical Biology, 17 (2013) 699-707.

[13] K.K.-W. Lo, A.W.-T. Choi, W.H.-T. Law, Applications of luminescent inorganic and organometallic transition metal complexes as biomolecular and cellular probes, Dalton Transactions, 41 (2012) 6021-6047.

[14] Y. Jeong, J. Yoon, Recent progress on fluorescent chemosensors for metal ions, Inorganica Chimica Acta, 381 (2012) 2-14.

[15] J. Chan, S.C. Dodani, C.J. Chang, Reaction-based small-molecule fluorescent probes for chemoselective bioimaging, Nature Chemistry, 4 (2012) 973-984.

[16] Q. Zhao, C. Huang, F. Li, Phosphorescent heavy-metal complexes for bioimaging, Chemical Society Reviews, 40 (2011) 2508-2524.

[17] H. Wu, T. Yang, Q. Zhao, J. Zhou, C. Li, F. Li, A cyclometalated iridium(iii) complex with enhanced phosphorescence emission in the solid state (EPESS): synthesis, characterization and its application in bioimaging, Dalton Transactions, 40 (2011) 1969-1976.

[18] W.-C. Wu, C.-Y. Chen, Y. Tian, S.-H. Jang, Y. Hong, Y. Liu, R. Hu, B.Z. Tang, Y.-T. Lee, C.-T. Chen, W.-C. Chen, A.K.Y. Jen, Enhancement of Aggregation-Induced Emission in Dye-Encapsulating Polymeric Micelles for Bioimaging, Advanced Functional Materials, 20 (2010) 1413-1423.

[19] W. Lv, T. Yang, Q. Yu, Q. Zhao, K.Y. Zhang, H. Liang, S. Liu, F. Li, W. Huang, A Phosphorescent Iridium(III) Complex-Modified Nanoprobe for Hypoxia Bioimaging Via Time-Resolved Luminescence Microscopy, Advanced Science, 2 (2015) 1500107.

[20] G. Ambrosi, E. Borgogelli, M. Formica, V. Fusi, L. Giorgi, M. Micheloni, E. Rampazzo, M. Sgarzi, N. Zaccheroni, L. Prodi, PluS Nanoparticles as a tool to control the metal complex stoichiometry of a new thio-aza macrocyclic chemosensor for Ag(I) and Hg(II) in water, Sensors and Actuators B: Chemical, 207, Part B (2015) 1035-1044.

[21] D. En, Y. Guo, B.-T. Chen, B. Dong, M.-J. Peng, Coumarin-derived Fe3+-selective fluorescent turn-off chemosensors: synthesis, properties, and applications in living cells, RSC Advances, 4 (2014) 248-253.

[22] H.S. Jung, X. Chen, J.S. Kim, J. Yoon, Recent progress in luminescent and colorimetric chemosensors for detection of thiols, Chemical Society Reviews, 42 (2013) 6019-6031.

[23] Y. Zhou, J. Yoon, Recent progress in fluorescent and colorimetric chemosensors for detection of amino acids, Chemical Society Reviews, 41 (2012) 52-67.

[24] M. Formica, V. Fusi, L. Giorgi, M. Micheloni, New fluorescent chemosensors for metal ions in solution, Coordination Chemistry Reviews, 256 (2012) 170-192.

[25] V. Guerchais, J.-L. Fillaut, Sensory luminescent iridium(III) and platinum(II) complexes for cation recognition, Coordination Chemistry Reviews, 255 (2011) 2448-2457.

[26] Q. Zhao, F. Li, C. Huang, Phosphorescent chemosensors based on heavy-metal complexes, Chemical Society Reviews, 39 (2010) 3007-3030.

[27] M. Wang, G. Zhang, D. Zhang, D. Zhu, B.Z. Tang, Fluorescent bio/chemosensors based on silole and tetraphenylethene luminogens with aggregation-induced emission feature, Journal of Materials Chemistry, 20 (2010) 1858-1867.

[28] K.M.-C. Wong, V.W.-W. Yam, Luminescence platinum(II) terpyridyl complexes—From fundamental studies to sensory functions, Coordination Chemistry Reviews, 251 (2007) 2477-2488.

[29] G.-G. Shan, H.-B. Li, D.-X. Zhu, Z.-M. Su, Y. Liao, Intramolecular π-stacking in cationic iridium(iii) complexes with a triazole-pyridine type ancillary ligand: synthesis, photophysics, electrochemistry properties and piezochromic behavior, Journal of Materials Chemistry, 22 (2012) 12736-12744.

[30] C. Ulbricht, B. Beyer, C. Friebe, A. Winter, U.S. Schubert, Recent Developments in the Application of Phosphorescent Iridium(III) Complex Systems, Advanced Materials, 21 (2009) 4418-4441.

[31] Z. Ning, Z. Chen, Q. Zhang, Y. Yan, S. Qian, Y. Cao, H. Tian, Aggregation-induced Emission (AIE)-active Starburst Triarylamine Fluorophores as Potential Non-doped Red Emitters for Organic Light-emitting Diodes and Cl₂ Gas Chemodosimeter, Advanced Functional Materials, 17 (2007) 3799-3807.

[32] T. Kato, Hydrogen-bonded liquid crystals: Molecular self-assembly for dynamically functional materials, Struct. Bond., 96 (2000) 95-146.

[33] G. Scheibe, Über die Veränderlichkeit der Absorptionsspektren in Lösungen und die Nebenvalenzen als ihre Ursache, Angewandte Chemie, 50 (1937) 212-219.

[34] E.E. Jelley, Spectral Absorption and Fluorescence of Dyes in the Molecular State, Nature, 138 (1936) 1009-1010.

[35] M. Yang, Y. Zhang, W. Zhu, H. Wang, J. Huang, L. Cheng, H. Zhou, J. Wu, Y. Tian, Difunctional chemosensor for Cu(II) and Zn(II) based on Schiff base modified anthryl derivative with aggregation-induced emission enhancement and piezochromic characteristics, Journal of Materials Chemistry C, 3 (2015) 1994-2002.

[36] K. Benelhadj, W. Muzuzu, J. Massue, P. Retailleau, A. Charaf-Eddin, A.D. Laurent, D. Jacquemin, G. Ulrich, R. Ziessel, White Emitters by Tuning the Excited-State Intramolecular Proton-Transfer Fluorescence Emission in 2-(2'-Hydroxybenzofuran)benzoxazole Dyes, Chemistry – A European Journal, 20 (2014) 12843-12857.

[37] Q. Zhao, S. Zhang, Y. Liu, J. Mei, S. Chen, P. Lu, A. Qin, Y. Ma, J.Z. Sun, B.Z. Tang, Tetraphenylethenyl-modified perylene bisimide: aggregation-induced red emission, electrochemical properties and ordered microstructures, Journal of Materials Chemistry, 22 (2012) 7387-7394.

[38] J. Jortner, Spiers Memorial Lecture On Dynamics From isolated molecules to biomolecules, Faraday Discussions, 108 (1997) 1-22.

[39] E. Matayoshi, G. Wang, G. Krafft, J. Erickson, Novel fluorogenic substrates for assaying retroviral proteases by resonance energy transfer, Science, 247 (1990) 954-958.

[40] F. Würthner, T.E. Kaiser, C.R. Saha-Möller, J-Aggregates: From Serendipitous Discovery to Supramolecular Engineering of Functional Dye Materials, Angewandte Chemie International Edition, 50 (2011) 3376-3410.

[41] J. Hoche, H.-C. Schmitt, A. Humeniuk, I. Fischer, R. Mitrić, M.I.S. Röhr, The mechanism of excimer formation: an experimental and theoretical study on the pyrene dimer, Physical Chemistry Chemical Physics, 19 (2017) 25002-25015.

[42] R.E. Cook, B.T. Phelan, R.J. Kamire, M.B. Majewski, R.M. Young, M.R. Wasielewski, Excimer Formation and Symmetry-Breaking Charge Transfer in Cofacial Perylene Dimers, The Journal of Physical Chemistry A, 121 (2017) 1607-1615.

[43] E.A. Chandross, C.J. Dempster, Intramolecular excimer formation and fluorescence quenching in dinaphthylalkanes, Journal of the American Chemical Society, 92 (1970) 3586-3593.

[44] M.A. Slifkin, Charge Transfer and Excimer Formation, Nature, 200 (1963) 766.

[45] X.-M. Liu, C. He, X.-T. Hao, L.-W. Tan, Y. Li, K.S. Ong, Hyperbranched Blue-Light-Emitting Alternating Copolymers of Tetrabromoarylmethane/Silane and 9,9-Dihexylfluorene-2,7-diboronic Acid, Macromolecules, 37 (2004) 5965-5970.

[46] S. Hecht, J.M.J. Fréchet, Dendritic Encapsulation of Function: Applying Nature's Site Isolation Principle from Biomimetics to Materials Science, Angewandte Chemie International Edition, 40 (2001) 74-91.

[47] A.W. Freeman, S.C. Koene, P.R.L. Malenfant, M.E. Thompson, J.M.J. Fréchet, Dendrimer-Containing Light-Emitting Diodes: Toward Site-Isolation of Chromophores, Journal of the American Chemical Society, 122 (2000) 12385-12386.

[48] J. Luo, Z. Xie, J.W.Y. Lam, L. Cheng, H. Chen, C. Qiu, H.S. Kwok, X. Zhan, Y. Liu, D. Zhu, B.Z. Tang, Aggregation-induced emission of 1-methyl-1,2,3,4,5-pentaphenylsilole, Chemical Communications, (2001) 1740-1741.

[49] Z. Zhao, B. He, B.Z. Tang, Aggregation-induced emission of siloles, Chemical Science, 6 (2015) 5347-5365.

[50] J. Mei, Y. Hong, J.W.Y. Lam, A. Qin, Y. Tang, B.Z. Tang, Aggregation-Induced Emission: The Whole Is More Brilliant than the Parts, Advanced Materials, 26 (2014) 5429-5479.

[51] Y. Hong, J.W.Y. Lam, B.Z. Tang, Aggregation-induced emission, Chemical Society Reviews, 40 (2011) 5361-5388.

[52] J. Mei, N.L.C. Leung, R.T.K. Kwok, J.W.Y. Lam, B.Z. Tang, Aggregation-Induced Emission: Together We Shine, United We Soar!, Chemical Reviews, 115 (2015) 11718-11940.

[53] R. Hu, Q. Zang, B.Z. Tang, Recent Progress in New AIE Structural Motifs, in: Aggregation-Induced Emission: Materials and Applications Volume 1, American Chemical Society, 2016, pp. 193-219.

[54] V.W.-W. Yam, V.K.-M. Au, S.Y.-L. Leung, Light-Emitting Self-Assembled Materials Based on d8 and d10 Transition Metal Complexes, Chemical Reviews, 115 (2015) 7589-7728.

[55] V. Sathish, A. Ramdass, P. Thanasekaran, K.-L. Lu, S. Rajagopal, Aggregation-induced phosphorescence enhancement (AIPE) based on transition metal complexes—An overview, Journal of Photochemistry and Photobiology C: Photochemistry Reviews, 23 (2015) 25-44.

[56] R.T.K. Kwok, C.W.T. Leung, J.W.Y. Lam, B.Z. Tang, Biosensing by luminogens with aggregation-induced emission characteristics, Chemical Society Reviews, 44 (2015) 4228-4238.

[57] H. Braunschweig, T. Dellermann, R.D. Dewhurst, B. Hupp, T. Kramer, J.D. Mattock, J. Mies, A.K. Phukan, A. Steffen, A. Vargas, Strongly Phosphorescent Transition Metal π-Complexes of Boron–Boron Triple Bonds, Journal of the American Chemical Society, 139 (2017) 4887-4893.

[58] Z. He, C. Ke, B.Z. Tang, Journey of Aggregation-Induced Emission Research, ACS Omega, 3 (2018) 3267-3277.

[59] X. Cai, F. Hu, G. Feng, R.T.K. Kwok, B. Liu, B.Z. Tang, Organic Mitoprobes based on Fluorogens with Aggregation-Induced Emission, Israel Journal of Chemistry, 58 (2018) 860-873.

[60] J. Zhao, Z. Feng, D. Zhong, X. Yang, Y. Wu, G. Zhou, Z. Wu, Cyclometalated Platinum Complexes with Aggregation-Induced Phosphorescence Emission Behavior and Highly Efficient Electroluminescent Ability, Chemistry of Materials, 30 (2018) 929-946.

[61] Y. Jiang, G. Li, D. Zhu, Z. Su, M.R. Bryce, An AIE-active phosphorescent Ir(iii) complex with piezochromic luminescence (PCL) and its application for monitoring volatile organic compounds (VOCs), Journal of Materials Chemistry C, 5 (2017) 12189-12193.

[62] Z. Song, R. Liu, Y. Li, H. Shi, J. Hu, X. Cai, H. Zhu, AIE-active Ir(iii) complexes with tunable emissions, mechanoluminescence and their application for data security protection, Journal of Materials Chemistry C, 4 (2016) 2553-2559.

[63] J. Wang, S. Tang, A. Sandström, L. Edman, Combining an Ionic Transition Metal Complex with a Conjugated Polymer for Wide-Range Voltage-Controlled Light-Emission Color, ACS Applied Materials & Interfaces, 7 (2015) 2784-2789.

[64] S.M. Parke, E. Rivard, Aggregation Induced Phosphorescence in the Main Group, Israel Journal of Chemistry, 58 (2018) 915-926.

[65] L. Ravotto, P. Ceroni, Aggregation induced phosphorescence of metal complexes: From principles to applications, Coordination Chemistry Reviews, 346 (2017) 62-76.

[66] M. Mauro, C. Cebrián, Aggregation-induced Phosphorescence Enhancement in Ir(III) Complexes, Israel Journal of Chemistry, 58 (2018) 901-914.

[67] K.A. King, P.J. Spellane, R.J. Watts, Excited-state properties of a triply ortho-metalated iridium(III) complex, Journal of the American Chemical Society, 107 (1985) 1431-1432.

[68] S. Lamansky, P. Djurovich, D. Murphy, F. Abdel-Razzaq, H.-E. Lee, C. Adachi, P.E. Burrows, S.R. Forrest, M.E. Thompson, Highly Phosphorescent Bis-Cyclometalated Iridium Complexes: Synthesis, Photophysical Characterization, and Use in Organic Light Emitting Diodes, Journal of the American Chemical Society, 123 (2001) 4304-4312.

[69] Y. You, S.Y. Park, Inter-Ligand Energy Transfer and Related Emission Change in the Cyclometalated Heteroleptic Iridium Complex: Facile and Efficient Color Tuning over the Whole Visible Range by the Ancillary Ligand Structure, Journal of the American Chemical Society, 127 (2005) 12438-12439.

[70] F.N. Castellano, I.E. Pomestchenko, E. Shikhova, F. Hua, M.L. Muro, N. Rajapakse, Photophysics in bipyridyl and terpyridyl platinum(II) acetylides, Coordination Chemistry Reviews, 250 (2006) 1819-1828.

[71] Y. You, W. Nam, Photofunctional triplet excited states of cyclometalated Ir(iii) complexes: beyond electroluminescence, Chemical Society Reviews, 41 (2012) 7061-7084.

[72] G. Stokes George, XVI. On the change of refrangibility of light.—No. II, Philosophical Transactions of the Royal Society of London, 143 (1853) 385-396.

[73] Y. Kawamura, K. Goushi, J. Brooks, J.J. Brown, H. Sasabe, C. Adachi, 100% phosphorescence quantum efficiency of Ir(III) complexes in organic semiconductor films, Applied Physics Letters, 86 (2005) 071104.

[74] N. Nirmalananthan, T. Behnke, K. Hoffmann, D. Kage, C.F. Gers-Panther, W. Frank, T.J.J. Müller, U. Resch-Genger, Crystallization and Aggregation-Induced Emission in a Series of Pyrrolidinylvinylquinoxaline Derivatives, The Journal of Physical Chemistry C, 122 (2018) 11119-11127.

[75] J. Tong, Y.J. Wang, Z. Wang, J.Z. Sun, B.Z. Tang, Crystallization-Induced Emission Enhancement of a Simple Tolane-Based Mesogenic Luminogen, The Journal of Physical Chemistry C, 119 (2015) 21875-21881.

[76] Crystallization-Induced Phosphorescence for Purely Organic Phosphors at Room Temperature and Liquid Crystals with Aggregation-Induced Emission Characteristics, in: Aggregation-Induced Emission: Fundamentals and Applications, Volumes 1 and 2.

[77] Y.Q. Dong, J.W.Y. Lam, B.Z. Tang, Mechanochromic Luminescence of Aggregation-Induced Emission Luminogens, The Journal of Physical Chemistry Letters, 6 (2015) 3429-3436.

[78] X. Luo, J. Li, C. Li, L. Heng, Y.Q. Dong, Z. Liu, Z. Bo, B.Z. Tang, Reversible Switching of the Emission of Diphenyldibenzofulvenes by Thermal and Mechanical Stimuli, Advanced Materials, 23 (2011) 3261-3265.

[79] N.-W. Tseng, J. Liu, J.C.Y. Ng, J.W.Y. Lam, H.H.Y. Sung, I.D. Williams, B.Z. Tang, Deciphering mechanism of aggregation-induced emission (AIE): Is E-Z isomerisation involved in an AIE process?, Chemical Science, 3 (2012) 493-497.

[80] J. Wang, J. Mei, R. Hu, J.Z. Sun, A. Qin, B.Z. Tang, Click Synthesis, Aggregation-Induced Emission, E/Z Isomerization, Self-Organization, and Multiple Chromisms of Pure Stereoisomers of a Tetraphenylethene-Cored Luminogen, Journal of the American Chemical Society, 134 (2012) 9956-9966.

[81] N.L.C. Leung, N. Xie, W. Yuan, Y. Liu, Q. Wu, Q. Peng, Q. Miao, J.W.Y. Lam, B.Z. Tang, Restriction of Intramolecular Motions: The General Mechanism behind Aggregation-Induced Emission, Chemistry – A European Journal, 20 (2014) 15349-15353.

[82] J. Liang, H. Shi, R.T.K. Kwok, M. Gao, Y. Yuan, W. Zhang, B.Z. Tang, B. Liu, Distinct optical and kinetic responses from E/Z isomers of caspase probes with aggregation-induced emission characteristics, Journal of Materials Chemistry B, 2 (2014) 4363-4370.

[83] Z. He, L. Shan, J. Mei, H. Wang, J.W.Y. Lam, H.H.Y. Sung, I.D. Williams, X. Gu, Q. Miao, B.Z. Tang, Aggregation-induced emission and aggregation-promoted photochromism of bis(diphenylmethylene)dihydroacenes, Chemical Science, 6 (2015) 3538-3543.

[84] T.F.a.K. Kasper, Ein Konzentrationsumschlag der Fluoreszenz, in: Zeitschrift für Physikalische Chemie, 1954, pp. 275.

[85] J. Gierschner, S.Y. Park, Luminescent distyrylbenzenes: tailoring molecular structure and crystalline morphology, Journal of Materials Chemistry C, 1 (2013) 5818-5832.

[86] S. Yin, Q. Peng, Z. Shuai, W. Fang, Y.-H. Wang, Y. Luo, Aggregation-enhanced luminescence and vibronic coupling of silole molecules from first principles, Physical Review B, 73 (2006) 205409.

[87] C. Deng, Y. Niu, Q. Peng, A. Qin, Z. Shuai, B.Z. Tang, Theoretical study of radiative and non-radiative decay processes in pyrazine derivatives, The Journal of Chemical Physics, 135 (2011) 014304.

[88] Q. Wu, C. Deng, Q. Peng, Y. Niu, Z. Shuai, Quantum chemical insights into the aggregation induced emission phenomena: A QM/MM study for pyrazine derivatives, Journal of Computational Chemistry, 33 (2012) 1862-1869.

[89] X.-L. Peng, S. Ruiz-Barragan, Z.-S. Li, Q.-S. Li, L. Blancafort, Restricted access to a conical intersection to explain aggregation induced emission in dimethyl tetraphenylsilole, Journal of Materials Chemistry C, 4 (2016) 2802-2810.

[90] R. Crespo-Otero, Q. Li, L. Blancafort, Exploring Potential Energy Surfaces for Aggregation-Induced Emission—From Solution to Crystal, Chemistry – An Asian Journal, 14 (2019) 700-714.

[91] Q. Zhao, L. Li, F. Li, M. Yu, Z. Liu, T. Yi, C. Huang, Aggregation-induced phosphorescent emission (AIPE) of iridium(iii) complexes, Chemical Communications, (2008) 685-687.

[92] Y. You, H.S. Huh, K.S. Kim, S.W. Lee, D. Kim, S.Y. Park, Comment on 'aggregation-induced phosphorescent emission (AIPE) of iridium(iii) complexes': origin of the enhanced phosphorescence, Chemical Communications, (2008) 3998-4000.

[93] S. Maji, P. Alam, G.S. Kumar, S. Biswas, P.K. Sarkar, B. Das, I. Rehman, B.B. Das, N.R. Jana, I.R. Laskar, S. Acharya, Induced Aggregation of AIE-Active Mono-Cyclometalated Ir(III) Complex into Supramolecular Branched Wires for Light-Emitting Diodes, Small, 13 (2017) 1603780.

[94] C. Climent, P. Alam, S.S. Pasha, G. Kaur, A.R. Choudhury, I.R. Laskar, P. Alemany, D. Casanova, Dual emission and multi-stimuli-response in iridium(iii) complexes with aggregation-induced enhanced emission: applications for quantitative CO2 detection, Journal of Materials Chemistry C, 5 (2017) 7784-7798.

[95] P. Alam, G. Kaur, A. Sarmah, R.K. Roy, A.R. Choudhury, I.R. Laskar, Highly Selective Detection of H+ and OH– with a Single-Emissive Iridium(III) Complex: A Mild Approach to Conversion of Non-AIEE to AIEE Complex, Organometallics, 34 (2015) 4480-4490.

[96] P. Alam, G. Kaur, S. Chakraborty, A. Roy Choudhury, I.R. Laskar, "Aggregation induced phosphorescence" active "rollover" iridium(iii) complex as a multi-stimuli-responsive luminescence material, Dalton Transactions, 44 (2015) 6581-6592.

[97] P. Alam, G. Kaur, C. Climent, S. Pasha, D. Casanova, P. Alemany, A. Roy Choudhury, I.R. Laskar, New 'aggregation induced emission (AIE)' active cyclometalated iridium(iii) based phosphorescent sensors: high sensitivity for mercury(ii) ions, Dalton Transactions, 43 (2014) 16431-16440.

[98] P. Alam, M. Karanam, A. Roy Choudhury, I. Rahaman Laskar, One-pot synthesis of strong solid state emitting mono-cyclometalated iridium(iii) complexes: study of their aggregation induced enhanced phosphorescence, Dalton Transactions, 41 (2012) 9276-9279.

[99] P. Alam, P. Das, C. Climent, M. Karanam, D. Casanova, A.R. Choudhury, P. Alemany, N.R. Jana, I.R. Laskar, Facile tuning of the aggregation-induced emission wavelength in a common framework of a cyclometalated iridium(iii) complex: micellar encapsulated probe in cellular imaging, Journal of Materials Chemistry C, 2 (2014) 5615-5628.

[100] P. Alam, M. Karanam, D. Bandyopadhyay, A.R. Choudhury, I.R. Laskar, Aggregation-Induced Emission Activity in Iridium(III) Diimine Complexes: Investigations of Their Vapochromic Properties, European Journal of Inorganic Chemistry, 2014 (2014) 3710-3719.

[101] P. Alam, C. Climent, G. Kaur, D. Casanova, A. Roy Choudhury, A. Gupta, P. Alemany, I.R. Laskar, Exploring the Origin of "Aggregation Induced Emission" Activity and "Crystallization Induced Emission" in Organometallic Iridium(III) Cationic Complexes: Influence of Counterions, Crystal Growth & Design, 16 (2016) 5738-5752.

[102] G.-G. Shan, H.-B. Li, J.-S. Qin, D.-X. Zhu, Y. Liao, Z.-M. Su, Piezochromic luminescent (PCL) behavior and aggregation-induced emission (AIE) property of a new cationic iridium(iii) complex, Dalton Transactions, 41 (2012) 9590-9593.

[103] Y. Wu, H.-Z. Sun, H.-T. Cao, H.-B. Li, G.-G. Shan, Y.-A. Duan, Y. Geng, Z.-M. Su, Y. Liao, Stepwise modulation of the electron-donating strength of ancillary ligands: understanding the AIE mechanism of cationic iridium(iii) complexes, Chemical Communications, 50 (2014) 10986-10989.

[104] Y. Jiang, G. Li, W. Che, Y. Liu, B. Xu, G. Shan, D. Zhu, Z. Su, M.R. Bryce, A neutral dinuclear Ir(iii) complex for anti-counterfeiting and data encryption, Chemical Communications, 53 (2017) 3022-3025.

[105] G. Li, X. Ren, G. Shan, W. Che, D. Zhu, L. Yan, Z. Su, M.R. Bryce, New AIE-active dinuclear Ir(iii) complexes with reversible piezochromic phosphorescence behaviour, Chemical Communications, 51 (2015) 13036-13039.

[106] G. Li, W. Guan, S. Du, D. Zhu, G. Shan, X. Zhu, L. Yan, Z. Su, M.R. Bryce, A.P. Monkman, Anion-specific aggregation induced phosphorescence emission (AIPE) in an ionic iridium complex in aqueous media, Chemical Communications, 51 (2015) 16924-16927.

[107] G. Li, Y. Wu, G. Shan, W. Che, D. Zhu, B. Song, L. Yan, Z. Su, M.R. Bryce, New ionic dinuclear Ir(iii) Schiff base complexes with aggregation-induced phosphorescent emission (AIPE), Chemical Communications, 50 (2014) 6977-6980.

[108] J. Ma, Y. Zeng, Y. Liu, D. Wu, Thermostable polymeric nanomicelles of iridium(iii) complexes with aggregation-induced phosphorescence emission characteristics and their recyclable double-strand DNA monitoring, Journal of Materials Chemistry B, 5 (2017) 123-133.

[109] K. Ohno, T. Sakata, M. Shiiba, A. Nagasawa, T. Fujihara, A water-soluble cyclometalated iridium(iii) complex for pH sensing based on aggregation-induced enhanced phosphorescence, Dalton Transactions, (2019).

[110] L.A. Galán, D.B. Cordes, A.M.Z. Slawin, D. Jacquemin, M.I. Ogden, M. Massi, E. Zysman-Colman, Analyzing the Relation between Structure and Aggregation Induced Emission (AIE) Properties of Iridium(III) Complexes through Modification of Non-Chromophoric Ancillary Ligands, European Journal of Inorganic Chemistry, 2019 (2019) 152-163.

[111] M. Saremi, A. Amini, H. Heydari, An aptasensor for troponin I based on the aggregation-induced electrochemiluminescence of nanoparticles prepared from a cyclometallated iridium(III) complex and

poly(4-vinylpyridine-co-styrene) deposited on nitrogen-doped graphene, Microchimica Acta, 186 (2019) 254.

[112] Y. Wang, T. Yang, X. Liu, G. Li, W. Che, D. Zhu, Z. Su, New cationic Ir(iii) complexes without "any soft substituents": aggregation-induced emission and piezochromic luminescence, Journal of Materials Chemistry C, 6 (2018) 12217-12223.

[113] S.S. Pasha, P. Alam, S. Dash, G. Kaur, D. Banerjee, R. Chowdhury, N. Rath, A. Roy Choudhury, I.R. Laskar, Rare observation of 'aggregation induced emission' in cyclometalated platinum(ii) complexes and their biological activities, RSC Advances, 4 (2014) 50549-50553.

[114] H. Honda, Y. Ogawa, J. Kuwabara, T. Kanbara, Emission Behavior of Secondary Thioamide-Based Cationic Pincer Platinum(II) Complexes in the Aggregate State, European Journal of Inorganic Chemistry, 2014 (2014) 1865-1869.

[115] H. Honda, J. Kuwabara, T. Kanbara, Aggregation-induced emission behavior of a pincer platinum(II) complex bearing a poly(ethylene oxide) chain in aqueous solution, Journal of organometallic chemistry, 772–773 (2014) 139-142.

[116] Y.-Z. Xie, G.-G. Shan, P. Li, Z.-Y. Zhou, Z.-M. Su, A novel class of Zn (II) Schiff base complexes with aggregation-induced emission enhancement (AIEE) properties: synthesis, characterization and photophysical/electrochemical properties, Dyes and Pigments, 96 (2013) 467-474.

[117] D. Wang, S.-M. Li, J.-Q. Zheng, D.-Y. Kong, X.-J. Zheng, D.-C. Fang, L.-P. Jin, Coordination-Directed Stacking and Aggregation-Induced Emission Enhancement of the Zn(II) Schiff Base Complex, Inorganic Chemistry, 56 (2017) 984-990.

[118] X.-L. Xin, M. Chen, Y.-b. Ai, F.-l. Yang, X.-L. Li, F. Li, Aggregation-Induced Emissive Copper (I) Complexes for Living Cell Imaging, Inorganic Chemistry, 53 (2014) 2922-2931.

[119] R. Liu, M.-M. Huang, X.-X. Yao, H.-H. Li, F.-L. Yang, X.-L. Li, Synthesis, structures and aggregation-induced emissive properties of copper(I) complexes with 1H-imidazo[4,5-f][1,10]phenanthroline derivative and diphosphine as ligands, Inorganica Chimica Acta, 434 (2015) 172-180.

[120] X. Jia, J. Li, E. Wang, Cu Nanoclusters with Aggregation Induced Emission Enhancement, Small, 9 (2013) 3873-3879.

[121] X. Kang, S. Wang, Y. Song, S. Jin, G. Sun, H. Yu, M. Zhu, Bimetallic Au_2Cu_6 Nanoclusters: Strong Luminescence Induced by the Aggregation of Copper(I) Complexes with Gold(0) Species, Angewandte Chemie International Edition, 55 (2016) 3611-3614.

[122] X. Liu, Y. Shan, J. Xu, X. Zhang, S. Shang, X.-L. Li, Alcohol soluble Cu(I) complexes with aggregation-induced phosphorescent emission in ethanol/water solvents, Polyhedron, 164 (2019) 152-158.

[123] B. Manimaran, P. Thanasekaran, T. Rajendran, R.-J. Lin, I.-J. Chang, G.-H. Lee, S.-M. Peng, S. Rajagopal, K.-L. Lu, Luminescence enhancement induced by aggregation of alkoxy-bridged rhenium (I) molecular rectangles, Inorganic Chemistry, 41 (2002) 5323-5325.

[124] E.Q. Procopio, M. Mauro, M. Panigati, D. Donghi, P. Mercandelli, A. Sironi, G. D'ALFONSO, L. De Cola, Highly Emitting Concomitant Polymorphic Crystals of a Dinuclear Rhenium Complex, Journal of the American Chemical Society, 132 (2010) 14397-14399.

[125] M. Mauro, C.-H. Yang, C.-Y. Shin, M. Panigati, C.-H. Chang, G. D'Alfonso, L. De Cola, Phosphorescent Organic Light-Emitting Diodes with Outstanding External Quantum Efficiency using Dinuclear Rhenium Complexes as Dopants, Advanced Materials, 24 (2012) 2054-2058.

[126] C. Cebrian, M. Natali, D. Villa, M. Panigati, M. Mauro, G. D'Alfonso, L. De Cola, Luminescent supramolecular soft nanostructures from amphiphilic dinuclear Re(i) complexes, Nanoscale, 7 (2015) 12000-12009.

[127] M. Mauro, G. De Paoli, M. Otter, D. Donghi, G. D'Alfonso, L. De Cola, Aggregation induced colour change for phosphorescent iridium(iii) complex-based anionic surfactants, Dalton Transactions, 40 (2011) 12106-12116.

[128] V. Sathish, A. Ramdass, Z.-Z. Lu, M. Velayudham, P. Thanasekaran, K.-L. Lu, S. Rajagopal, Aggregation-Induced Emission Enhancement in Alkoxy-Bridged Binuclear Rhenium(I) Complexes:

Application as Sensor for Explosives and Interaction with Microheterogeneous Media, The Journal of Physical Chemistry B, 117 (2013) 14358-14366.

[129] Y.-J. Pu, R.E. Harding, S.G. Stevenson, E.B. Namdas, C. Tedeschi, J.P.J. Markham, R.J. Rummings, P.L. Burn, I.D.W. Samuel, Solution processable phosphorescent rhenium(I) dendrimers, Journal of Materials Chemistry, 17 (2007) 4255-4264.

[130] C. Chen, Y. Xu, Y. Wan, W. Fan, Z. Si, Aggregation-Induced Phosphorescent Emission from ReI Complexes: Synthesis and Property Studies, European Journal of Inorganic Chemistry, 2016 (2016) 1340-1347.

[131] M.T. Gabr, F.C. Pigge, Rhenium tricarbonyl complexes of AIE-active tetraarylethylene ligands: tuning luminescence properties and HSA-specific binding, Dalton Transactions, 46 (2017) 15040-15047.

[132] Front Matter, in: Mechanochromic Fluorescent Materials: Phenomena, Materials and Applications, The Royal Society of Chemistry, 2014, pp. P001-P004.

[133] Y. Chen, W.-C. Xu, J.-F. Kou, B.-L. Yu, X.-H. Wei, H. Chao, L.-N. Ji, Aggregation-induced emission of ruthenium (II) polypyridyl complex [Ru(bpy)$_2$(pzta)]$^{2+}$, Inorganic Chemistry Communications, 13 (2010) 1140-1143.

[134] E. Babu, P.M. Mareeswaran, M.M. Krishnan, V. Sathish, P. Thanasekaran, S. Rajagopal, Unravelling the aggregation induced emission enhancement in Tris(4,7-diphenyl-1,10-phenanthroline)ruthenium(II) complex, Inorganic Chemistry Communications, 98 (2018) 7-10.

[135] S.K. Sheet, B. Sen, S.K. Patra, M. Rabha, K. Aguan, S. Khatua, Aggregation-Induced Emission-Active Ruthenium(II) Complex of 4,7-Dichloro Phenanthroline for Selective Luminescent Detection and Ribosomal RNA Imaging, ACS Applied Materials & Interfaces, 10 (2018) 14356-14366.

[136] J. Kuwabara, Y. Ogawa, A. Taketoshi, T. Kanbara, Enhancement of the photoluminescence of a thioamide-based pincer palladium complex in the crystalline state, Journal of organometallic chemistry, 696 (2011) 1289-1293.

[137] C. Zhu, S. Li, M. Luo, X. Zhou, Y. Niu, M. Lin, J. Zhu, Z. Cao, X. Lu, T. Wen, Stabilization of anti-aromatic and strained five-membered rings with a transition metal, Nature chemistry, 5 (2013) 698-703.

[138] G.-X. Sun, M.-G. Ju, H. Zang, Y. Zhao, W. Liang, Mechanisms of large Stokes shift and aggregation-enhanced emission of osmapentalyne cations in solution: combined MD simulations and QM/MM calculations, Physical Chemistry Chemical Physics, 17 (2015) 24438-24445.

[139] V.W.-W. Yam, E.C.-C. Cheng, Highlights on the recent advances in gold chemistry-a photophysical perspective, Chemical Society Reviews, 37 (2008) 1806-1813.

[140] K.M.-C. Wong, V.W.-W. Yam, Self-Assembly of Luminescent Alkynylplatinum(II) Terpyridyl Complexes: Modulation of Photophysical Properties through Aggregation Behavior, Accounts of Chemical Research, 44 (2011) 424-434.

[141] A. Pinto, N. Svahn, J.C. Lima, L. Rodríguez, Aggregation induced emission of gold(I) complexes in water or water mixtures, Dalton Transactions, 46 (2017) 11125-11139.

[142] Z. Chi, X. Zhang, B. Xu, X. Zhou, C. Ma, Y. Zhang, S. Liu, J. Xu, Recent advances in organic mechanofluorochromic materials, Chemical Society Reviews, 41 (2012) 3878-3896.

[143] Z. Luo, X. Yuan, Y. Yu, Q. Zhang, D.T. Leong, J.Y. Lee, J. Xie, From Aggregation-Induced Emission of Au(I)–Thiolate Complexes to Ultrabright Au(0)@Au(I)–Thiolate Core–Shell Nanoclusters, Journal of the American Chemical Society, 134 (2012) 16662-16670.

[144] J. Liang, Z. Chen, J. Yin, G.-A. Yu, S.H. Liu, Aggregation-induced emission (AIE) behavior and thermochromic luminescence properties of a new gold(i) complex, Chemical Communications, 49 (2013) 3567-3569.

[145] K. Fujisawa, S. Yamada, Y. Yanagi, Y. Yoshioka, A. Kiyohara, O. Tsutsumi, Tuning the photoluminescence of condensed-phase cyclic trinuclear Au(I) complexes through control of their aggregated structures by external stimuli, Scientific Reports, 5 (2015) 7934.

[146] Z. Chen, D. Wu, X. Han, J. Liang, J. Yin, G.-A. Yu, S.H. Liu, A novel fluorene-based gold (I) complex with aggregate fluorescence change: A single-component white light-emitting luminophor, Chemical Communications, 50 (2014) 11033-11035.

[147] Z. Chen, G. Liu, S. Pu, S.H. Liu, Bipyridine-based aggregation-induced phosphorescent emission (AIPE)-active gold(I) complex with reversible phosphorescent mechanochromism and self-assembly characteristics, Dyes and Pigments, 152 (2018) 54-59.

[148] J. Zhang, Q. Liu, W. Wu, J. Peng, H. Zhang, F. Song, B. He, X. Wang, H.H.Y. Sung, M. Chen, B.S. Li, S.H. Liu, J.W.Y. Lam, B.Z. Tang, Real-Time Monitoring of Hierarchical Self-Assembly and Induction of Circularly Polarized Luminescence from Achiral Luminogens, ACS Nano, 13 (2019) 3618-3628.

[149] H. Yersin, D. Donges, Low-Lying Electronic States and Photophysical Properties of Organometallic Pd(II) and Pt(II) Compounds. Modern Research Trends Presented in Detailed Case Studies, in: H. Yersin (Ed.) Transition Metal and Rare Earth Compounds: Excited States, Transitions, Interactions II, Springer Berlin Heidelberg, Berlin, Heidelberg, 2001, pp. 81-186.

[150] G. Magnus, Ueber einige Verbindungen des Platinchlorürs, Annalen der Physik, 90 (1828) 239-242.

[151] D.M. Roundhill, H.B. Gray, C.M. Che, Pyrophosphito-bridged diplatinum chemistry, Accounts of Chemical Research, 22 (1989) 55-61.

[152] S.-W. Lai, C.-M. Che, Luminescent Cyclometalated Diimine Platinum(II) Complexes: Photophysical Studies and Applications, in: Transition Metal and Rare Earth Compounds: Excited States, Transitions, Interactions III, Springer Berlin Heidelberg, Berlin, Heidelberg, 2004, pp. 27-63.

[153] M. Mauro, A. Aliprandi, D. Septiadi, N.S. Kehr, L. De Cola, When self-assembly meets biology: luminescent platinum complexes for imaging applications, Chemical Society Reviews, 43 (2014) 4144-4166.

[154] K.H.-Y. Chan, H.-S. Chow, K.M.-C. Wong, M.C.-L. Yeung, V.W.-W. Yam, Towards thermochromic and thermoresponsive near-infrared (NIR) luminescent molecular materials through the modulation of inter- and/or intramolecular Pt···Pt and π···π interactions, Chemical Science, 1 (2010) 477-482.

[155] Y. Li, D.P.-K. Tsang, C.K.-M. Chan, K.M.-C. Wong, M.-Y. Chan, V.W.-W. Yam, Synthesis of Unsymmetric Bipyridine–PtII–Alkynyl Complexes through Post-Click Reaction with Emission Enhancement Characteristics and Their Applications as Phosphorescent Organic Light-Emitting Diodes, Chemistry – A European Journal, 20 (2014) 13710-13715.

[156] J.A. Bailey, M.G. Hill, R.E. Marsh, V.M. Miskowski, W.P. Schaefer, H.B. Gray, Electronic Spectroscopy of Chloro(terpyridine)platinum(II), Inorganic Chemistry, 34 (1995) 4591-4599.

[157] V.W.-W. Yam, K.M.-C. Wong, N. Zhu, Solvent-Induced Aggregation through Metal···Metal/π···π Interactions: Large Solvatochromism of Luminescent Organoplatinum(II) Terpyridyl Complexes, Journal of the American Chemical Society, 124 (2002) 6506-6507.

[158] L.J. Grove, J.M. Rennekamp, H. Jude, W.B. Connick, A New Class of Platinum(II) Vapochromic Salts, Journal of the American Chemical Society, 126 (2004) 1594-1595.

[159] M.-X. Zhu, W. Lu, N. Zhu, C.-M. Che, Structures and Solvatochromic Phosphorescence of Dicationic Terpyridyl–Platinum(II) Complexes with Foldable Oligo(ortho-phenyleneethynylene) Bridging Ligands, Chemistry – A European Journal, 14 (2008) 9736-9746.

[160] W. Lu, Y. Chen, V.A.L. Roy, S.S.-Y. Chui, C.-M. Che, Supramolecular Polymers and Chromonic Mesophases Self-Organized from Phosphorescent Cationic Organoplatinum(II) Complexes in Water, Angewandte Chemie International Edition, 48 (2009) 7621-7625.

[161] H.-F. Xiang, S.-C. Chan, K.K.-Y. Wu, C.-M. Che, P.T. Lai, High-efficiency red electrophosphorescence based on neutral bis(pyrrole)-diimine platinum(ii) complex, Chemical Communications, (2005) 1408-1410.

[162] S.C.F. Kui, Y.-C. Law, G.S.M. Tong, W. Lu, M.-Y. Yuen, C.-M. Che, Spectacular luminescent behaviour of tandem terpyridyl platinum(ii) acetylide complexes attributed to solvent effect on ordering of excited states, "ion-pair" formation and molecular conformations, Chemical Science, 2 (2011) 221-228.

[163] H.-Y. Shiu, H.-C. Chong, Y.-C. Leung, T. Zou, C.-M. Che, Phosphorescent proteins for bio-imaging and site selective bio-conjugation of peptides and proteins with luminescent cyclometalated iridium(iii) complexes, Chemical Communications, 50 (2014) 4375-4378.

[164] J.L.-L. Tsai, T. Zou, J. Liu, T. Chen, A.O.-Y. Chan, C. Yang, C.-N. Lok, C.-M. Che, Luminescent platinum(ii) complexes with self-assembly and anti-cancer properties: hydrogel, pH dependent emission color and sustained-release properties under physiological conditions, Chemical Science, 6 (2015) 3823-3830.

[165] C.A. Strassert, C.-H. Chien, M.D. Galvez Lopez, D. Kourkoulos, D. Hertel, K. Meerholz, L. De Cola, Switching On Luminescence by the Self-Assembly of a Platinum(II) Complex into Gelating Nanofibers and Electroluminescent Films, Angewandte Chemie International Edition, 50 (2011) 946-950.

[166] N. Komiya, M. Okada, K. Fukumoto, D. Jomori, T. Naota, Highly Phosphorescent Crystals of Vaulted trans-Bis(salicylaldiminato)platinum(II) Complexes, Journal of the American Chemical Society, 133 (2011) 6493-6496.

[167] N. Komiya, T. Muraoka, M. Iida, M. Miyanaga, K. Takahashi, T. Naota, Ultrasound-Induced Emission Enhancement Based on Structure-Dependent Homo- and Heterochiral Aggregations of Chiral Binuclear Platinum Complexes, Journal of the American Chemical Society, 133 (2011) 16054-16061.

[168] S. Yu-Lut Leung, V. Wing-Wah Yam, Hierarchical helices of helices directed by Pt···Pt and π–π stacking interactions: reciprocal association of multiple helices of dinuclear alkynylplatinum(ii) complex with luminescence enhancement behavior, Chemical Science, 4 (2013) 4228-4234.

[169] J. Liang, X. Zheng, L. He, H. Huang, W. Bu, Remarkable luminescence enhancement of chloroplatinum(ii) complexes of hexaethylene glycol methyl ether substituted 2,6-bis(benzimidazol-2[prime or minute]-yl)pyridine in water triggered by PF6, Dalton Transactions, 43 (2014) 13174-13177.

[170] J. Song, M. Wang, X. Zhou, H. Xiang, Unusual Circularly Polarized and Aggregation-Induced Near-Infrared Phosphorescence of Helical Platinum(II) Complexes with Tetradentate Salen Ligands, Chemistry – A European Journal, 24 (2018) 7128-7132.

[171] J. Song, M. Wang, X. Xu, L. Qu, X. Zhou, H. Xiang, 1D-helical platinum(ii) complexes bearing metal-induced chirality, aggregation-induced red phosphorescence, and circularly polarized luminescence, Dalton Transactions, 48 (2019) 4420-4428.

[172] J. Wu, Y. Li, C. Tan, X. Wang, Y. Zhang, J. Song, J. Qu, W.-Y. Wong, Aggregation-induced near-infrared emitting platinum(ii) terpyridyl complex: cellular characterisation and lysosome-specific localisation, Chemical Communications, 54 (2018) 11144-11147.

[173] L. Qu, C. Li, G. Shen, F. Gou, J. Song, M. Wang, X. Xu, X. Zhou, H. Xiang, Syntheses, crystal structures, chirality and aggregation-induced phosphorescence of stacked binuclear platinum(II) complexes with bridging Salen ligands, Materials Chemistry Frontiers, 3 (2019) 1199-1208.

[174] S. Liu, H. Sun, Y. Ma, S. Ye, X. Liu, X. Zhou, X. Mou, L. Wang, Q. Zhao, W. Huang, Rational design of metallophosphors with tunable aggregation-induced phosphorescent emission and their promising applications in time-resolved luminescence assay and targeted luminescence imaging of cancer cells, Journal of Materials Chemistry, 22 (2012) 22167-22173.

[175] D.A. Evans, L.M. Lee, I. Vargas-Baca, A.H. Cowley, Photophysical tuning of the aggregation-induced emission of a series of para-substituted aryl bis(imino)acenaphthene zinc complexes, Dalton Transactions, 44 (2015) 11984-11996.

[176] D.A. Evans, L.M. Lee, I. Vargas-Baca, A.H. Cowley, Aggregation-Induced Emission of Bis(imino)acenaphthene Zinc Complexes: Photophysical Tuning via Methylation of the Flanking Aryl Substituents, Organometallics, 34 (2015) 2422-2428.

[177] G. Zhang, Q. Chen, Y. Zhang, L. Kong, X. Tao, H. Lu, Y. Tian, J. Yang, Bulky group functionalized porphyrin and its Zn (II) complex with high emission in aggregation, Inorganic Chemistry Communications, 46 (2014) 85-88.

[178] G.-G. Shan, H.-B. Li, H.-Z. Sun, D.-X. Zhu, H.-T. Cao, Z.-M. Su, Controllable synthesis of iridium(iii)-based aggregation-induced emission and/or piezochromic luminescence phosphors by simply adjusting the substitution on ancillary ligands, Journal of Materials Chemistry C, 1 (2013) 1440-1449.

[179] J. Liang, Z. Chen, L. Xu, J. Wang, J. Yin, G.-A. Yu, Z.-N. Chen, S.H. Liu, Aggregation-induced emission-active gold(i) complexes with multi-stimuli luminescence switching, Journal of Materials Chemistry C, 2 (2014) 2243-2250.

[180] Z. Chen, J. Zhang, M. Song, J. Yin, G.-A. Yu, S.H. Liu, A novel fluorene-based aggregation-induced emission (AIE)-active gold(i) complex with crystallization-induced emission enhancement (CIEE) and reversible mechanochromism characteristics, Chemical Communications, 51 (2015) 326-329.

[181] S.S. Pasha, P. Alam, A. Sarmah, R.K. Roy, I.R. Laskar, Encapsulation of multi-stimuli AIE-active platinum(ii) complex: a facile and dry approach for luminescent mesoporous silica, RSC Advances, 6 (2016) 87791-87795.

[182] N. Leventis, Electrogenerated Chemiluminescence Edited by Allen J. Bard (University of Texas at Austin). Marcel Dekker, Inc.: New York. 2004. viii + 540 pp. $165.00. ISBN 0-8247-5347-X, Journal of the American Chemical Society, 127 (2005) 2015-2016.

[183] N.E. Tokel, A.J. Bard, Electrogenerated chemiluminescence. IX. Electrochemistry and emission from systems containing tris(2,2'-bipyridine)ruthenium(II) dichloride, Journal of the American Chemical Society, 94 (1972) 2862-2863.

[184] M.M. Richter, Electrochemiluminescence (ECL), Chemical Reviews, 104 (2004) 3003-3036.

[185] D. Ege, W.G. Becker, A.J. Bard, Electrogenerated chemiluminescent determination of tris(2,2'-bipyridine)ruthenium ion ($Ru(bpy)_3^{2+}$) at low levels, Analytical Chemistry, 56 (1984) 2413-2417.

[186] I. Rubinstein, A.J. Bard, Electrogenerated chemiluminescence. 37. Aqueous ecl systems based on tris(2,2'-bipyridine)ruthenium(2+) and oxalate or organic acids, Journal of the American Chemical Society, 103 (1981) 512-516.

[187] S. Carrara, A. Aliprandi, C.F. Hogan, L. De Cola, Aggregation-Induced Electrochemiluminescence of Platinum(II) Complexes, Journal of the American Chemical Society, 139 (2017) 14605-14610.

[188] T.-B. Gao, J.-J. Zhang, R.-Q. Yan, D.-K. Cao, D. Jiang, D. Ye, Aggregation-Induced Electrochemiluminescence from a Cyclometalated Iridium(III) Complex, Inorganic Chemistry, 57 (2018) 4310-4316.

[189] J.R. Lakowicz, Radiative Decay Engineering: Biophysical and Biomedical Applications, Analytical Biochemistry, 298 (2001) 1-24.

[190] F. Tam, G.P. Goodrich, B.R. Johnson, N.J. Halas, Plasmonic Enhancement of Molecular Fluorescence, Nano Letters, 7 (2007) 496-501.

[191] J.S. Becker, M. Zoriy, A. Matusch, B. Wu, D. Salber, C. Palm, J.S. Becker, Bioimaging of metals by laser ablation inductively coupled plasma mass spectrometry (LA-ICP-MS), Mass Spectrometry Reviews, 29 (2010) 156-175.

[192] F. Zhang, G.B. Braun, Y. Shi, Y. Zhang, X. Sun, N.O. Reich, D. Zhao, G. Stucky, Fabrication of Ag@SiO2@Y2O3:Er Nanostructures for Bioimaging: Tuning of the Upconversion Fluorescence with Silver Nanoparticles, Journal of the American Chemical Society, 132 (2010) 2850-2851.

[193] J. Liu, Y. Liu, Q. Liu, C. Li, L. Sun, F. Li, Iridium(III) Complex-Coated Nanosystem for Ratiometric Upconversion Luminescence Bioimaging of Cyanide Anions, Journal of the American Chemical Society, 133 (2011) 15276-15279.

[194] Y. Chen, M. Li, Y. Hong, J.W.Y. Lam, Q. Zheng, B.Z. Tang, Dual-Modal MRI Contrast Agent with Aggregation-Induced Emission Characteristic for Liver Specific Imaging with Long Circulation Lifetime, ACS Applied Materials & Interfaces, 6 (2014) 10783-10791.

[195] E.S. Shibu, K. Ono, S. Sugino, A. Nishioka, A. Yasuda, Y. Shigeri, S.-i. Wakida, M. Sawada, V. Biju, Photouncaging Nanoparticles for MRI and Fluorescence Imaging in Vitro and in Vivo, ACS Nano, 7 (2013) 9851-9859.

[196] A.M. Smith, M.C. Mancini, S. Nie, Second window for in vivo imaging, Nature Nanotechnology, 4 (2009) 710.

[197] G. Mandal, M. Darragh, Y.A. Wang, C.D. Heyes, Cadmium-free quantum dots as time-gated bioimaging probes in highly-autofluorescent human breast cancer cells, Chemical Communications, 49 (2013) 624-626.

[198] N.-N. Dong, M. Pedroni, F. Piccinelli, G. Conti, A. Sbarbati, J.E. Ramírez-Hernández, L.M. Maestro, M.C. Iglesias-de la Cruz, F. Sanz-Rodriguez, A. Juarranz, F. Chen, F. Vetrone, J.A. Capobianco, J.G. Solé, M. Bettinelli, D. Jaque, A. Speghini, NIR-to-NIR Two-Photon Excited CaF2:Tm3+,Yb3+ Nanoparticles: Multifunctional Nanoprobes for Highly Penetrating Fluorescence Bio-Imaging, ACS Nano, 5 (2011) 8665-8671.

[199] H. Lu, Y. Zheng, X. Zhao, L. Wang, S. Ma, X. Han, B. Xu, W. Tian, H. Gao, Highly Efficient Far Red/Near-Infrared Solid Fluorophores: Aggregation-Induced Emission, Intramolecular Charge Transfer, Twisted Molecular Conformation, and Bioimaging Applications, Angewandte Chemie, 128 (2016) 163-167.

[200] J. Qi, C. Sun, A. Zebibula, H. Zhang, R.T.K. Kwok, X. Zhao, W. Xi, J.W.Y. Lam, J. Qian, B.Z. Tang, Real-Time and High-Resolution Bioimaging with Bright Aggregation-Induced Emission Dots in Short-Wave Infrared Region, Advanced Materials, 30 (2018) 1706856.

[201] S. Xie, A.Y.H. Wong, R.T.K. Kwok, Y. Li, H. Su, J.W.Y. Lam, S. Chen, B.Z. Tang, Fluorogenic Ag+—Tetrazolate Aggregation Enables Efficient Fluorescent Biological Silver Staining, Angewandte Chemie International Edition, 57 (2018) 5750-5753.

[202] J. Liu, C. Jin, B. Yuan, X. Liu, Y. Chen, L. Ji, H. Chao, Selectively lighting up two-photon photodynamic activity in mitochondria with AIE active iridium(III) complexes, Chemical Communications, 53 (2017) 2052-2055.

[203] K. Qiu, M. Ouyang, Y. Liu, H. Huang, C. Liu, Y. Chen, L. Ji, H. Chao, Two-photon photodynamic ablation of tumor cells by mitochondria-targeted iridium(III) complexes in aggregate states, Journal of Materials Chemistry B, 5 (2017) 5488-5498.

[204] D.-L. Ma, H.-Z. He, K.-H. Leung, D.S.-H. Chan, C.-H. Leung, Bioactive Luminescent Transition-Metal Complexes for Biomedical Applications, Angewandte Chemie International Edition, 52 (2013) 7666-7682.

[205] M. Gao, B.Z. Tang, Aggregation-induced emission probes for cancer theranostics, Drug Discovery Today, 22 (2017) 1288-1294.

[206] G. Feng, B. Liu, Aggregation-Induced Emission (AIE) Dots: Emerging Theranostic Nanolights, Accounts of Chemical Research, 51 (2018) 1404-1414.

[207] S.S. Pasha, L. Fageria, C. Climent, N.P. Rath, P. Alemany, R. Chowdhury, A. Roy, I.R. Laskar, Evaluation of novel platinum(ii) based AIE compound-encapsulated mesoporous silica nanoparticles for cancer theranostic application, Dalton Transactions, 47 (2018) 4613-4624.

[208] Q. Zhao, X. Zhou, T. Cao, K.Y. Zhang, L. Yang, S. Liu, H. Liang, H. Yang, F. Li, W. Huang, Fluorescent/phosphorescent dual-emissive conjugated polymer dots for hypoxia bioimaging, Chemical Science, 6 (2015) 1825-1831.

[209] T. Yoshihara, S. Murayama, S. Tobita, Ratiometric Molecular Probes Based on Dual Emission of a Blue Fluorescent Coumarin and a Red Phosphorescent Cationic Iridium(III) Complex for Intracellular Oxygen Sensing, Sensors, 15 (2015) 13503.

[210] S. Kim, M.S. Eom, S. Yoo, M.S. Han, Development of a highly selective colorimetric pyrophosphate probe based on a metal complex and gold nanoparticles: change in selectivity induced by metal ion tuning of the metal complex, Tetrahedron Letters, 56 (2015) 5030-5033.

[211] Z. Hai, Y. Bao, Q. Miao, X. Yi, G. Liang, Pyridine–Biquinoline–Metal Complexes for Sensing Pyrophosphate and Hydrogen Sulfide in Aqueous Buffer and in Cells, Analytical Chemistry, 87 (2015) 2678-2684.

[212] Y. Fu, F. Qiu, F. Zhang, Y. Mai, Y. Wang, S. Fu, R. Tang, X. Zhuang, X. Feng, A dual-boron-cored luminogen capable of sensing and imaging, Chemical Communications, 51 (2015) 5298-5301.

[213] K.-C. Chang, S.-S. Sun, M.O. Odago, A.J. Lees, Anion recognition and sensing by transition-metal complexes with polarized NH recognition motifs, Coordination Chemistry Reviews, 284 (2015) 111-123.

[214] B. Chen, X. Sun, X. Li, H. Ågren, Y. Xie, TICT based fluorescence "turn-on" hydrazine probes, Sensors and Actuators B: Chemical, 199 (2014) 93-100.

[215] J. Hu, Z. He, Z. Wang, X. Li, J. You, G. Gao, A simple approach to aggregation-induced emission in difluoroboron dibenzoylmethane derivatives, Tetrahedron Letters, 54 (2013) 4167-4170.

[216] K. Zhang, S. Liu, Q. Zhao, F. Li, W. Huang, Phosphorescent Iridium(III) Complexes for Bioimaging, in: K.K.-W. Lo (Ed.) Luminescent and Photoactive Transition Metal Complexes as Biomolecular Probes and Cellular Reagents, Springer Berlin Heidelberg, 2015, pp. 131-180.

[217] M.G. Mohamed, R.-C. Lin, J.-H. Tu, F.-H. Lu, J.-L. Hong, K.-U. Jeong, C.-F. Wang, S.-W. Kuo, Thermal property of an aggregation-induced emission fluorophore that forms metal-ligand complexes with $Zn(ClO_4)_2$ of salicylaldehyde azine-functionalized polybenzoxazine, RSC Advances, 5 (2015) 65635-65645.

[218] S. Lee, K.K.Y. Yuen, K.A. Jolliffe, J. Yoon, Fluorescent and colorimetric chemosensors for pyrophosphate, Chemical Society Reviews, 44 (2015) 1749-1762.

[219] D.G. Khandare, H. Joshi, M. Banerjee, M.S. Majik, A. Chatterjee, Fluorescence Turn-on Chemosensor for the Detection of Dissolved CO2 Based on Ion-Induced Aggregation of Tetraphenylethylene Derivative, Analytical Chemistry, 87 (2015) 10871-10877.

[220] F. Yan, Q. Mei, L. Wang, B. Tong, Z. Xu, J. Weng, L. Wang, W. Huang, A highly selective and ratiometric sensor for Hg^{2+} based on a phosphorescent iridium (III) complex, Inorganic Chemistry Communications, 22 (2012) 178-181.

[221] Y. Liu, Y. Tang, N.N. Barashkov, I.S. Irgibaeva, J.W.Y. Lam, R. Hu, D. Birimzhanova, Y. Yu, B.Z. Tang, Fluorescent Chemosensor for Detection and Quantitation of Carbon Dioxide Gas, Journal of the American Chemical Society, 132 (2010) 13951-13953.

[222] Q. Zhao, S. Liu, F. Li, T. Yi, C. Huang, Multisignaling detection of Hg2+ based on a phosphorescent iridium(iii) complex, Dalton Transactions, (2008) 3836-3840.

[223] N.K. Hien, N.C. Bao, N.T. Ai Nhung, N.T. Trung, P.C. Nam, T. Duong, J.S. Kim, D.T. Quang, A highly sensitive fluorescent chemosensor for simultaneous determination of Ag(I), Hg(II), and Cu(II) ions: Design, synthesis, characterization and application, Dyes and Pigments, 116 (2015) 89-96.

[224] J. Du, M. Hu, J. Fan, X. Peng, Fluorescent chemodosimeters using "mild" chemical events for the detection of small anions and cations in biological and environmental media, Chemical Society Reviews, 41 (2012) 4511-4535.

[225] N. Zhao, Y.-H. Wu, J. Luo, L.-X. Shi, Z.-N. Chen, Aggregation-induced phosphorescence of iridium(iii) complexes with 2,2[prime or minute]-bipyridine-acylhydrazone and their highly selective recognition to Cu^{2+}, Analyst, 138 (2013) 894-900.

[226] Y. Guo, X. Tong, L. Ji, Z. Wang, H. Wang, J. Hu, R. Pei, Visual detection of Ca^{2+} based on aggregation-induced emission of Au(i)–Cys complexes with superb selectivity, Chemical Communications, 51 (2015) 596-598.

[227] P. Alam, G. Kaur, V. Kachwal, A. Gupta, A. Roy Choudhury, I.R. Laskar, Highly sensitive explosive sensing by "aggregation induced phosphorescence" active cyclometalated iridium(III) complexes, Journal of Materials Chemistry C, 3 (2015) 5450-5456.

[228] X.-G. Hou, Y. Wu, H.-T. Cao, H.-Z. Sun, H.-B. Li, G.-G. Shan, Z.-M. Su, A cationic iridium(iii) complex with aggregation-induced emission (AIE) properties for highly selective detection of explosives, Chemical Communications, 50 (2014) 6031-6034.

[229] K.S. Bejoymohandas, T.M. George, S. Bhattacharya, S. Natarajan, M.L.P. Reddy, AIPE-active green phosphorescent iridium(III) complex impregnated test strips for the vapor-phase detection of 2,4,6-trinitrotoluene (TNT), Journal of Materials Chemistry C, 2 (2014) 515-523.

[230] W. Che, G. Li, X. Liu, K. Shao, D. Zhu, Z. Su, M.R. Bryce, Selective sensing of 2,4,6-trinitrophenol (TNP) in aqueous media with "aggregation-induced emission enhancement" (AIEE)-active iridium(III) complexes, Chemical Communications, 54 (2018) 1730-1733.

[231] A.J. Howarth, D.L. Davies, F. Lelj, M.O. Wolf, B.O. Patrick, Tuning the Emission Lifetime in Bis-cyclometalated Iridium(III) Complexes Bearing Iminopyrene Ligands, Inorganic Chemistry, 53 (2014) 11882-11889.

[232] S. Kumar, Y. Hisamatsu, Y. Tamaki, O. Ishitani, S. Aoki, Design and Synthesis of Heteroleptic Cyclometalated Iridium(III) Complexes Containing Quinoline-Type Ligands that Exhibit Dual Phosphorescence, Inorganic Chemistry, 55 (2016) 3829-3843.

[233] S. Ladouceur, L. Donato, M. Romain, B.P. Mudraboyina, M.B. Johansen, J.A. Wisner, E. Zysman-Colman, A rare case of dual emission in a neutral heteroleptic iridium(III) complex, Dalton Transactions, 42 (2013) 8838-8847.

[234] K.K.-W. Lo, K.Y. Zhang, S.-K. Leung, M.-C. Tang, Exploitation of the Dual-emissive Properties of Cyclometalated Iridium(III)–Polypyridine Complexes in the Development of Luminescent Biological Probes, Angewandte Chemie International Edition, 47 (2008) 2213-2216.

[235] Y. You, Y. Han, Y.-M. Lee, S.Y. Park, W. Nam, S.J. Lippard, Phosphorescent Sensor for Robust Quantification of Copper(II) Ion, Journal of the American Chemical Society, 133 (2011) 11488-11491.

[236] K.Y. Zhang, H.-W. Liu, M.-C. Tang, A.W.-T. Choi, N. Zhu, X.-G. Wei, K.-C. Lau, K.K.-W. Lo, Dual-Emissive Cyclometalated Iridium(III) Polypyridine Complexes as Ratiometric Biological Probes and Organelle-Selective Bioimaging Reagents, Inorganic Chemistry, 54 (2015) 6582-6593.

[237] K.Y. Zhang, P. Gao, G. Sun, T. Zhang, X. Li, S. Liu, Q. Zhao, K.K.-W. Lo, W. Huang, Dual-Phosphorescent Iridium(III) Complexes Extending Oxygen Sensing from Hypoxia to Hyperoxia, Journal of the American Chemical Society, 140 (2018) 7827-7834.

[238] W. Lv, T. Yang, Q. Yu, Q. Zhao, K.Y. Zhang, H. Liang, S. Liu, F. Li, W. Huang, A Phosphorescent Iridium(III) Complex-Modified Nanoprobe for Hypoxia Bioimaging Via Time-Resolved Luminescence Microscopy, Advanced Science, (2015) 1500107.

[239] J. Zhuang, W. Li, W. Su, Y. Liu, Q. Shen, L. Liao, M. Zhou, Highly efficient phosphorescent organic light-emitting diodes using a homoleptic iridium(III) complex as a sky-blue dopant, Organic Electronics, 14 (2013) 2596-2601.

[240] D. Kourkoulos, C. Karakus, D. Hertel, R. Alle, S. Schmeding, J. Hummel, N. Risch, E. Holder, K. Meerholz, Photophysical properties and OLED performance of light-emitting platinum(ii) complexes, Dalton Transactions, 42 (2013) 13612-13621.

[241] L. Flamigni, A. Barbieri, C. Sabatini, B. Ventura, F. Barigelletti, Photochemistry and Photophysics of Coordination Compounds: Iridium, in: V. Balzani, S. Campagna (Eds.) Photochemistry and Photophysics of Coordination Compounds II, Springer Berlin Heidelberg, 2007, pp. 143-203.

[242] B. Ma, P.I. Djurovich, M.E. Thompson, Excimer and electron transfer quenching studies of a cyclometalated platinum complex, Coordination Chemistry Reviews, 249 (2005) 1501-1510.

[243] M. Ito, Y. Morita, H. Saigusa, Transformation of van der Waals complexes to excimer and exciplex in jet-cooled fluorene and 9-ethylfluorene, The Journal of Physical Chemistry, 92 (1988) 5693-5696.

[244] Y.C. Zhu, L. Zhou, H.Y. Li, Q.L. Xu, M.Y. Teng, Y.X. Zheng, J.L. Zuo, H.J. Zhang, X.Z. You, Highly Efficient Green and Blue-Green Phosphorescent OLEDs Based on Iridium Complexes with the Tetraphenylimidodiphosphinate Ligand, Advanced Materials, 23 (2011) 4041-4046.

[245] P. Li, Q.-Y. Zeng, H.-Z. Sun, M. Akhtar, G.-G. Shan, X.-G. Hou, F.-S. Li, Z.-M. Su, Aggregation-induced emission (AIE) active iridium complexes toward highly efficient single-layer non-doped electroluminescent devices, Journal of Materials Chemistry C, 4 (2016) 10464-10470.

[246] C. Borek, K. Hanson, P.I. Djurovich, M.E. Thompson, K. Aznavour, R. Bau, Y. Sun, S.R. Forrest, J. Brooks, L. Michalski, J. Brown, Highly Efficient, Near-Infrared Electrophosphorescence from a Pt–Metalloporphyrin Complex, Angewandte Chemie International Edition, 46 (2007) 1109-1112.

[247] X.-H. Zhao, G.-H. Xie, Z.-D. Liu, W.-J. Li, M.-d. Yi, L.-H. Xie, C.-P. Hu, R. Zhu, Q. Zhao, Y. Zhao, J.-F. Zhao, Y. Qian, W. Huang, A 3-dimensional spiro-functionalized platinum(II) complex to suppress intermolecular [small pi]-[small pi] and Pt[three dots, centered]Pt supramolecular interactions for a high-performance electrophosphorescent device, Chemical Communications, 48 (2012) 3854-3856.

[248] Y. Li, D.P.K. Tsang, C.K.M. Chan, K.M.C. Wong, M.Y. Chan, V.W.W. Yam, Synthesis of Unsymmetric Bipyridine–PtII–Alkynyl Complexes through Post-Click Reaction with Emission Enhancement Characteristics and Their Applications as Phosphorescent Organic Light-Emitting Diodes, Chemistry – A European Journal, 20 (2014) 13710-13715.

[249] R. Liu, Z. Song, Y. Li, Y. Li, W. Yao, H. Sun, H. Zhu, An AIPE-active heteroleptic Ir(III) complex for latent fingermarks detection, Sensors and Actuators B: Chemical, 259 (2018) 840-846.